

NOVEL REGULATORY MECHANISMS OF PROTEIN KINASE B ON APOPTOSIS
SUSCEPTIBILITY AND CANCER DEDIFFERENTIATION



A Dissertation Submitted in Partial Fulfillment of the Requirements
for the Degree of Doctor of Philosophy in Pharmacology and Toxicology

Department of Pharmacology and Physiology

Faculty of Pharmaceutical Sciences

Chulalongkorn University

Academic Year 2018

Copyright of Chulalongkorn University

กลไกการควบคุมใหม่ของโปรตีนโคเนสปีต่อความไวในการอะพอพโทซิสและการเกิดวิวัฒนาการถอย
หลังของมะเร็ง



วิทยานิพนธ์นี้เป็นส่วนหนึ่งของการศึกษาตามหลักสูตรปริญญาเภสัชศาสตรดุษฎีบัณฑิต
สาขาวิชาเภสัชวิทยาและพิษวิทยา ภาควิชาเภสัชวิทยาและสรีรวิทยา
คณะเภสัชศาสตร์ จุฬาลงกรณ์มหาวิทยาลัย
ปีการศึกษา 2561
ลิขสิทธิ์ของจุฬาลงกรณ์มหาวิทยาลัย

Thesis Title NOVEL REGULATORY MECHANISMS OF PROTEIN KINASE B ON
APOPTOSIS SUSCEPTIBILITY AND CANCER DEDIFFERENTIATION
By Mr. Arnatchai Maiuthed
Field of Study Pharmacology and Toxicology
Thesis Advisor Associate Professor Pithi Chanvorachote, Ph.D.
Thesis Co Advisor Professor Doctor rerum naturalium Regine Schneider-Stock
Professor Jutta Eichler, Ph.D.

Accepted by the Faculty of Pharmaceutical Sciences, Chulalongkorn University in Partial
Fulfillment of the Requirement for the Doctor of Philosophy

..... Dean of the Faculty of Pharmaceutical
Sciences
(Assistant Professor Rungpetch Sakulbumrungsil, Ph.D.)

DISSERTATION COMMITTEE

..... Chairman
(Associate Professor Suree Jianmongkol, Ph.D.)

..... Thesis Advisor
(Associate Professor Pithi Chanvorachote, Ph.D.)

..... Thesis Co-Advisor
(Professor Doctor rerum naturalium Regine Schneider-Stock)

..... Thesis Co-Advisor
(Professor Jutta Eichler, Ph.D.)

..... Examiner
(Assistant Professor Rataya Luechapudiporn, Ph.D.)

..... Examiner
(Assistant Professor SUPANNIKAR TAWINWUNG, Ph.D.)

..... External Examiner
(Associate Professor Chanitra Thuwajit (Toraksa), Ph.D.)

อาณัฐชัย ม้ายอุเทศ : กลไกการควบคุมใหม่ของโปรตีนไคเนสบีต่อความไวในการอะพอพโทซิสและ
 การเกิดวิวัฒนาการถอยหลังของมะเร็ง. (NOVEL REGULATORY MECHANISMS OF PROTEIN
 KINASE B ON APOPTOSIS SUSCEPTIBILITY AND CANCER DEDIFFERENTIATION) อ.ที่ปรึกษา
 หลัก : รศ. ภก. ดร.ปิติ จันทร์วรโชติ, อ.ที่ปรึกษาร่วม : ศ. ดร.เรจิน่า ซไนเดอร์ สต็อก, ศ. ดร.ยุทธะ
 ไอซ์เลอร์



สาขาวิชา เภสัชวิทยาและพิษวิทยา
 ปีการศึกษา 2561

ลายมือชื่อนิสิต
 ลายมือชื่อ อ.ที่ปรึกษาหลัก
 ลายมือชื่อ อ.ที่ปรึกษาร่วม
 ลายมือชื่อ อ.ที่ปรึกษาร่วม

5776454933 : MAJOR PHARMACOLOGY AND TOXICOLOGY

KEYWORD:

Arnatchai Maiuthed : NOVEL REGULATORY MECHANISMS OF PROTEIN KINASE B ON APOPTOSIS SUSCEPTIBILITY AND CANCER DEDIFFERENTIATION. Advisor: Assoc. Prof. Pithi Chanvorachote, Ph.D. Co-advisor: Prof. Dr. rer. nat. Regine Schneider-Stock, Prof. Jutta Eichler, Ph.D.



Field of Study:	Pharmacology and Toxicology	Student's Signature
Academic Year:	2018	Advisor's Signature
		Co-advisor's Signature
		Co-advisor's Signature

ACKNOWLEDGEMENTS

First, I would like to express my deepest gratitude and appreciation to Associate Professor Pithi Chanvorachote (Ph.D.), my major advisor, Professor Dr. rer. Nat. Regine Schneider-Stock (Ph.D.), my co-advisor, and Professor Jutta Eichler (Ph.D.), my co-advisor, for giving me expert guidance, their invaluable advice, kind support, supervision and friendliness. Most importantly, their graciousness will always be unforgettable.

My special thanks are extended to all co-authors in my publications, for their helpful guidance and criticism, superb supervision, kind support and abundant encouragement throughout the research work. Their enthusiasm and creativity will continue to inspire me.

My great appreciation is extended to all staffs at Department of Pharmacology and Physiology, Faculty of Pharmaceutical Sciences, Chulalongkorn University, Thailand and all staffs at Department of Experimental Tumor-pathology, Institute of Pathology, University of Erlangen-Nürnberg, Germany, for warm welcome, work flow helpful, and nice technique training.

I appreciate to thank grants as follows: Thailand Research Fund through The Royal Golden Jubilee Ph.D. program (PHD/0063/2557) (for 2 semester 2014 - 2 semester 2017) and The 100th Anniversary Chulalongkorn University Fund for Doctoral Scholarship (for 1st semester of 2014) which supported my life and my research work while I was as Ph.D. student.

I would like to thank all my friends and my colleagues at Faculty of Pharmaceutical Sciences, Chulalongkorn University, for friendship, kind support and cheerfulness.

Last but not least, I would like to express my deep appreciation to my dearest parents and my family for their love, understand, support my life which help me to reach the goal that I want.

CHULALONGKORN UNIVERSITY

Amatchai Maiuthed

TABLE OF CONTENTS

	Page
ABSTRACT (THAI).....	iii
ABSTRACT (ENGLISH).....	iv
ACKNOWLEDGEMENTS	v
TABLE OF CONTENTS	vi
CHAPTER I.....	1
INTRODUCTION.....	1
Alteration of Protein kinase B is the cause of cancer progression	1
Protein kinase B.....	1
Akt signaling in physiology	4
Akt Dysregulation in cancer	7
Cancer	7
Upregulation of Akt activity in cancer	7
Akt promoting and maintaining cancer hallmarks.....	8
Lung and colorectal cancers	10
Epidemiology	10
Akt-related molecular pathophysiology of lung cancer	11
Lung cancer recurrence is major cause of death.....	13
Akt-related proteins in the regulation of cancer stem cells.....	14
Caveolin-1	15
Caveolin-1 and cancer.....	16
Nitric oxide promotes cancer stem cell.....	17

Dedifferentiation and cancer stem cell	18
Epidemiology	19
Akt-related molecular pathophysiology of colorectal cancer	20
Chemoresistance in colorectal cancer	22
Cancer therapeutics targeting AKT	24
Natural compounds are promising source for developing cancer drug	27
Natural product.....	27
Renieramycin (natural product from the Thai blue sponge).....	28
Research Questions	29
Objectives.....	29
Hypotheses.....	29
Expected benefits	29
Novel finding in this research	30
CHAPTER II	42
NITRIC OXIDE PROMOTES CANCER CELL DEDIFFERENTIATION BY DISRUPTING AN OCT4:CAVEOLIN-1 COMPLEX : A NEW REGULATORY MECHANISM FOR CANCER STEM CELL FORMATION.....	42
Approval of the co-authors on the use of publication material in the dissertation of Arnatchai Maiuthed	43
Abstract	44
Introduction.....	45
Results.....	46
Nitric oxide increases CSC-like phenotypes of human lung cancer cells.	46
Nitric oxide increases the expression of stemness-related proteins.....	49
Microarray gene profiles of nitric oxide-mediated gene expression.	51

Nitric oxide suppresses the degradation of Oct4 by diminishing its ubiquitin proteasomal degradation.....	53
Nitric oxide increases phosphorylated Akt (Ser-473) and caveolin-1 levels.....	54
Caveolin-1 enhances the degradation of Oct4 via ubiquitin–proteasome pathway.....	54
Caveolin-1 interacts with Oct-4	57
NO-mediated phosphorylation of Akt promotes Oct4 expression by dissociating it from caveolin-1 complex.....	60
Tyrosine 14 of caveolin-1 is required for its interaction with Oct4.....	62
Cav-1:Oct4 complex models.....	63
Discussion	65
Experimental procedures.....	68
Cells and reagents.....	68
Cytotoxicity assay	68
Cell death assay.....	69
Spheroid formation assay	69
Microarray analysis.....	69
RNA isolation and RT-PCR.....	69
Plasmid construction and transfection	69
Co-immunoprecipitation	70
Western blot analysis.....	70
Immunofluorescence.....	71
Proximity ligation assay	71
Computational method.....	71
Statistical analysis.....	72

Supplement data	73
References	78
CHAPTER III	86
CYTOPLASMIC p21 MEDIATES 5-FLUOROURACIL RESISTANCE BY INHIBITING PRO- APOPTOTIC CHK2	86
Approval of the co-authors on the use of publication material in the dissertation of Arnatchai Maiuthed	87
Abstract	94
Introduction	95
Results	96
Cytotoxic effect of 5FU on colorectal cancer cell lines	96
Cytoplasmic localization of p21 in 5FU-resistant cells in vitro and in vivo	96
Cytoplasmic p21 induces apoptosis resistance after 5FU treatment	100
Cytoplasmic p21 activates cell survival signals and attenuates the pro- apoptotic effect of Chk2 in vitro and in vivo	102
p21 interacts with p-Chk2 in 5-FU resistant cells.	105
Discussion	109
Material and Methods	111
Cell lines	111
Cytotoxicity assay	111
Annexin-Propidium iodide apoptosis assay by flow cytometry	111
Western Blot analysis	112
Immunofluorescence	112
Plasmids and Transfection	113
Immunoprecipitation	113

Human phospho-kinase antibody array	113
Chorioallantoic membrane assay (CAM assay)	114
Immunohistochemistry (IHC) Staining Assay.....	114
Proximity ligation assay (In situ PLA).....	115
Structural modeling.....	115
Statistics	115
Conclusions	115
Supplementary materials:	117
References	121
CHAPTER IV	127
APOPTOSIS-INDUCING EFFECT OF HYDROQUINONE 5-O-CINNAMOYL ESTER ANALOG OF RENIERAMYCIN M ON NON-SMALL CELL LUNG CANCER CELLS	127
Approval of the co-authors on the use of publication material in the dissertation of Arnatchai Maiuthed	128
Abstract	129
Introduction.....	130
Materials and Methods	131
Preparation of CIN-RM.....	131
Chemicals.....	132
Cell culture and treatment.....	132
Cell viability assay.....	132
Nuclear staining assay.....	132
Membrane integrity analysis.....	133
Western blot analysis.....	133

Statistical analysis.....	133
Results.....	133
Evaluation of the cytotoxic effect of CIN-RM and RM on H292 cells.....	133
CIN-RM induces apoptotic cell death.....	134
CIN-RM triggers apoptosis via a p53-dependent mechanism and suppresses AKT.	135
Discussion	137
References.....	139
CHAPTER V	143
CONCLUSION AND SUGGESTION FOR FUTHER STUDY	143
Conclusion.....	143
Suggestion for further projects.....	143
REFERENCES	144
VITA.....	146

CHAPTER I

INTRODUCTION

Alteration of Protein kinase B is the cause of cancer progression

Protein kinase B

Protein kinase B (PKB), also known as Akt, is a 57-kDa serine/threonine kinase which act as a central of multiple cellular processes (1). Akt has three isoforms which are encoded by distinct gene sequences in different chromosomes (14q32.33 for Akt1/PKB-alpha, 19q13.2 for Akt2/PKB-beta, 1q43-q44 for Akt3/PKB-gamma) (2). Although, the three Akt isoforms share 80% homology of amino acid sequences (2). More than 100 cellular molecules have been identified as Akt substrate without reported with isoform specificity. However, different in physiological effects of each isoform depend on its specific tissue expression (3). A key Akt substrates are described in Table1. Most of the Akt substrates contain at least Arg-X-Arg-X-X-Ser/Thr-Hyd motif, where x is any amino acid and Hyd is a hydrophobic amino acid (1). Akt is composed with 480 amino acids which can be divided to four major functional domains, an N-terminal pleckstrin homology (PH) domain, central catalytic domain, a hinge region (HR) between the PH domain and the catalytic domain, and a C-terminal regulatory domain (C-tail) (1). The illustration of Akt functional domain of three isoforms are showed below in Figure1. The N-terminus PH domain allows the translocation of Akt from the cytoplasm to the plasma membrane and binding with phosphatidyl inositol (3,4,5) phosphate. The Akt activation occurs after it bound to the plasma membrane. Once binding at the plasma membrane, the Akt is activated by multiple processes which resulted in phosphorylation both of Thr308 in the central catalytic domain and Ser473 in the C-tail regulatory domain (1).

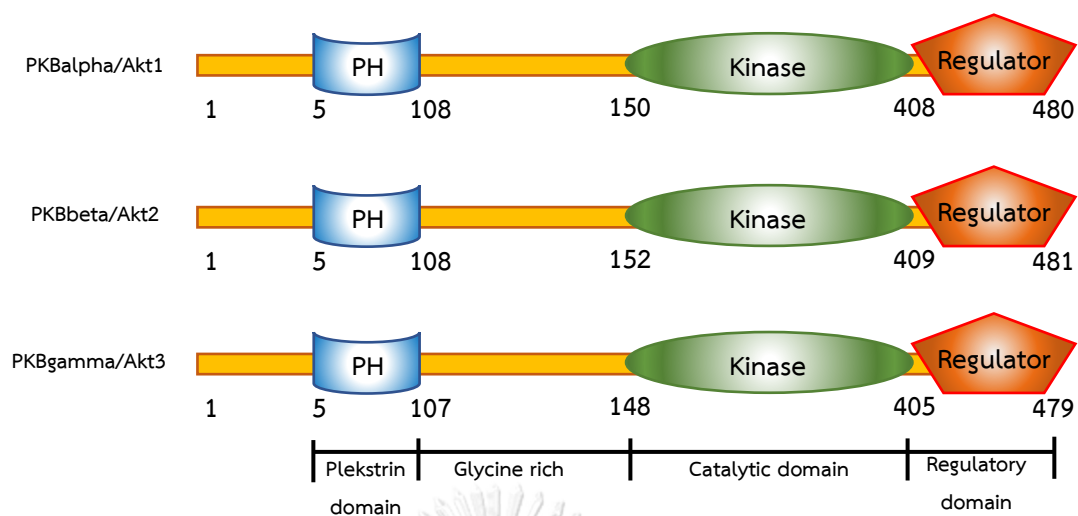


Figure. 1. Structure of the three human Akt/PKB isoforms. All isoform contains a pleckstrin homology-domain (PH) in the N-terminal region, a glycine rich link region, a central catalytic domain, and a regulatory C-terminal region.

Table 1. The key Akt substrates.

Substrate protein	Phosphorylation site(s)	Sequences	Effect of phosphorylation
Glucose homeostasis			
AS160	Ser-588 and Thr-642	QFRRRAHtFsHPPss	Stimulates AS160 and GLUT4 trafficking
GSK3-alpha	Ser-21	SGRARTssFAEPGGG	Inhibits the enzyme activity
GSK3-beta	Ser-9	SGRPRttsFAESCKP	Inhibits the enzyme activity
PFK-2	Ser-466 and Ser-483	PVRMRRNsFtPLSSS, IRRPRNysVGSRPLK	Activates the protein
PGC-1alpha	Ser-570	RMRSRsRsFsRHRSC	Inhibits its transcriptional co-function
PTP1B	Ser-50	RNRyRDVsPFDHsRI	Inhibits its phosphatases activity

Cell proliferation			
Androgen receptor	Ser-210 and Ser-790	LLCLRRssLKAYGNG	Inhibits its transcriptional activity
BRCA1	Thr-509	QTSKRHDSDTFPELK, LKRKRPPtsGLHPED	Prevent its nuclear localization
EZH2	Ser-21	CWRKRVKsEYMRLRQ	Suppresses its methyltransferase activity
Mdm2	Ser-166, Ser-186, Ser-188	SsRRRAIsEtEENSd, RQRKRHKsDsIsLsF, RKRHKsDsIsLsFDE	Prevention its degradation
p21	Ser-146, Thr-145	GRkRRQtsMTDFYHs, QGRkRRQtsMTDFYH	Cytoplasmic localization
p27	Ser-10, Thr-157, Thr-198	NVRVNGsPsLErMD, GIRkrPAtdDSSTQN, PGLRRRQt_____	Cytoplasmic localization
WNK1	Thr-60	EYRRRRHtMDKDSRG	Induces mitogenesis by insulin
Cell survival			
ASK1	Ser-83	ATRGRGssVGGGSRR	Inhibits ASK1 activity
BAD	Ser-136	PFRGRsRsAPPNLWA	Inhibits BAD activity
CHK1	Ser-280	AKRPRVtsGGVsEsP	Inhibits its function
Caspase9	Ser-196	KLRRRFssLHFMVEV	Prevents its activation
FoxO1	Thr-24, Ser-256, Ser319	sPrRrAAsMDNNSKF, TFRPRtssNAsTIsG, LPRPRsCtWPLPRPE	Inhibits its activity
FoxO3A	Thr-32, Ser-253	APRRRAVsMDNSNKY, QSRPRsCtWPLORPE	Inhibits its activity
FoxO4	Thr-28, Ser-193, Ser-258	APRRRAAsMDSSSKL, TFRPRsSsNASSVST, QSRPRsCtWPLPRPE	Inhibits its activity

Par-4	Ser-249	SRHNRDTsAPANFAS	Inhibits its function
Nurr-77	Ser-350	GRRGRLPsKPKQPPD	Inhibits its function
Cell growth and protein synthesis			
mTORC1	Ser-2448	RsRtRtDsysAGQsV	Activates its activity
PRAS40	Thr-246	LPRPRLNtsDFQKLK	Inhibits its negative role on mTORC1
TSC2	Ser-939, Ser-981, Thr-1462	sFRARstsLNERPKs, AFRCRSIsVSEHVVR, GLRPRGytIsDSAPs	Inhibits its negative role on mTORC1
Cell Migration and Invasion			
b-Raf	Ser-365, Ser-429,	GQRDRsssAPNVHIN, PQERKsssSsEDRN	Inhibits it signaling
EDG-1	Thr-236	RTRSRLtFRKNISK	Promotes its function
Rac-1	Ser-71	yDRLRPLsYPQTDVF	Promotes its function
Angiogenesis			
eNOS	Ser-615, Ser-1177	SYKIRFNsISCDPL, TsRIRtQsFsLQERQ	Promotes its function

Akt signaling in physiology

Glucose homeostasis

Glucose homeostasis and metabolism is well known function of Akt. Among three isoforms of Akt, Akt2 is the predominant expressed in insulin responsive-tissue thus it has high responsibility to control glucose homeostasis (4). Glucose intolerance, insulin resistance, and severe diabetes are occurred in Akt2 knock out mice but did not observed in Akt1 and Akt3 null mice. At the molecular level, insulin promotes cellular glucose uptake by stimulating the translocation of glucose transporter GLUT4 from cytoplasmic GLUT4 storage vesicle to the cell membrane (4). Akt stimulates GLUT4 translocation through phosphorylates AS160 (Akt substrate 160 kDa) and PIKfyve. The Akt mediated AS160 phosphorylation inhibits activity of AS160-GAP (GTPase-activating protein) domain which resulted in promotes Rab mediated-GLUT4 storage vesicle trafficking to plasma membrane. Phosphorylated-PIKfyve activates moving of GLUT4 protein from endosome to GLUT4 storage vesicles. Moreover, Akt activation leads to promote expression of another isoform of glucose transporter GLUT1 (5). GLUT1 is a glucose transporter

expressed in the most cell and its cellular level is dominantly regulated by its gene transcription. Akt phosphorylates and activates mTORC1 resulted in promotes HIF1-alpha dependent transcription of GLUT1 gene (6). In addition, Akt also regulates glucose and lipid homeostasis at other aspects. For example, Akt mediated-inactivation of GSK3 β increases glycogen storage, cholesterol and fatty acid biosynthesis by which induces its regulated gene transcription (7). Likewise, regulation of Forkhead transcription factor FoxO1 by Akt inhibit hepatic gluconeogenesis and fatty acid oxidation (8). Thus, Akt involves in various aspects of metabolism and homeostasis of glucose and lipid. The alteration of these regulations could promote abnormality of cellular and tissue functions which might be led to several diseases including cancer.

Cell proliferation

Akt regulates cellular proliferation by multiple mechanisms. For example, Akt inhibits cell cycle inhibitors, p21waf1 and p27kip1, by direct phosphorylating these proteins resulted in promotes their cytoplasmic localization (9). For Mdm2-mediated p53 proteasomal degradation, Akt phosphorylates and sustains Mdm2 nuclear localization where it forms a complex with p53 subsequently promotes p53 ubiquitination and proteasomal degradation (10). The decreasing of p53 level is relevant in the cell cycle check points induced by DNA damage. For cell cycle checkpoint, Akt promotes the cellular level of cyclin D1 both by increase the protein stability and promotes it translation (11). Thus, tumor suppressors and cell cycle regulators are controlled by Akt. Interestingly, Akt could promote unlimited cell replication by phosphorylating and maintaining reverse transcriptase subunit telomerase (12). Furthermore, Akt can regulates genes expression through control Enhancer of Zeste homolog2 (EZH2)-mediated DNA methylation (13). Akt phosphorylates EZH2 which suppress its methyltransferase function, therefore resulted in re-activation of gene expression that may influence in various diseases and oncogenesis.

Cell survival

Akt increases survival signals resulted in prevent cell death through a variety of mechanisms. Akt phosphorylates the pro-apoptotic protein BAD subsequently preventing cytochrome C release from the mitochondria (14). The release of mitochondrial cytochrome C triggers caspase activity thereby stimulates the programmed cell death. Akt directly phosphorylates pro-caspase-9 (on Ser-196) and diminishes its activity which protect cell death from apoptosis stimuli (15). Akt prevent caspase-3 activation-mediated apoptosis through increase the stability of a cytosolic caspase-3 inhibitor, PED/PEA15, by phosphorylation processes (16). Likewise, effects of Akt on p21 and p27 that mentions above, Akt phosphorylation promotes

cytoplasmic retention of transcription factors of Forkhead box (FOX) family. In particular, Akt phosphorylates FoxO proteins, FoxO1, FoxO3 and FoxO4, enhances their interaction with 14-3-3 protein subsequently promotes its nuclear exportation (17). After FoxO nuclear exportation, various pro-apoptotic genes such as BIM, Fas ligand, and TRADD are inhibited its transcription (17). On the other hand, Akt promotes nuclear translocation of NF- κ B through phosphorylates and activates IKK kinase (IKK). Once NF- κ B locates in the nucleus (18), it induces transcription of several anti-apoptotic genes including cIAP1, cIAP2, and BFL1 (19). In summary, down-regulation of apoptosis machinery by Akt promotes cell growth and survival in physiological condition but Akt hyper-activation or dysregulation becomes causes of disease progression such as cancer.

Cell Migration and Invasion

Mounting of evidence indicates that Akt can positively regulates cell migration. Akt promotes fibroblast migration by phosphorylating an actin binding protein, Girdin, facilitates stress fiber and lamellipodia formation (20). Akt1 overexpression resulted in increased matrix metalloproteinase-2 (MMP2) expression and invasiveness phenotype of mouse mammary epithelial cells (21). In breast cancer cells only Akt2, not Akt1 or Akt3, has been shown to promote migration and invasion behaviors through upregulates beta-1 integrin (22). Thus, Akt can promotes cell migration and invasion both in normal physiological and diseases.

Cell growth and protein translation

Akt regulates cell growth and protein synthesis through modulation of TSC-2/mTORC1 pathway (23). TSC1 and TSC2 form a heterodimeric complex which acts as a negative regulator of mTORC1 (23). TSC2 contains a GAP (GTPase-activating protein) domain which enhancing the conversion of Rheb into inactive state (GDP-bound). The GTP-bound Rheb (active form) can stimulates the activity of mTORC1. Akt diminishes TSC1-TSC2 complex activity via directly phosphorylates TSC2, thereby activating mTORC1 resulted in response to growth factors-mediated cell growth (23). Moreover, the proline-rich Akt substrate or 40 KDa (PRAS40), another Akt substrate mediated mTORC1 activity, is a negative regulator of mTORC1 via protein-protein interaction (24). Once Akt phosphorylates PRAS40 at Thr-246, phosphorylated PRAS40 favor to bind with 14-3-3 protein resulted in activation of mTORC1 (24). Thus, Akt activates mTORC1 via regulating both TSC2 and PRAS40. The activation of mTORC1 promotes cell growth by regulating cellular nutrients response and cellular protein synthesis. The regulation of cell growth and protein translation are a crucial role in both normal homeostasis and aggressiveness of cancer.

Angiogenesis

Numerous studies show that Akt promote could promote angiogenesis. Akt1 is predominant expressed in vascular endothelial cells and promotes the nitric oxide synthase (eNOS) activity by phosphorylating eNOS at Ser-1117 (25). Nitric oxide (NO) is the product of activated eNOS which promotes vasodilation, vascular remodeling, and angiogenesis (26). In addition, Akt also modulates various aspects of Vascular Endothelial Growth Factor (VEGF)-mediated angiogenesis (27). Akt activates Girdin by direct phosphorylation process which intern promoting VEGF-dependent endothelial cell migration for new vessel formation (28). On the other hands, Akt activates VEGF expression in endothelial cell via HIF1alpha-dependent pathway (29). In summary, angiogenesis is an essential for normal physiological function of all organs and it can be used to promote cancer cell survival and metastasis.

Akt Dysregulation in cancer

Cancer

Cancer has been recognized as the dynamic diseases which can be modulated by intrinsic or environmental factors. The accumulation of mutation in specific genes associates with gain function of proto-oncogenes or loss of tumor suppressor gene activity results in uncontrolled cell division and spread of these uncontrolled cells to other organs (30). These mutation accumulations are subsequently to unique characteristics of cancer, called cancer hallmarks (31). The cancer cells cause normal organs function failure by their hallmarks are the major cause of cancer related death.

Upregulation of Akt activity in cancer

Aberrant Akt activation have been found in various type of human cancers. Most type of cancers, Akt over-activation has been shown the correlation with poor prognosis and advance stage of the disease (32). Genes mutation or genes alteration responsible for dysregulating Akt activation in human cancer are described below.

Receptor Tyrosine Kinase signaling Gene alteration

Accumulation of genetic mutations in cancer exhibit their oncogenic role at least in part via promoting PI3K/Akt signaling cascade. Activating mutation in Receptor tyrosine kinase (RTK) such as Epidermal Growth Factor Receptor (EGFR), Platelet Derived Growth Factor receptor (PDGFR), c-KIT, and ABL kinase result in upregulated Akt activation (33). Cancer frequently addicts to overexpression of PI3K/Akt which can be used as cancer therapeutic target. Anticancer drugs

targeting these receptors diminish both RTK and its downstream PI3K/Akt to achieve the therapeutic goals. The refractory of Akt signaling can promote resistance to certain therapeutics.

Inactivating mutation of Phosphatase and tensin homolog

Deletion and inactivating mutation of Phosphatase and tensin homolog (PTEN) are observed in a variety of human cancer. Both dysregulations in transcriptional and post-translational processes cause the loss of PTEN protein function. PTEN germline mutations are underlie pathogenesis which increasing risk for breast and thyroid cancer. PTEN somatic mutations have been commonly observed in advanced prostate cancer, endometrial cancer, and glioblastoma (34). Loss of PTEN function results in upregulation of Akt activation.

Activating mutation of PI3K

PIK3CA gene which encodes the catalytic p110 α subunit of PI3K have been frequency mutated in cancers. This mutation leading to gain of PI3K function almost 30% of breast, endometrial and colorectal cancer and with lower frequency in other cancer types (35). More than 80% of cancer cases involved in *PIK3CA* activating mutation either the kinase domain (exon 20; such as H1047R) or the helical domain (exon 9 such as E542K and E545K) of p110 α subunit (35). The mutation of negative regulator subunit of PI3K, p85, have been documented in cancers. Mutation of p85 results in release p110 from p85-p110 complex (36), thereby promoting AKT with bypassing RTK and PI3K activation.

Activating mutation of Akt

Activating *AKT1* gene mutation has been discovered in cancers. In particular, an activating mutation in PH domain by E17K of Akt1 has been identified in colorectal, breast, ovarian, and endometrial cancer (37, 38). The E17K mutation promotes PI3K-independent membrane translocation and activation of Akt (38).

Akt promoting and maintaining cancer hallmarks

Since the Akt phosphorylates and regulates the function of various cellular proteins involved in many processes including metabolism, proliferation, differentiation, survival/apoptosis, migration, and angiogenesis. The activating mutation of Akt that occurred in cancers have crucial roles in regulating cancer cells behaviors called “cancer hallmarks”.

In January 2000, Douglas Hanahan and Robert Weinberg proposed the concept of cancer hallmarks which provided the general cancer virulent characteristics (31). The role of Akt in regulating cancer hallmarks are described below.

Self-sufficiency in growth signals

Tumor cells contains cell growth self-activation without growth-stimulating signal of the other cells, thereby reducing their dependence on growth stimulating signal from the body system. Since Akt is a central regulation of cell growth by act as a downstream signaling of growth factors then promoting protein synthesis at least in part of mTORC1 (23). The activating mutation of Akt can promotes cancer growth by stimulating mTORC1 activity event absence of growth factors (23).

Insensitivity to growth-inhibitory signals

Anti-growth signals are importance for normal physiological regulation and homeostasis through inhibiting protein synthesis and cell growth. Cancer cells can omit the anti-growth signal results in its unlimited growth capacity. Since Akt controls cellular protein synthesis and cell growth through various pathway, activating mutation of Akt in cancer can against the anti-growth signal. In particular, Akt inhibits negative regulatory effect of TSC2 on mTORC1-dependent cell growth by phosphorylating TSC2. Phosphorylated TSC2 cannot bind and inhibit the function of mTORC1 results in cell growth (39). Moreover, Akt phosphorylates p21 and p27 which promotes their cytoplasmic retention. The cytoplasmic localization of p21 and p27 prevent their transcriptional function, thereby promoting cell cycle progression (9).

Evasion of programmed cell death

Cancer cells can resist apoptosis by various strategies which primarily involving in loss of expression or function of pro-apoptosis regulators. Most of apoptosis regulatory proteins such as FoxO family, BCL₂-family, and caspases are controlled its function and stability by phosphorylation process (17). Akt phosphorylation on these proteins favors to inhibit pro-apoptotic protein and activate pro-survival protein function, thereby over activated Akt in cancer cell can promotes cell survival event in stress- or cytotoxic drugs-induced cell death condition (17).

Limitless replicative potential

Cancer cells have unlimited replicative capacity by promoting the expression of telomerase enzyme which adds hexanucleotide repeated motif onto the end of the telomeric DNA (12). Over-activating Akt in cancer cell promotes the telomerase function which intern un-limit cell replication.

Sustained angiogenesis

The initially tumor lacks the ability to promote blood vessel growth, this ability must be developed once tumor need to be a bigger size. This process involves in the alteration of angiogenesis regulatory signals including angiogenic activators/inhibitors and their receptors. Cancer cell with upregulating of Akt1 can promotes angiogenesis through promoting eNOS activity and VEGF expression (25, 27).

Tissue invasion and metastasis

Tissue invasion and metastasis behavior of cancer cells require the expressing alteration of cell-cell adhesion molecules (CAM), integrins pattern, and extracellular matrix proteases especially MMP-2. Akt modulates these alterations through both transcriptional and post-translational levels resulting in promotes migration and invasion of certain cancer cells (21, 22).

Lung and colorectal cancers

Cancer statistic

Nowadays, cancer is the globally second leading cause of death. The estimated new cases and estimated cancer related deaths in 2018 are 18.1 million and 9.6 million cases, respectively (40). Worldwide, 20% men and 16% women develop cancer in their lifetime and death rate are 12.5% and 9% in men and women, respectively (40). The top three of high incidence cancer which responsible for 30% of disease incidence and mortality are lung cancer, breast cancer in female and colorectal cancer (40). In terms of mortality rate, lung and colorectal cancer are the first (1.8 million death cases, 18.4% of total cases) and second (881,000 death cases, 9.2% of total) most common cause of estimated cancer death in 2018, respectively (40). Interestingly, the primarily causes of cancer-related death are depend on their chemoresistance and recurrence capabilities.

Lung cancer

Epidemiology

Lung cancer (LC) rises from normal epithelial cells of the airway and alveolar which continuously genetic damage leading to uncontrolled proliferation and abnormal cells growth in the lung (41). Lung cancer can be divided into two major types, non-small cell lung cancer (NSCLC; 85% of all lung cancer cases) and small cell lung cancer (SCLC; about 15%). Moreover, histological classification divides LC into three major subtypes including squamous cell

carcinoma, adenocarcinoma and large-cell carcinoma (41). At the present day, surgery, radiation, chemotherapy and targeted therapy are used in lung cancer treatment. However, the prognosis for patients with LC remains poor, with overall 5-year survival only 15-18% after treatment (42). Moreover, cancer relapse and metastasis are important factors influencing the death of LC patients by lowering the overall 5-year survival to 4-5% (42).

Akt-related molecular pathophysiology of lung cancer

The lung is a complex organ composed of different cell types with discrete functions for supporting gas exchanged of the body. These cells can undergo an accumulation of genetic mutation which trigger by both genetics and environmental factors. Genetics and epigenetics changed subsequently alter the function of onco-genes and tumor suppressor genes (41). The formation of neoplastic lesions in lung by losing their control in genetics and epigenetics are principally of LC initiation. The genes alteration promoting LC are summarized in Table 2.

Table 2. Akt-related genetic and epigenetic alteration in lung cancer

Gene / Biomarker	Chromosome	Function	Molecular alteration	Frequency (%)
Proto-oncogenes				
<i>AKT1</i>	14	Regulates proliferation and differentiation	Mutation	1
<i>PIK3CA</i>	3	Regulates PI3K-AKT pathway	Activating-mutation Amplification	1-3
<i>EGFR</i>	7	Involved in AKT, MAPK, and JNK pathway	Activating-mutation	10-35
<i>FGFR1</i>	8	Regulates proliferation via Akt pathway	Amplification	20
<i>KRAS</i>	12	Involved in PI3K-Akt pathway	Mutation	15-25
<i>TTF-1</i>	14	Regulates genes transcription involving in EGFR expression	Amplification	15
<i>ALK</i>	2	Regulates proliferation and phosphorylation of	Rearrangement	3-7

		Akt		
<i>DDR2</i>	1	Regulates proliferation, differentiation and apoptosis	Mutation	4
<i>HER2</i>	17	Regulates Akt, MAPK pathway	Mutation	2-4
<i>MET</i>	7	Regulates angiogenesis	Amplification	2-4
<i>BRAF</i>	17	Involved in Akt MAPK pathway	Mutation	1-3
<i>MEK1</i>	15	Regulates Akt, MAPK pathway	Mutation	1
<i>NRAS</i>	1	Co-activation with Akt signaling	Mutation	1
<i>ROS1</i>	6	Regulates proliferation and differentiation via PI3K/AKT/mTOR, p-STAT3, and SHP-2 phosphatase pathway	Rearrangement	1
<i>MYC</i>	8	Downstream target of Akt involving in proliferation and differentiation	Translocation	9
<i>NTRK1</i>	1	Regulates Erk/Akt pathways	Translocation	3
<i>NRG1</i>	8	Involved in PI3k/Akt and MAPK pathway	Translocation	1
Tumor suppressor genes				
<i>TP53</i>	17	Regulates the expression of target genes involved in cell cycle progression, DNA repair and apoptosis	Mutation	60-70
<i>PTEN</i>	10	Regulates PI3K-AKT pathway	Mutation	4-8
<i>LKB1</i>	19	Regulates cell polarity	Mutation	34

		and apoptosis via Akt activity		
--	--	--------------------------------	--	--

AKT1, protein kinase B; ALK, anaplastic lymphoma kinase ; DDR2, discoidin domain-containing receptor 2 ; EGFR, epidermal growth factor receptor; FGFR1, fibroblast growth factor receptor 1; GDNF, glial cell-derived neurotrophic factor; HER2, human epidermal growth factor receptor 2; LKB1, liver kinase B1; MET, tyrosine-protein kinase MET; MAPK, mitogen-activated protein kinase; MEK1, mitogen-activated protein kinase kinase 1; MYC; NTRK1, neurotrophic tyrosine kinase receptor type 1; NRG1, Neuregulin 1 ; PIK3CA, phosphatidylinositol-4,5-bisphosphate 3-kinase catalytic subunit-alpha; PTEN, phosphatase and tensin homologue; ROS1, Proto-oncogene tyrosine-protein kinase ROS; TP53, tumor protein p53 ; TTF-1, thyroid transcription factor 1

Lung cancer recurrence is major cause of death

Cancer recurrence is the occurrence of cancer after treatment or after a detection-free period. There are various types of cancer recurrence: Local recurrence is the cancer that found again in the same place it first detected, Regional recurrence is the cancer that come back in the lymph nodes near the place it first detected, Distant recurrence is that cancer has come back in other organs of the body (43). Lung cancer is one of cancer that exhibit high capacity to recurrence which is the major cause of lung cancer-related death (40).

Cancer stem cells are the seed of cancer recurrence

Cancer stem cells

It is now well accepted that cancer is containing of cell heterogeneity as resulted from their distinct cellular signaling. Among the different lineage of cancer cells residing in the tumor, there is a specific small population of cancer cells that has stem cell characteristics including the self-renewal capacity and multi-lineage differentiation (44, 45). The cancer cells containing the stem cell capacities exhibit highly aggressive phenotypes such as tumorigenic potency, migration and invasion, recurrence and metastasis, and chemotherapeutic resistance (44). These specific subpopulation of cancer cells were first named “cancer initiating cells”, as they were believed to be the beginning seed of the whole cancer and have now become the main focus of cancer cell biology as well as anti-cancer drug discovery research. CSCs were first identified in acute myeloid leukemia (AML) by their cell surface marker CD34+Cd38- (46). These cells were shown to have a high capacity to self-renew in bone marrow and differentiate to leukemic cells when transplanted into severe combined immunodeficient (SCID) mice (47). After these observations were made, CSCs of various cancer types including lung cancer were discovered through specific cell-surface proteins by numerous research groups (48).

The key CSC properties compose of:

- Self-renewal capacity; a unique ability of the CSC (just like normal stem cells) to generate the identical daughter cells with identical stem cell characteristics.
- Ability to drive tumor heterogeneity and survival of tumor; an ability to differentiate into different cancer cell lineages, facilitate cell growth, and survival of whole tumor.
- High tumorigenic potential; an ability of CSC to proliferate and create non-CSC lineages and form new tumors.

Akt-related proteins in the regulation of cancer stem cells

Octamer-binding transcription factor4 (Oct-4)

Oct-4 is a POU domain-containing transcription factor that binds to the octamer sequence, ATGCAAAT, of the target genes. Oct-4 is encoded by POU5F1 gene located at chromosome 6p21.31. The human Oct-4 gene consists of five exons which can be spliced into three main isoforms OCT4A, OCT4B and OCT4B1. These gene isoforms provide four isoform proteins Oct4A, Oct4B-190, Oct4B-265, and Oct4B-164. All forms of Oct-4 are functionally and structurally divided into three domains including an N-terminal transcriptional activation domain, a central POU domain, and a C-terminus containing a cell type-specific transactivation domain. Oct4A, is generally referred as Oct-4, and regulates the stemness of embryonic stem cells. Oct-4 is highly expressed in embryonic stem (ES) cells and low expressed when ES cell differentiates and there is consequently loss of pluripotency. Oct-4 and its activities were shown to be required for maintaining the ES cell capacity (49). Several target genes of Oct-4 in ES cells have been identified, including Fgf4, Utf1, Opn, Rex1/Zfp42, and Fbx15 (49). Additionally, high levels of Oct-4 have been identified in highly aggressive tumors, poor prognosis patients, and relapse cancer. It has been documented that overexpression of Oct-4 is associated with tumorigenicity, metastasis, and cancer relapse in certain cancers (50). Oct-4 level and activity are known to be regulated by several steps, such as transcription, translation, and post-translational modifications.

Akt is one of the key regulators controlling Oct-4 expression and function through phosphorylation-mediated protein post-translational modification. Ubiquitination is the main pathway responsible for eliminating short-lived proteins. Oct-4 can be ubiquitinated by an HECT type E3 ubiquitin ligase, Wwp2. Wwp2 regulates Oct-4 level by mediating its ubiquitination and degradation during ESC differentiation. Oct-4 can be phosphorylated by Akt at Ser229, Ser236 and Tyr327. Phosphorylation at these residues by Akt regulates Oct-4 stability and transcriptional

activity (51). In contrast, the small ubiquitin related modifier (SUMO) have a functionally divergent from ubiquitin. SUMO can modify many nuclear proteins to increase their protein stability and promote their nuclear localization, thereby enhancing genes expression (52). Studies show that Oct-4 can be sumoylated at a lysine 118, which is promoted by Akt activity. Sumoylation of Oct-4 significantly increases its stability, DNA binding, and thus the transcriptional activity (53).

Cluster of differentiation-133 (CD133, prominin-1, PROM-1)

CD133 is an 865 amino acids penta-span transmembrane protein which is encoded on chromosome 4 (4p15.32). CD133 have been accepted as a principle marker of stemness in several solid tumors (54). In general, CD133 is an important marker used for the isolation and identification of the stem cells from normal tissue like human hematopoietic stem cells (54). The function of CD133 in the cells is not fully known yet but several studies have shown that CD133 expression is linked with stem and progenitor cell characteristics as well as the stage of cell regeneration and differentiation (48). Later on, evidence has shown that CD133 is not only a biomarker and is functioning in normal stem cells, but also in cancer cells. Expression of CD133 has been used for the identification of CSC in several cancers including lung, pancreatic adenocarcinoma, hepatocellular carcinoma, prostate, neural, colorectal, and renal cancers(54).

In addition, evidence has shown that the expression of CD133 is associated with tumor aggressiveness through upregulation at least in part of Akt (55). CD133 promotes the CSC phenotype by stabilizing the EGFR-Akt signaling. The interaction of CD133 with p85 promotes the activation of Akt resulting promotes tumorigenesis capacity of CSC.

Caveolin-1

Caveolins (Cav) is a family of integral membrane proteins which are the primarily components of caveolae, cave-like invagination of the cell membrane. Caveolin involves in various cell signaling cascade. Caveolin protein are interaction with various classes of signaling molecules including, non-receptor and receptor tyrosine kinase, G-protein subunit, endothelial nitric oxide synthase, and small GTPase, through caveolin-scaffolding motif. These interactions of protein are involved in various cellular signaling pathway including endocytosis, lipid homeostasis and signaling transduction. The caveolin gene family, located at chromosome 7q31.1, are consisted with 3 member, *CAV1*, *CAV2*, and *CAV3* which coding for protein caveolin-1, caveolin-2 and caveolin-3, respectively. The predicted domains span almost the same number of residues in

all three protein isoforms: the amino-terminal domain comprises the first 101 residues in Cav-1 α and the first 70-86 residues in Cav-1 β , Cav-2, and Cav-3, with the putative transmembrane domain occupying 33 amino acids and the carboxy-terminal domain containing 43-44 amino acids (56).

Caveolin-1 function

Caveolin-1 (Cav-1), a 21 kDa protein, localizes to the cellular membrane, the membrane of Golgi apparatus and the membrane of the trans-Golgi-derived transport vesicles. Cav-1 have a specific tightly interaction with cholesterol in caveolae. This interaction between Cav-1 and cholesterol control intracellular cholesterol balance through regulating cellular cholesterol uptake. Moreover, caveolae containing Cav-1 serve as signaling platforms which promoting the compartmentalizing and concentrating of signaling molecules. The high variety of signaling molecule families, including G-protein subunits, receptor and non-receptor tyrosine kinases, endothelial nitric oxide synthase (eNOS), and small GTPases, can be modulated their signaling cascade through binding with Cav-1. Cav-1 favors to inhibit the activation of various bound proteins, including c-Src, H-Ras, mitogen-activated protein (MAP) kinases, and eNOS (57).

Caveolin-1 and cancer

Cav-1 has implicated roles in the carcinogenesis and aggressiveness of cancer. Cav-1 has paradoxically effects on cancer by containing both tumor suppressive and onco-protein function. Highly expression of Cav-1 in certain cancer promotes the cancerous aggressiveness such as migration, invasion, and chemoresistance (58). In contrast, the overexpression of Cav-1 in other cancer seem to be suppressing cancer virulently including migration and chemoresistance (59). Thus, the enhancing or suppressing roles of Cav-1 on the aggressiveness of cancer is a tissue-specific function. Moreover, the evidences show that Cav-1 act as a tumor suppressor in initial step of oncogenesis but might be as a oncoprotein for latter stage of tumor development due to it promotes cell survival, metastasis and chemoresistance (60).

Akt can be induced by the highly expression of Cav-1. Cav-1 exhibit direct interaction with serine/threonine phosphatase PP1 and PP2A which suppressing negative role of PP1 and PP2A on Akt activation (61). Cav-1 can be induced by mechanobiological of low shear stress subsequently promotes breast cancer motility through activation of PI3K/Akt/mTOR pathway (62). Cav-1 promotes lamellipodia formation in lung cancer via activating Akt pathway (63). Modulation

of Caveolin-1 Expression alter cellular response to Insulin-like Growth factor1 (IGF1) through the Phosphatidylinositol 3-Kinase/Akt Pathway (64). Thus Cav-1 modulates Akt signaling both direct and indirect pathway. However, regulation role of Akt on Cav-1 function is still unknown.

Nitric oxide promotes cancer stem cell

Biological function of nitric oxide

Nitric oxide (NO) is a water-soluble gas, which plays key role in various physiological as well as pathological processes (65). Role of nitric oxide (NO) has been first discovered as the mediator which regulate blood pressure and prevent cardiovascular diseases. After that, NO have also been documented its role involving in immune system, nervous system, inflammation process, tumorigenesis and cancer progression. The biological action of NO is primarily through cGMP (66) signaling pathway and S-nitrosylation reaction (67). cGMP is a second messenger cyclic nucleotide which responsible for several cellular processes. NO stimulates cGMP by activating guanylyl cyclase (sGC) which subsequently to converse guanosine 5'-triphosphate (GTP) to cyclic guanosine 3',5'-monophosphate (cGMP). In addition of downstream target, cGMP activates cGMP-dependent protein kinase (PKG) which trigger the activated form of AKT (phosphorylated AKT) which plays a role in activation of several cellular function (66). S-nitrosylation is a process to produce covalent bond between nitrogen monoxide and thiol group of cysteine residue in targeted protein. These processes occur in protein post-translational modification. After the S-nitrosylation, the conformation and properties of proteins are changed which alter their biological functions (67).

Nitric oxide and cancer

Under normal physiological conditions, NO serves as a key signaling molecule for various physiology functions such as smooth muscle relaxation, blood flow regulation, iron homeostasis, and platelet reactivity (65). On the other hand, excessive and uncontrolled NO production, or elevation of NO levels have been contributing to pathological events such as infection, chronic inflammation and cancer (65). Clinical data has been shown that, an increasing of NO is frequently detected in cancer patients and the higher level of NO is correlated with the advancing stage and poor prognosis (68). There are strong evidences reported that, the increasing of NO which always found in cancer environment is concerned with up-regulation of inducible nitric oxide synthase (iNOS) (65). In addition, iNOS is widely presence in cancer cells and distinct neighboring cells such as tumor-associated endothelium, and cancer-associated fibroblast (68).

According to clinical finding, *in vivo* study has demonstrated that, NO plays a role in tumor metastasis by promotion of migration, matrix degradation and angiogenesis (68).

Nitric oxide and cancer stem cell

Interestingly, the aggressive CSC-like behaviors of the cancer cells as mentioned were shown to be augmented in the lung cancer cell receiving nitric oxide (NO) (69). NO treatment was shown to increased cell motility, invasion, and mediated anoikis resistance phenotypes in human lung cancer cells (70). As the NO is a gaseous endogenous substance found in physiologic tissue and its level was shown to be elevated in cancer environments (68), NO may have a significant impact on CSC-like phenotypes.

Dedifferentiation and cancer stem cell

There are well accepted that cells in tumor population exhibited multiple levels of genetics heterogeneity which resulted from their genome instability (71). There are not only genetics heterogeneity, but also phenotypic heterogeneity was detected in several cancers (72). Phenotypic heterogeneity is the diverse functions of cells which can be observed through different lineage markers expression. Observational by stem cell markers, there are distinct sub-line of cancer stem cells with in the same tumor indicating that cancer genome instability not only generate genetics heterogeneity but also might provide multi-lineage of cancer with distinct differentiation state of the cell (73). The CSC with genetics instability might be cause of the heterogeneous lineage of cancer cells. Although CSCs do not necessarily genetics transformation from normal stem cells. The recent studies suggested that not only CSCs but also certain populations of cancer cells within tumors have stem cell properties (stemness) (74). Moreover, fully differentiated cancer cells can be transformed to be cancer stem-like cells (CSC-like cells) by the activity of certain cancer microenvironment substances such as nitric oxide, hypoxia condition, and interleukin or by the mutation of certain genes (74). These indicated that “stemness” is a phenotype which can be acquired via proper extracellular stimulation signals or accumulation of specific gene mutations within the cells. Nevertheless, both CSC and CSC-like cells show the same characteristics as normal stem cells. Mounting of evidences suggested that non-CSC can generated from dedifferentiation process which acquired CSC-like phenotypes by certain stimulating condition (ref). The non-CSC dedifferentiation can be triggered by both intracellular signals and microenvironmental stimulation.

For intracellular factors, gene mutation or epigenetics changed can be determined as a CSC stimulant. In glioblastoma (GBM), loss of p16INK4a and p19ARF enables drive dedifferentiation of mature astrocyte when activation of EGFR (75). Moreover, observation of TUJ1-positive neurons in GBM which originating from fully differentiated cell, astrocytes, indicating that GBM can originate from variety of brain cells through dedifferentiation process (76)). In addition, synapsin L-Cre neurons and glial cells induced the formation of GBM through promoted expression of nestin and Sox2 (77). The dedifferentiation of non-CSCs to be CSCs was also found in tumors of intestine by activation of NF- κ B/Wnt signalling pathway (78). Moreover, combination of Kras overactivation and NF- κ B induction promotes the stabilization of β -catenin which leading to conversion non-stem cell to be tumor-initiating cells (79). For breast cancer, the conversion from non-CSC to CSC required the activity of Zeb1, a transcription for EMT regulation (80). Zeb1 is not only converse non-CSC to CSC but also maintenance CSC-like characteristics of the cells (81). These data supporting that bidirectional interconvertibility of non-CSC to CSC model instead of unidirectional of stem cell hierarchy model (82).

For microenvironmental factors, tumor microenvironment provides various stimuli such as TGF- β , TNF-alpha, nitric oxide (NO), and hypoxia condition enhanced the dedifferentiation process from non-CSC to CSC by different pathway (83). Moreover, surrounding cells of the tumor can promote the transformation of non-CSC to CSC by secreted certain substance enhancing dedifferentiation process (83). Myofibroblast is colorectal stromal cell enhancing dedifferentiation of non-CSC by secreting hepatocyte growth factor (HGF) (84). HGF promotes stem cell phenotypes of differentiated cancer cells by promoting β -catenin nuclear localization which facilitate induction of Wnt pathway (85).

Colorectal cancer

Epidemiology

Colorectal cancer (CRC) is the expanding of tumor from the colon and rectum. Most case of CRCs are due to age and environment factors; a small number of patients are due to underlying genetic inheritance (86). CRC is the third most common type of cancer which more prevalence in developed countries and also common in men. CRC treatments are surgery, chemotherapy, radiotherapy and targeted therapy. However, the successful of therapy in terms of overall 5-year survival is only 58-65% after treatment (40). Moreover, chemoresistance with

cancer relapse and metastasis are major influencing factors of CRC patient's death by lowering the overall 5-year survival to 10-14% (40).

Akt-related molecular pathophysiology of colorectal cancer

The environmental and genetic factors caused CRC by promoting the acquisition of cancer hallmarks in colorectal epithelial cells through enhance the accumulation of genetic mutation and epigenetic alteration (86). The changed in genetics and epigenetics activate oncogenes and inactivate tumor suppressor genes. The formation of neoplastic lesions in colon by losing genetics and epigenetics stability is thought to be the initiation of CRC. The hierarchy cancer stem cell model believes that the origin of CRC is a stem cell or progenitor cell that resides in colon crypts (87). The genetics alteration in the stem cell lead to the formation of cancer stem cells (CSCs) which promote tumorigenesis and maintain cancer aggressiveness. Generally, the transformation of normal colon epithelial cells to colorectal cancer cell by accumulation of genetics and epigenetics alteration takes 10-15 years (87). The genes alteration promoting colorectal cancer are summarized in Table 3.

Table 3. Akt-related genetic and epigenetic alteration in colorectal cancer

Gene / Biomarker	Chromosome	Function	Molecular alteration	Frequency (%)
Proto-oncogenes				
<i>PIK3CA</i>	3	Regulates PI3K-AKT pathway	Mutation	20
<i>KRAS</i>	12	Involved in Akt, MAPK pathway	Activating mutation	40
<i>ERBB2</i>	17	Involved in EGF-Akt-MAPK pathway	Amplification	35
<i>BRAF</i>	7	Involved in the Akt, MAPK pathway	Activating mutation	8-28
<i>GNAS</i>	20	Regulates G protein signaling Involved in PI3K, MAPK	Mutation	20
<i>IGF2</i>	11	Co-ordinate with Akt signaling and promotes IGF pathway	Copy number gain and loss	7 (mutation) 10 (methylation)
<i>RSPO2 and RSPO3</i>	8 6	Involved in WNT/Akt/Beta-catenin pathway	Gene fusion and translocation	10
<i>SOX9</i>	17	Mediated-Akt regulates survival and differentiation	Copy number gain	9 (mutation) <5 (CNV gain)
<i>TCF7L2</i>	10	Regulates WNT/Akt/beta-	Gene fusion and	10

		catenin pathway	translocation	
<i>MYC</i>	8	Downstream signaling of Akt and MAPK	Amplification	2 (mutation) 10 (CNV gain)
<i>NRAS</i>	1	Co-activation with Akt regulates proliferation, survival, and carcinogenesis	Mutation	2
Tumor suppressor				
<i>PTEN</i>	10	Regulates PI3K-AKT pathway	Inactivating mutation and loss of protein	10 (mutation) 30 (loss of expression)
<i>APC</i>	5	Regulates the WNT-Akt pathways	Inactivating mutation	40-70
<i>TP53</i>	17	Regulates the expression of target genes involved in cell cycle progression, DNA repair and apoptosis	Inactivating mutation	50
<i>SMAD4</i>	18	Suppressing Akt signaling	Inactivating mutation and deletion	25
<i>FBXW7</i>	4	Regulates proteasome-mediated protein degradation, repressing Akt-activated mTORC1	Inactivating mutation	20
<i>ABID1A</i>	1	Regulates chromatin structure and gene transcription	Inactivating mutation	15
<i>FAM123B</i>	X	Involved in PI3K/Akt/WNT pathway	Inactivating mutation	10
<i>RET</i>	10	Suppress Akt-induced oncogenesis	Inactivating mutation and aberrant DNA methylation	7 (mutation) 60 (methylation)
<i>DCC</i>	18	Involved in Akt-regulated apoptosis	Deletion or LOH	9 (deletion) 70 (LOH)
<i>CTNNB1</i>	3	Regulates PI3K/Akt/WNT pathway	Activating mutation	1

APC, adenomatous polyposis coli; ARID1A, AT-rich interactive domain 1A; BMP, bone morphogenetic protein; CNV, copy number variation; CTNNB1, catenin- β 1; DCC, DCC nerin 1 receptor; EGF, epidermal growth factor; FAM123B, family with sequence similarity 123B; FBXW7, F-box and WD repeat domain-containing 7, E3 ubiquitin protein ligase; GDNF, glial cell-derived neurotrophic factor; GNAS, guanine nucleotide-binding protein, alpha-stimulating complex locus; IGF, insulin-like growth factor; LGR, leucine-rich repeat-containing G

protein-coupled receptor; LOH, loss of heterozygosity; MAPK, mitogen-activated protein kinase; N/A, not applicable; NDRG4, NDRG family member 4; PI3K, phosphatidylinositol 3-kinase; PIK3CA, phosphatidylinositol-4,5-bisphosphate 3-kinase catalytic subunit- α ; PTEN, phosphatase and tensin homologue; RSPO, R-spondin; SEPT9, septin 9; SMAD4, SMAD family member 4; SOX9, SRY (sex-determining region Y) box 9; TCF7L2, transcription factor 7-like 2; TGF β , transforming growth factor- β ; TGFBR2, TGF β receptor 2; VIM, vimentin.

Chemoresistance in colorectal cancer

Resistance to chemotherapy initiate disease relapse and metastasis which impact clinical outcomes by decreasing overall survival (88). Chemoresistance in colorectal cancer is one of the major cause of cancer relapse and death (88). For these reasons, there are very essential for understanding the mechanisms controlling cancer chemoresistance and searching novel therapeutic targets to improve the therapy. The molecular mechanisms of chemoresistance usually involve with transporter, onco-proteins, tumor suppressor proteins, alteration of mitochondrial proteins, DNA repair system, and cancer stem cells (89). The major molecule involve in these mechanisms regulated chemoresistance is participate in PI3K/Akt pathway (90).

Akt-related proteins in the regulation of chemoresistance

PI3K/Akt

Akt is also known as protein kinase B (PKB), a serine/threonine protein kinase, that involves in many cellular processes such as growth and proliferation, differentiation, self-renewal, apoptosis, transcription and translation control, cellular movement. Akt could promote chemo- and radio-resistance of cancer cell by alteration of pro-survival/pro-death protein ratio (90). Akt could promote the pro-survival proteins function including Bcl_{x_l} (91), and mcl-1 (92). Akt mediated overexpression of pro-survival proteins can alter the activation of p53-inducing death after receiving cytotoxic drugs (93). Overexpression of Akt by amplification of Akt gene, increase its upstream activators, or down regulation of its negative regulatory proteins resulted in chemoresistance in many cancer types (93). In addition, miRNA-130b diminished the expression of PTEN protein which confer chemoresistance via PI3K/Akt activation (94). Suppression of PI3K/Akt pathway by activation of endoplasmic reticulum stress or dephosphorylation of Akt by USP49 enhancing cellular response to cytotoxic drugs (95). Thus, Akt promotes cancer chemoresistance mostly on inhibiting pro-apoptotic function of various proteins. However, role of Akt on certain tumor suppressor for increasing cancer chemoresistance capacity is under elucidated.

p21

The p21 protein (also known as WAF1 or CIP1) have primarily function to inhibit cell cycle via inhibit cyclin-dependent kinase (CDK) and proliferating cell nuclear antigen (PCNA) functions (96). Thus, p21 are tumor suppressor protein by which its capacity to inhibit cancer cell proliferation and promote cancer apoptosis after received chemotherapeutic drugs (96).

The evidences have revealed that p21 may also containing an oncogenic role. Regrading to high expression of p21 level in various cancer have a correlation with tumor progression (97). There are suggested that bidirectional role of p21 may depend on its sub-cellular localization. P21 nuclear localization confers its tumor suppressive function, while more oncogenic capacity is associated with cytoplasmic localization of p21 (98). As an example, cytoplasmic p21 has been shown to mediate cisplatin and paclitaxel resistance in various cancers (99, 100). P21 sub-cellular localization might diverge its response to various stimuli, promote apoptosis or rather stimulates pro-survival signal, which could contribute to cancer prognosis and chemotherapeutic resistance. However, it has no clear the mechanisms of cytoplasmic-p21 promotes chemoresistance.

Chk2

Checkpoint kinase2 (Chk2), 65 kDa protein consist of 543 amino acid residues, is a conserved protein in mouse, rat *Drosophila* spp., *Caenorhabditis elegans*, zebrafish, and human (101). Chk2 have three different functional domains. The N-terminus domain with serine-glutamine (SQ) and threonine-glutamine (TQ) repeated rich region called SQ/TQ cluster domain (SCD) which are phosphorylation site by PI3K protein family such as ATM and ATR. The forkhead-associated (FHA) domain between residues 112 and 175 is responsible for the interaction with phosphorylated proteins. The C-terminus kinase domain spans residues from 220 to 486 (101).

During normal physiological condition, Chk2 is located in the nucleus in an inactive form. After DNA damage, activated ATM (sensor of DNA break) phosphorylates Chk2 at Threonine-68 on SCD domain. This T68 phosphorylation resulting in a conformational change induces Chk2 homo-dimerization of phosphorylated SCD of one Chk2 monomer with the FHA domain of another molecule. The dimerization promotes kinase domain activation through autophosphorylation at residues S260 and T432 followed by residues T383, T387, and S516 which triggering the dissociation or the homo-dimer into activated-monomers. After phosphorylation, phosphorylated Chk2 can acts as tumor suppressive protein by inducing apoptosis. The phosphorylation of PML,

E2F1, and p53 by p-Chk2 resulted in triggering apoptosis (102). Thus, Chk2 acts as a tumor suppressor protein.

Several evidences suggested that the over-activation or over-expression of Akt promotes chemoresistance in various cancer types. Activated-Akt inhibits p-Chk2-mediated apoptosis during DNA damage through direct or indirect inhibiting p-Chk2 signaling (103, 104). However, the precise mechanisms Akt-inhibit Chk2-mediated apoptotic is under elucidated.

Cancer therapeutics targeting AKT

There is clear that PI3K-AKT signaling involves in different human diseases including cancer. Since, more than 50% of human cancer exhibits hyperactivation of AKT, therapeutics targeting AKT for treating cancer have been exclusively developed in the past decade (105). Numerous small molecules with high specificity and potency to inhibit PI3K and AKT pathway have enrolled clinical trials (105).

Two PI3K inhibitors, LY294002 and wortmannin, have been used *in vitro* for decoding various of the mechanism which initiate by PI3K activity, including AKT activation (106). However, subsequent studies showed that both compounds inhibited all isoform of PI3K. Since more specific and potent PI3K and Akt inhibitors have been developed, LY294002 and wortmannin have no longer recommended to use for specific conclusion regarding the function of PI3K or AKT. The new classes of PI3K inhibitors have been observed their efficacy and therapeutic outcomes in patients, but their clinical use can be limited by severe toxicity (106). Moreover, small molecule AKT inhibitors have been developed and tested in clinical trials.

Although, various ATP-competitive AKT inhibitors have been developed, the specificity of these compounds is still lacking due to the high similarity of ATP-binding motif of AGC kinase family. GSK690693 can inhibits all AKT isoforms and exhibit clinical implication in preclinical studies, but toxicity due to its unspecific inhibition activity lead to termination of the clinical development of this drug (107). AZD5363 is a pan-AKT inhibitor used in nanomolar range, show efficacy in studies of solid tumors (108). GDC0068 (Ipatasertib), orally high potent AKT inhibitor, has showed efficacy in preclinical models with PTEN inactivation or PI3KCA mutation, but not showed significant effects against cancer in a phase I clinical trial (109). GSK2110183 (Aføresertib), nanomolar AKT inhibitor, with more specificity to AKT1 showed significant activity in preclinical models and well-tolerated in phase II trial (110).

Catalytic AKT inhibitors block the phosphorylation of its downstream substrates which out dephosphorylation of T308 and S463 of AKT. However, catalytic inhibitors have less efficacy in triggering cell death than allosteric inhibitors. Unlike catalytic inhibitors, allosteric inhibitors can prevent AKT phosphorylation and its downstream activation. MK2206 is a specific allosteric AKT inhibitor with orally bioavailable that induces cancer cell death both using alone or in combination with other compounds (111). ARQ092, allosteric AKT inhibitor, is target three isoforms AKT with under evaluation in phase I clinical trials (112). The limited efficacy of both catalytic and allosteric AKT inhibitors in clinical trials may be cause by the lack of patients with activating AKT or PI3KCA mutation. In clinical trial of AZD5363 with patients that presence of the mutation, AZD5363 showed significant effects on some patient who carried the mutation (113). The summary of clinical trials of PI3K and AKT inhibitors are in Table4.

Table 4. inhibitors of the PI3K-AKT signaling pathway that complete the clinical trials as single agents or in combination. (<https://clinicaltrials.gov/>)

Target of inhibition		Compound	Phase of the clinical trials	Condition	ClinicalTrials.gov identifier
PI3K	Pan-PI3K	BKM120	I, II, III	Metastatic breast cancer, NSCLC, endometrial cancer, GBM, CRPC, prostate cancer, renal cell carcinoma, lymphoma, advanced solid tumors, skin cancer, plus with radiotherapy	NCT02128724, NCT02439489, NCT02404844, NCT01297452, NCT01473901, NCT01470209, NCT01633060, NCT01693614, NCT01363232, NCT01719250, NCT01512251, NCT02088684, NCT02303041, NCT01923168, NCT02058381
		XL147	I, II	Metastatic breast cancer, endometrial cancer, NSCLC, lymphoma, GBM, advanced solid tumors	NCT01013324, NCT01042925, NCT00692640, NCT01082068, NCT00692640,

					NCT01082068, NCT01240460, NCT01357330, NCT01587040, NCT01436565
		GDC 0941	I, II	Metastatic breast cancer, Non-Hodgkin's lymphoma, NSCLC, advanced solid tumors	NCT00876109, NCT01740336, NCT00876122, NCT01437566, NCT00960960, NCT00928330, NCT01493843,
		BAY80 6946	I, II	large B-cell lymphoma, advanced cancer	NCT01411410, NCT00962611, NCT01404390, NCT02391116, NCT01392521, NCT01460537,
		PX 866	I, II	Prostate cancer, glioblastoma, colorectal cancer, metastasis of head and neck cancer, advance solid tumor, NSCLC	NCT01331083, NCT01259869, NCT01252628, NCT00726583, NCT01204099
	p110 α specific	BYL719	I, II	Breast cancer, head and neck cancer, advanced solid tumor, metastatic gastric cancer, multiple myeloma, acute myeloid lymphoma, esophageal cancer, breast cancer,	NCT02051751, NCT01928459, NCT01613950, NCT02144038, NCT01449058, NCT01735968, NCT01387321, NCT01822613, NCT02088684,
		INK1117	I	Metastatic solid tumors	NCT01449370
		GDC-0032	I	Metastatic breast cancer, NSCLC, breast cancer,	NCT01862081, NCT02273973
	p110 δ specific	CAL 101	I, II, III	Lymphoma,	NCT01306643, NCT02242045, NCT01393106, NCT01090414, NCT01539291, NCT01282424,

					NCT00710528, NCT01659021, NCT01796470, NCT01539512, NCT01838434, NCT01088048, NCT01644799, NCT02603445
AKT		AZD5363	I, II	Invasive breast cancer, advanced solid tumor, metastatic prostate cancer	NCT02077569, NCT01353781, NCT01692262,
		GDC-0068	I, II	Neoplasms, breast cancer	NCT01562275, NCT02301988,
		GSK2141795	I, II	Melanoma,	NCT00920257, NCT01979523,
		MK-2206	I, II	Lymphatic leukemia, colorectal cancer, pancreases cancer, ovarian cancer, oral carcinoma, advanced solid tumor, endometrial cancer, breast cancer, lung carcinoma, Gastro intestinal adenocarcinoma,	NCT01369849, NCT01333475, NCT01169649, NCT01283035, NCT01604772, NCT01253447, NCT01370070, NCT01071018, NCT01349933, NCT01307631, NCT01258998, NCT01277757, NCT01481129, NCT01231919, NCT01245205, NCT01294306, NCT01260701,

Natural compounds are promising source for developing cancer drug

Natural product

Natural products are the most important source for developing anti-cancer agents. Most of potential anti-cancer drugs is derived from secondary metabolite in the natural sources. About 70% of anti-cancer compounds used in therapeutic regimens are natural products or its

derivatives (114). More than 60% of small molecule anti-cancer agents are developed from natural compound (114, 115). 57% of cancer drugs in clinical trials were natural products or related to them which target at least 86 cancer types. Six per cent are natural products, 27% are derivatives of natural products, 5% are synthetic with natural product pharmacophores, and 23% are synthetic mimics of natural products (114, 115).

Natural compounds with anti-cancer activity are categorized to several structural classes including anthracyclines, enediynes, indolocarbazoles, isoprenoids, polyketide, polyketide macrolides, glycol-peptides, and others. The natural products for treating cancer are working by various mechanisms such as promoting apoptosis, altering cancer metabolism, inhibiting cell growth, and inhibiting angiogenesis (114). Thus, novel high efficacy and specificity drugs finding to conquer cancer are the most interested in oncological research fields.

Renieramycin (natural product from the Thai blue sponge)

The ocean is a big source for searching and developing the natural compounds with potential pharmacological effects (116, 117). Marine sponges are fruitful secondary metabolites which can be developed to be promising cancer therapeutics drugs. Recently, drugs derived from marine sponges have been approved for treating breast cancer, lymphoma, and Hodgkin's disease by USA-Food and Drug Administrative (116-118). The mechanisms of sponge-derived anti-cancer compounds are consisted with multiple mechanisms including apoptosis inducing, cell-cycle alteration, anti-inflammation, and increasing chemosensitivity to conventional anti-cancer drugs(117, 118).

Renieramycin M (RM) is a bis-tetrahydroisoquinolinequinone alkaloid which isolated from the Thai blue sponge *Xestospongia sp.* RM showed high potency cytotoxic activity against certain cancer cell lines including lung cancer (118, 119). Moreover, subtoxic concentration of RM exhibits its anti-metastatic potential (119), anti-anoikis resistant phenotype (120), and suppress stem-like phenotypes of lung cancer cells (121). These activities of RM against cancer aggressiveness phenotypes are rely on at least in part of the Akt-related mechanisms. Recently, derivatives of RM were synthesized by series of 22-O-acyl and hydroquinone 5-O-acyl ester analogs. Interestingly, most of these derivatives showed high potency of cytotoxicity in dose range at nanomolar concentration (122). Some of these derivatives exhibited more potency than their parent compound. Among the derivatives, hydroquinone 5-O-cinnamoyl ester of Renieramycin M (CIN-RM) is a structurally promising as an anticancer candidate (122). However, the Akt dependent anti-cancer mechanisms of CIN-RM are under elucidated.

Research Questions

1. Does Akt have the novel regulatory mechanisms on apoptosis resistance behavior?
2. Does Akt have the novel mechanisms on the regulation of cancer stem cells?
3. Does CIN-RM exhibit cytotoxicity on cancer cell through alteration of Akt pathway?

Objectives

1. To investigate the novel mechanisms of Akt on apoptosis susceptibility of cancer.
2. To determine the novel regulatory roles of Akt on cancer stem cell.
3. To determine the Akt suppression mechanisms of CIN-RM inducing cancer cell death.

Hypotheses

1. Akt have the novel mechanisms on the regulation of apoptosis resistance in cancer.
2. Akt have the novel regulatory roles on cancer stem cell.
3. CIN-RM have the Akt suppressive capacity inducing cancer cell death.

Expected benefits

This research project could clarify novel roles of Akt on the regulation of apoptosis susceptibility and cancer stem cell formation in the high mortality-rate cancers, NSCLC and CRC. This discovery could provide a better understanding of the crosstalk between Akt and other cellular proteins in the regulation of apoptosis resistance and cancer stem cell maintenance. Moreover, the semi-synthetic natural compound from Thai blue sponge, CIN-RM, would be tested its anti-cancer activity through diminishing Akt-activated survival pathways. Together, these discoveries could be used for designing novel targeted-drug and therapeutics strategy for cancer treatment.

Novel finding in this research

This project unravels the novel information explaining the regulatory role of Akt on apoptosis susceptibility and CSCs.

(i) For regulation of cancer dedifferentiation, cancer dedifferentiation processes are recognized as one of cancer stem cells (CSCs) origins. The accumulation of evidences indicated that Akt could promote CSCs in various cancer including prostate cancer, myeloid and acute lymphoblastic leukemia, breast cancer, NSCLC, and CRC. The mechanisms that Akt promotes CSCs, are increases ABCG2 expression, promotes expression of chemokine (C-X-C motif) receptor 4 (CXCR4) which subsequently stimulates STAT3 signaling pathway, and promotes mTOR induced HIF-1 α upregulation. However, the direct link between Akt and the regulation of CSC transcription factor Oct4 is still unclear.

Oct4 is a POU domain-containing transcription factor that binds to an octamer sequence, ATGCAAAT, of the target genes. Oct4 is the most important mediator for maintaining CSCs by functioning as a master transcription factor controlling stem cell self-renewal and pluripotency. Oct4 acts as a core of transcription factor complex by holding the other transcription factors together and promotes stemness gene expression. In addition, there have been documented that overexpression of Oct4 is associated with CSC characteristics including tumorigenicity, metastasis, and cancer relapse in certain cancer. There are various cellular processes for regulating and controlling Oct4 protein level and activity. Phosphorylation is one of post-translational modifications process that linked to cellular level and activity of various protein including Oct4. Oct4 can be phosphorylated at Ser229, Ser236 and tyr327. The phosphorylation on these residues regulate Oct4 stability and transcriptional activity. Together, Akt could be the one that regulates Oct4 at post-translational level. However, the certain mechanisms are still unclear.

Here, we provide an evidence that alteration of Akt activity by NO (tumor microenvironment substance) or Perifosine (clinical used drug for Akt inhibition) can modulate the cellular level of Oct4 protein through the alteration of Cav-1 mediated Oct4 degradation. Cav-1 control Oct4 protein level by promotes Oct4 degradation through protein-protein interaction enhancing ubiquitination proteasomal degradation pathway. This protein-protein

interaction between Cav-1 and Oct4 require OH-group of tyrosine 14 of Cav-1. NO mediated Akt activation alters the OH group of Cav-1 tyrosine 14 by facilitates phosphorylation on this site. This effect of NO diminishes the interaction between Cav-1 and Oct and promotes cellular level of Oct4. Moreover, Perifosine, a clinical used specific Akt inhibitor, can decreases level of p-Cav-1^{tyr14} subsequently increased complex formation between Cav-1 and Oct4 and decreased the level of Oct4 protein. In addition, point mutation be replacement tyrosine 14 of Cav-1 with phenylamine by using Cav-1 Y14F plasmid show absence of Cav-1 Y14F-Oct4 complex. which resulted in increased Oct4 stability and level. In silico computer molecular modelling also confirm that both phosphorylation at tyrosine 14 of Cav-1 and replacement tyrosine14 with phenylalanine increases ΔG_{free} energy between Cav-1 and Oct4 resulted in destabilizing the complex and increased half-life and cellular level of Oct4. The upregulation of Oct4 promotes dedifferentiation process which resulted in increases CD133 expression and promotes CSC behaviours. Thus, the kinase activity of Akt can overcome tumor suppressive function of Cav-1 resulting in upregulation of Oct4 and de-differentiation of NSCLC cell lines.

(ii) For apoptosis regulation, Akt has been shown to implicate enhanced survival and apoptosis resistance in lung and colorectal cancers. Since activated PI3K resulted in inhibition of apoptosis, Akt could be a target for mediating PI3K-dependent program cell death inhibition responses. Akt has implicated as an anti-apoptotic protein in several aspects of cell death control, including depletion the extracellular death stimulation signal, restraining harmful oxidative stress molecules, overcoming irradiation and chemotherapeutics triggering apoptosis. However, influencing role of Akt on p21 in the regulation of apoptosis resistance is largely unknown.

Here, we have provided the new role of p21 in regulation of drug resistance in colorectal cancer. Activated-Akt can drives the expression of cytoplasmic-p21 which promotes chemoresistance to 5FU through inhibiting pro-apoptosis function of p-Chk2^{T68}. Moreover, cytoplasmic-p21 or p-p21^{T145} forms protein-protein complex with p-Chk2^{T68} and diminishes its apoptosis inducing function by shuttling this complex out of nucleus. Nuclear exporting of the complex due to an effect of cytoplasmic-p21-mediated an increasing of NES (nuclear exporting signal) /NLS (nuclear localizing signal) ratio. These effects of cytoplasmic-p21 on p-Chk2^{T68} promote survival of CRC cell lines after 5FU exposure. Thus, activated-Akt could change cellular

localization and function of p21 from nuclear localization to cytoplasmic localization and from tumor suppressor to onco-protein.

(iii) Furthermore, we provided the pharmacological activity of semi-synthetic natural compound with anti-cancer activities that exhibit direct Akt suppression function. Hydroquinone 5-O-cinnamoyl ester of renieramycin-M (CIN-RM) is synthesized from renieramycin M (RM), an anticancer lead compound isolated from the blue sponge *Xestospongia sp.* CIN-RM show anticancer activity through the depletion of activated-Akt consequently augmenting p53 response in NSCLC cell line. The accumulation of p53 in treated cells altered the balance between Bcl₂ and Bax protein levels, by decreasing Bcl₂ and increasing Bax levels, leading to loss of mitochondria membrane integrity. Loss of mitochondria membrane potential activated caspase-dependent and -independent apoptosis cell death. Thus, the depletion of activated-Akt by CIN-RM could promote tumor suppressor function of p53 for activating apoptosis cell death.

In conclusion, we have provided the new information fulfilled the feature regarding how Akt controlling apoptosis susceptibility, and CSC properties especially Akt promotes cancer cell dedifferentiation which could have a benefit for better understanding of cancer cell biology and supporting Akt as an important anti-cancer drug targeting NSCLC and CRC. Moreover, we also provided the information regarding CIN-RM, a semi-synthetic natural compound, have a potential to develop to be an Akt-targeted cancer drug.

References

1. Manning BD, Toker A. AKT/PKB Signaling: Navigating the Network. *Cell*. 2017;169(3):381-405.
2. Gonzalez E, McGraw TE. The Akt kinases: isoform specificity in metabolism and cancer. *Cell cycle (Georgetown, Tex)*. 2009;8(16):2502-8.
3. Okano J, Gaslightwala I, Birnbaum MJ, Rustgi AK, Nakagawa H. Akt/protein kinase B isoforms are differentially regulated by epidermal growth factor stimulation. *J Biol Chem*. 2000;275(40):30934-42.
4. Hajduch E, Litherland GJ, Hundal HS. Protein kinase B (PKB/Akt) – a key regulator of glucose transport? *FEBS Letters*. 2001;492(3):199-203.
5. Barthel A, Okino ST, Liao J, Nakatani K, Li J, Whitlock JP, Jr., et al. Regulation of GLUT1 gene transcription by the serine/threonine kinase Akt1. *J Biol Chem*. 1999;274(29):20281-6.
6. He Q, Gao Z, Yin J, Zhang J, Yun Z, Ye J. Regulation of HIF-1{alpha} activity in adipose tissue by obesity-associated factors: adipogenesis, insulin, and hypoxia. *American journal of physiology Endocrinology and metabolism*. 2011;300(5):E877-E85.
7. Mackenzie RW, Elliott BT. Akt/PKB activation and insulin signaling: a novel insulin signaling pathway in the treatment of type 2 diabetes. *Diabetes, metabolic syndrome and obesity : targets and therapy*. 2014;7:55-64.
8. Das F, Ghosh-Choudhury N, Dey N, Bera A, Mariappan MM, Kasinath BS, et al. High glucose forces a positive feedback loop connecting Akt kinase and FoxO1 transcription factor to activate mTORC1 kinase for mesangial cell hypertrophy and matrix protein expression. *The Journal of biological chemistry*. 2014;289(47):32703-16.
9. Abukhdeir AM, Park BH. P21 and p27: roles in carcinogenesis and drug resistance. *Expert reviews in molecular medicine*. 2008;10:e19-e.
10. Ogawara Y, Kishishita S, Obata T, Isazawa Y, Suzuki T, Tanaka K, et al. Akt enhances Mdm2-mediated ubiquitination and degradation of p53. *J Biol Chem*. 2002;277(24):21843-50.
11. Muise-Helmericks RC, Grimes HL, Bellacosa A, Malstrom SE, Tsichlis PN, Rosen N. Cyclin D expression is controlled post-transcriptionally via a phosphatidylinositol 3-kinase/Akt-dependent pathway. *J Biol Chem*. 1998;273(45):29864-72.

12. Mendez-Pertuz M, Martinez P, Blanco-Aparicio C, Gomez-Casero E, Belen Garcia A, Martinez-Torrecedrada J, et al. Modulation of telomere protection by the PI3K/AKT pathway. *Nat Commun.* 2017;8(1):1278.
13. Cha TL, Zhou BP, Xia W, Wu Y, Yang CC, Chen CT, et al. Akt-mediated phosphorylation of EZH2 suppresses methylation of lysine 27 in histone H3. *Science.* 2005;310(5746):306-10.
14. Datta SR, Dudek H, Tao X, Masters S, Fu H, Gotoh Y, et al. Akt phosphorylation of BAD couples survival signals to the cell-intrinsic death machinery. *Cell.* 1997;91(2):231-41.
15. Cardone MH, Roy N, Stennicke HR, Salvesen GS, Franke TF, Stanbridge E, et al. Regulation of cell death protease caspase-9 by phosphorylation. *Science.* 1998;282(5392):1318-21.
16. Trecia A, Perfetti A, Cassese A, Vigliotta G, Miele C, Oriente F, et al. Protein kinase B/Akt binds and phosphorylates PED/PEA-15, stabilizing its antiapoptotic action. *Molecular and cellular biology.* 2003;23(13):4511-21.
17. Zhang X, Tang N, Hadden TJ, Rishi AK. Akt, FoxO and regulation of apoptosis. *Biochimica et Biophysica Acta (BBA) - Molecular Cell Research.* 2011;1813(11):1978-86.
18. Bai D, Ueno L, Vogt PK. Akt-mediated regulation of NFkappaB and the essentialness of NFkappaB for the oncogenicity of PI3K and Akt. *International journal of cancer.* 2009;125(12):2863-70.
19. Wang CY, Guttridge DC, Mayo MW, Baldwin AS, Jr. NF-kappaB induces expression of the Bcl-2 homologue A1/Bfl-1 to preferentially suppress chemotherapy-induced apoptosis. *Mol Cell Biol.* 1999;19(9):5923-9.
20. Enomoto A, Murakami H, Asai N, Morone N, Watanabe T, Kawai K, et al. Akt/PKB regulates actin organization and cell motility via Girdin/APE. *Dev Cell.* 2005;9(3):389-402.
21. Park BK, Zeng X, Glazer RI. Akt1 induces extracellular matrix invasion and matrix metalloproteinase-2 activity in mouse mammary epithelial cells. *Cancer Res.* 2001;61(20):7647-53.
22. Virtakoivu R, Pellinen T, Rantala JK, Perälä M, Ivaska J. Distinct roles of AKT isoforms in regulating β 1-integrin activity, migration, and invasion in prostate cancer. *Molecular biology of the cell.* 2012;23(17):3357-69.
23. Porta C, Paglino C, Mosca A. Targeting PI3K/Akt/mTOR Signaling in Cancer. *Frontiers in oncology.* 2014;4:64-.
24. Wiza C, Nascimento EB, Ouwens DM. Role of PRAS40 in Akt and mTOR signaling in health and disease. *Am J Physiol Endocrinol Metab.* 2012;302(12):E1453-60.
25. Dimmeler S, Fleming I, Fisslthaler B, Hermann C, Busse R, Zeiher AM. Activation of nitric oxide synthase in endothelial cells by Akt-dependent phosphorylation. *Nature.* 1999;399(6736):601-5.

26. Ziche M, Morbidelli L. Nitric oxide and angiogenesis. *J Neurooncol.* 2000;50(1-2):139-48.
27. Trinh XB, Tjalma WAA, Vermeulen PB, Van den Eynden G, Van der Auwera I, Van Laere SJ, et al. The VEGF pathway and the AKT/mTOR/p70S6K1 signalling pathway in human epithelial ovarian cancer. *British journal of cancer.* 2009;100(6):971-8.
28. Kitamura T, Asai N, Enomoto A, Maeda K, Kato T, Ishida M, et al. Regulation of VEGF-mediated angiogenesis by the Akt/PKB substrate Girdin. *Nat Cell Biol.* 2008;10(3):329-37.
29. Park ST, Kim BR, Park SH, Lee JH, Lee EJ, Lee SH, et al. Suppression of VEGF expression through interruption of the HIF1alpha and Akt signaling cascade modulates the antiangiogenic activity of DAPK in ovarian carcinoma cells. *Oncol Rep.* 2014;31(2):1021-9.
30. Imran A, Qamar HY, Ali Q, Naeem H, Riaz M, Amin S, et al. Role of Molecular Biology in Cancer Treatment: A Review Article. *Iranian journal of public health.* 2017;46(11):1475-85.
31. Hanahan D, Weinberg RA. The hallmarks of cancer. *Cell.* 2000;100(1):57-70.
32. Fresno Vara JA, Casado E, de Castro J, Cejas P, Belda-Iniesta C, Gonzalez-Baron M. PI3K/Akt signalling pathway and cancer. *Cancer Treat Rev.* 2004;30(2):193-204.
33. Regad T. Targeting RTK Signaling Pathways in Cancer. *Cancers.* 2015;7(3):1758-84.
34. Chalhoub N, Baker SJ. PTEN and the PI3-kinase pathway in cancer. *Annual review of pathology.* 2009;4:127-50.
35. Samuels Y, Waldman T. Oncogenic mutations of PIK3CA in human cancers. *Current topics in microbiology and immunology.* 2010;347:21-41.
36. Sun M, Hillmann P, Hofmann BT, Hart JR, Vogt PK. Cancer-derived mutations in the regulatory subunit p85alpha of phosphoinositide 3-kinase function through the catalytic subunit p110alpha. *Proceedings of the National Academy of Sciences of the United States of America.* 2010;107(35):15547-52.
37. Yi KH, Lauring J. Recurrent AKT mutations in human cancers: functional consequences and effects on drug sensitivity. *Oncotarget.* 2015;7(4):4241-51.
38. Kim MS, Jeong EG, Yoo NJ, Lee SH. Mutational analysis of oncogenic AKT E17K mutation in common solid cancers and acute leukaemias. *British journal of cancer.* 2008;98(9):1533-5.
39. Huang J, Manning BD. A complex interplay between Akt, TSC2 and the two mTOR complexes. *Biochem Soc Trans.* 2009;37(Pt 1):217-22.
40. Siegel RL, Miller KD, Jemal A. Cancer statistics, 2018. *CA Cancer J Clin.* 2018;68(1):7-30.
41. Massion PP, Carbone DP. The molecular basis of lung cancer: molecular abnormalities and therapeutic implications. *Respiratory research.* 2003;4(1):12-.
42. Torre LA, Siegel RL, Jemal A. Lung Cancer Statistics. *Adv Exp Med Biol.* 2016;893:1-19.

43. Maheu C, Galica J. The fear of cancer recurrence literature continues to move forward: a review article. *Curr Opin Support Palliat Care*. 2018;12(1):40-5.
44. Lobo NA, Shimono Y, Qian D, Clarke MF. The biology of cancer stem cells. *Annu Rev Cell Dev Biol*. 2007;23:675-99.
45. Cabrera MC, Hollingsworth RE, Hurt EM. Cancer stem cell plasticity and tumor hierarchy. *World Journal of Stem Cells*. 2015;7(1):27-36.
46. Bonnet D, Dick JE. Human acute myeloid leukemia is organized as a hierarchy that originates from a primitive hematopoietic cell. *Nat Med*. 1997;3(7):730-7.
47. Lapidot T, Sirard C, Vormoor J, Murdoch B, Hoang T, Caceres-Cortes J, et al. A cell initiating human acute myeloid leukaemia after transplantation into SCID mice. *Nature*. 1994;367(6464):645-8.
48. Li Z. CD133: a stem cell biomarker and beyond. *Experimental Hematology & Oncology*. 2013;2:17-.
49. Zeineddine D, Hammoud AA, Mortada M, Boeuf H. The Oct4 protein: more than a magic stemness marker. *American Journal of Stem Cells*. 2014;3(2):74-82.
50. Villodre ES, Kipper FC, Pereira MB, Lenz G. Roles of OCT4 in tumorigenesis, cancer therapy resistance and prognosis. *Cancer Treat Rev*. 2016;51:1-9.
51. Zhao QW, Zhou YW, Li WX, Kang B, Zhang XQ, Yang Y, et al. Akt-mediated phosphorylation of Oct4 is associated with the proliferation of stemlike cancer cells. *Oncol Rep*. 2015;33(4):1621-9.
52. Han Z-J, Feng Y-H, Gu B-H, Li Y-M, Chen H. The post-translational modification, SUMOylation, and cancer (Review). *International journal of oncology*. 2018;52(4):1081-94.
53. Wei F, Scholer HR, Atchison ML. Sumoylation of Oct4 enhances its stability, DNA binding, and transactivation. *J Biol Chem*. 2007;282(29):21551-60.
54. Glumac PM, LeBeau AM. The role of CD133 in cancer: a concise review. *Clinical and translational medicine*. 2018;7(1):18-.
55. Jang JW, Song Y, Kim SH, Kim JS, Kim KM, Choi EK, et al. CD133 confers cancer stem-like cell properties by stabilizing EGFR-AKT signaling in hepatocellular carcinoma. *Cancer Lett*. 2017;389:1-10.
56. Williams TM, Lisanti MP. The caveolin proteins. *Genome Biology*. 2004;5(3):214-.
57. Liu P, Rudick M, Anderson RG. Multiple functions of caveolin-1. *J Biol Chem*. 2002;277(44):41295-8.
58. Chatterjee M, Ben-Josef E, Thomas DG, Morgan MA, Zalupski MM, Khan G, et al. Caveolin-1 is Associated with Tumor Progression and Confers a Multi-Modality Resistance Phenotype in Pancreatic Cancer. *Sci Rep*. 2015;5:10867.

59. Han F, Gu D, Chen Q, Zhu H. Caveolin-1 acts as a tumor suppressor by down-regulating epidermal growth factor receptor-mitogen-activated protein kinase signaling pathway in pancreatic carcinoma cell lines. *Pancreas*. 2009;38(7):766-74.
60. Kato T, Miyamoto M, Kato K, Cho Y, Itoh T, Morikawa T, et al. Difference of caveolin-1 expression pattern in human lung neoplastic tissue. Atypical adenomatous hyperplasia, adenocarcinoma and squamous cell carcinoma. *Cancer Lett*. 2004;214(1):121-8.
61. Li L, Ren CH, Tahir SA, Ren C, Thompson TC. Caveolin-1 maintains activated Akt in prostate cancer cells through scaffolding domain binding site interactions with and inhibition of serine/threonine protein phosphatases PP1 and PP2A. *Mol Cell Biol*. 2003;23(24):9389-404.
62. Yang H, Guan L, Li S, Jiang Y, Xiong N, Li L, et al. Mechanosensitive caveolin-1 activation-induced PI3K/Akt/mTOR signaling pathway promotes breast cancer motility, invadopodia formation and metastasis in vivo. *Oncotarget*. 2016;7(13):16227-47.
63. Chanvorachote P, Chunchacha P, Pongrakhananon V. Caveolin-1 induces lamellipodia formation via an Akt-dependent pathway. *Cancer Cell International*. 2014;14:52-.
64. Salani B, Maffioli S, Hamoudane M, Parodi A, Ravera S, Passalacqua M, et al. Caveolin-1 is essential for metformin inhibitory effect on IGF1 action in non-small-cell lung cancer cells. *Faseb j*. 2012;26(2):788-98.
65. Hirst DG, Robson T. Nitric oxide physiology and pathology. *Methods Mol Biol*. 2011;704:1-13.
66. Ghalayini IF. Nitric oxide-cyclic GMP pathway with some emphasis on cavernosal contractility. *Int J Impot Res*. 2004;16(6):459-69.
67. Shahani N, Sawa A. Protein S-nitrosylation: role for nitric oxide signaling in neuronal death. *Biochim Biophys Acta*. 2012;1820(6):736-42.
68. Fukumura D, Kashiwagi S, Jain RK. The role of nitric oxide in tumour progression. *Nat Rev Cancer*. 2006;6(7):521-34.
69. Yongsanguanchai N, Pongrakhananon V, Mutirangura A, Rojanasakul Y, Chanvorachote P. Nitric oxide induces cancer stem cell-like phenotypes in human lung cancer cells. *Am J Physiol Cell Physiol*. 2015;308(2):C89-100.
70. Luanpitpong S, Chanvorachote P. Nitric Oxide and Aggressive Behavior of Lung Cancer Cells. *Anticancer Res*. 2015;35(9):4585-92.
71. Asatryan AD, Komarova NL. Evolution of genetic instability in heterogeneous tumors. *Journal of theoretical biology*. 2016;396:1-12.
72. Mahdipour-Shirayeh A, Kaveh K, Kohandel M, Sivaloganathan S. Phenotypic heterogeneity in modeling cancer evolution. *PloS one*. 2017;12(10):e0187000-e.

73. Vermeulen L, Todaro M, de Sousa Mello F, Sprick MR, Kemper K, Perez Alea M, et al. Single-cell cloning of colon cancer stem cells reveals a multi-lineage differentiation capacity. *Proc Natl Acad Sci U S A*. 2008;105(36):13427-32.
74. Friedmann-Morvinski D, Verma IM. Dedifferentiation and reprogramming: origins of cancer stem cells. *EMBO Rep*. 2014;15(3):244-53.
75. Zhu H, Acquaviva J, Ramachandran P, Boskovitz A, Woolfenden S, Pfannl R, et al. Oncogenic EGFR signaling cooperates with loss of tumor suppressor gene functions in gliomagenesis. *Proceedings of the National Academy of Sciences of the United States of America*. 2009;106(8):2712-6.
76. Su Z, Zang T, Liu ML, Wang LL, Niu W, Zhang CL. Reprogramming the fate of human glioma cells to impede brain tumor development. *Cell death & disease*. 2014;5(10):e1463-e.
77. Friedmann-Morvinski D, Bushong EA, Ke E, Soda Y, Marumoto T, Singer O, et al. Dedifferentiation of neurons and astrocytes by oncogenes can induce gliomas in mice. *Science (New York, NY)*. 2012;338(6110):1080-4.
78. Basu S, Haase G, Ben-Ze'ev A. Wnt signaling in cancer stem cells and colon cancer metastasis. *F1000Research*. 2016;5:F1000 Faculty Rev-699.
79. Lemieux E, Cagnol S, Beaudry K, Carrier J, Rivard N. Oncogenic KRAS signalling promotes the Wnt/beta-catenin pathway through LRP6 in colorectal cancer. *Oncogene*. 2015;34(38):4914-27.
80. Shibue T, Weinberg RA. EMT, CSCs, and drug resistance: the mechanistic link and clinical implications. *Nature reviews Clinical oncology*. 2017;14(10):611-29.
81. Zhou C, Jiang H, Zhang Z, Zhang G, Wang H, Zhang Q, et al. ZEB1 confers stem cell-like properties in breast cancer by targeting neurogenin-3. *Oncotarget*. 2017;8(33):54388-401.
82. van Neerven SM, Tieken M, Vermeulen L, Bijlsma MF. Bidirectional interconversion of stem and non-stem cancer cell populations: A reassessment of theoretical models for tumor heterogeneity. *Molecular & cellular oncology*. 2015;3(2):e1098791-e.
83. Plaks V, Kong N, Werb Z. The cancer stem cell niche: how essential is the niche in regulating stemness of tumor cells? *Cell stem cell*. 2015;16(3):225-38.
84. Grugan KD, Miller CG, Yao Y, Michaylira CZ, Ohashi S, Klein-Szanto AJ, et al. Fibroblast-secreted hepatocyte growth factor plays a functional role in esophageal squamous cell carcinoma invasion. *Proceedings of the National Academy of Sciences of the United States of America*. 2010;107(24):11026-31.

85. Parikh RA, Wang P, Beumer JH, Chu E, Appleman LJ. The potential roles of hepatocyte growth factor (HGF)-MET pathway inhibitors in cancer treatment. *Onco Targets Ther.* 2014;7:969-83.
86. Kuipers EJ, Grady WM, Lieberman D, Seufferlein T, Sung JJ, Boelens PG, et al. Colorectal cancer. *Nat Rev Dis Primers.* 2015;1:15065.
87. Munro MJ, Wickremesekera SK, Peng L, Tan ST, Itinteang T. Cancer stem cells in colorectal cancer: a review. *J Clin Pathol.* 2018;71(2):110-6.
88. Paldino E, Tesori V, Casalbore P, Gasbarrini A, Puglisi MA. Tumor initiating cells and chemoresistance: which is the best strategy to target colon cancer stem cells? *Biomed Res Int.* 2014;2014:859871.
89. Zheng H-C. The molecular mechanisms of chemoresistance in cancers. *Oncotarget.* 2017;8(35):59950-64.
90. Kim D, Dan HC, Park S, Yang L, Liu Q, Kaneko S, et al. AKT/PKB signaling mechanisms in cancer and chemoresistance. *Front Biosci.* 2005;10:975-87.
91. Qian J, Zou Y, Rahman JSM, Lu B, Massion PP. Synergy between phosphatidylinositol 3-kinase/Akt pathway and Bcl-xL in the control of apoptosis in adenocarcinoma cells of the lung. *Molecular cancer therapeutics.* 2009;8(1):101-9.
92. Longo PG, Laurenti L, Gobessi S, Sica S, Leone G, Efremov DG. The Akt/Mcl-1 pathway plays a prominent role in mediating antiapoptotic signals downstream of the B-cell receptor in chronic lymphocytic leukemia B cells. *Blood.* 2008;111(2):846-55.
93. Manning BD, Cantley LC. AKT/PKB signaling: navigating downstream. *Cell.* 2007;129(7):1261-74.
94. Miao Y, Zheng W, Li N, Su Z, Zhao L, Zhou H, et al. MicroRNA-130b targets PTEN to mediate drug resistance and proliferation of breast cancer cells via the PI3K/Akt signaling pathway. *Scientific reports.* 2017;7:41942-.
95. Luo K, Li Y, Yin Y, Li L, Wu C, Chen Y, et al. USP49 negatively regulates tumorigenesis and chemoresistance through FKBP51-AKT signaling. *Embo j.* 2017;36(10):1434-46.
96. Karimian A, Ahmadi Y, Yousefi B. Multiple functions of p21 in cell cycle, apoptosis and transcriptional regulation after DNA damage. *DNA Repair (Amst).* 2016;42:63-71.
97. Xia X, Ma Q, Li X, Ji T, Chen P, Xu H, et al. Cytoplasmic p21 is a potential predictor for cisplatin sensitivity in ovarian cancer. *BMC Cancer.* 2011;11:399.
98. Vincent AJ, Ren S, Harris LG, Devine DJ, Samant RS, Fodstad O, et al. Cytoplasmic translocation of p21 mediates NUPR1-induced chemoresistance: NUPR1 and p21 in chemoresistance. *FEBS Lett.* 2012;586(19):3429-34.

99. Koster R, di Pietro A, Timmer-Bosscha H, Gibcus JH, van den Berg A, Suurmeijer AJ, et al. Cytoplasmic p21 expression levels determine cisplatin resistance in human testicular cancer. *J Clin Invest.* 2010;120(10):3594-605.
100. Perez-Tenorio G, Berglund F, Esguerra Merca A, Nordenskjold B, Rutqvist LE, Skoog L, et al. Cytoplasmic p21WAF1/CIP1 correlates with Akt activation and poor response to tamoxifen in breast cancer. *Int J Oncol.* 2006;28(5):1031-42.
101. Zannini L, Delia D, Buscemi G. CHK2 kinase in the DNA damage response and beyond. *Journal of molecular cell biology.* 2014;6(6):442-57.
102. Stevens C, Smith L, La Thangue NB. Chk2 activates E2F-1 in response to DNA damage. *Nat Cell Biol.* 2003;5(5):401-9.
103. Hirose Y, Katayama M, Mirzoeva OK, Berger MS, Pieper RO. Akt activation suppresses Chk2-mediated, methylating agent-induced G2 arrest and protects from temozolomide-induced mitotic catastrophe and cellular senescence. *Cancer Res.* 2005;65(11):4861-9.
104. Liu Q, Turner KM, Alfred Yung WK, Chen K, Zhang W. Role of AKT signaling in DNA repair and clinical response to cancer therapy. *Neuro Oncol.* 2014;16(10):1313-23.
105. Nitulescu GM, Margina D, Juzenas P, Peng Q, Oлару OT, Saloustros E, et al. Akt inhibitors in cancer treatment: The long journey from drug discovery to clinical use (Review). *International journal of oncology.* 2015;48(3):869-85.
106. Gharbi SI, Zvelebil MJ, Shuttleworth SJ, Hancox T, Saghir N, Timms JF, et al. Exploring the specificity of the PI3K family inhibitor LY294002. *The Biochemical journal.* 2007;404(1):15-21.
107. Levy DS, Kahana JA, Kumar R. AKT inhibitor, GSK690693, induces growth inhibition and apoptosis in acute lymphoblastic leukemia cell lines. *Blood.* 2009;113(8):1723-9.
108. Crabb SJ, Birtle AJ, Martin K, Downs N, Ratcliffe I, Maishman T, et al. ProCAID: a phase I clinical trial to combine the AKT inhibitor AZD5363 with docetaxel and prednisolone chemotherapy for metastatic castration resistant prostate cancer. *Invest New Drugs.* 2017;35(5):599-607.
109. Lin J, Sampath D, Nannini MA, Lee BB, Degtyarev M, Oeh J, et al. Targeting activated Akt with GDC-0068, a novel selective Akt inhibitor that is efficacious in multiple tumor models. *Clin Cancer Res.* 2013;19(7):1760-72.
110. Arceci RJ, Allen CE, Dunkel IJ, Jacobsen E, Whitlock J, Vassallo R, et al. A phase IIa study of afuresertib, an oral pan-AKT inhibitor, in patients with Langerhans cell histiocytosis. *Pediatr Blood Cancer.* 2017;64(5).

111. Narayan RS, Fedrigo CA, Brands E, Dik R, Stalpers LJA, Baumert BG, et al. The allosteric AKT inhibitor MK2206 shows a synergistic interaction with chemotherapy and radiotherapy in glioblastoma spheroid cultures. *BMC cancer*. 2017;17(1):204-.
112. Yu Y, Hall T, Eathiraj S, Wick MJ, Schwartz B, Abbadessa G. In-vitro and in-vivo combined effect of ARQ 092, an AKT inhibitor, with ARQ 087, a FGFR inhibitor. *Anticancer Drugs*. 2017;28(5):503-13.
113. Banerji U, Dean EJ, Perez-Fidalgo JA, Batist G, Bedard PL, You B, et al. A Phase I Open-Label Study to Identify a Dosing Regimen of the Pan-AKT Inhibitor AZD5363 for Evaluation in Solid Tumors and in PIK3CA-Mutated Breast and Gynecologic Cancers. *Clin Cancer Res*. 2018;24(9):2050-9.
114. Cragg GM, Pezzuto JM. Natural Products as a Vital Source for the Discovery of Cancer Chemotherapeutic and Chemopreventive Agents. *Med Princ Pract*. 2016;25 Suppl 2:41-59.
115. Seca AML, Pinto DCGA. Plant Secondary Metabolites as Anticancer Agents: Successes in Clinical Trials and Therapeutic Application. *International journal of molecular sciences*. 2018;19(1):263.
116. Blunt JW, Carroll AR, Copp BR, Davis RA, Keyzers RA, Prinsep MR. Marine natural products. *Nat Prod Rep*. 2018;35(1):8-53.
117. Mehbub MF, Perkins MV, Zhang W, Franco CMM. New marine natural products from sponges (Porifera) of the order Dictyoceratida (2001 to 2012); a promising source for drug discovery, exploration and future prospects. *Biotechnol Adv*. 2016;34(5):473-91.
118. Calcabrini C, Catanzaro E, Bishayee A, Turrini E, Fimognari C. Marine Sponge Natural Products with Anticancer Potential: An Updated Review. *Mar Drugs*. 2017;15(10).
119. Halim H, Chunhacha P, Suwanborirux K, Chanvorachote P. Anticancer and antimetastatic activities of Renieramycin M, a marine tetrahydroisoquinoline alkaloid, in human non-small cell lung cancer cells. *Anticancer Res*. 2011;31(1):193-201.
120. Sirimangkalakitti N, Chamni S, Suwanborirux K, Chanvorachote P. Renieramycin M Sensitizes Anoikis-resistant H460 Lung Cancer Cells to Anoikis. *Anticancer Res*. 2016;36(4):1665-71.
121. Sirimangkalakitti N, Chamni S, Suwanborirux K, Chanvorachote P. Renieramycin M Attenuates Cancer Stem Cell-like Phenotypes in H460 Lung Cancer Cells. *Anticancer Res*. 2017;37(2):615-21.
122. Chamni S, Sirimangkalakitti N, Chanvorachote P, Saito N, Suwanborirux K. Chemistry of Renieramycins. 17. A New Generation of Renieramycins: Hydroquinone 5-O-Monoester Analogues of Renieramycin M as Potential Cytotoxic Agents against Non-Small-Cell Lung Cancer Cells. *J Nat Prod*. 2017;80(5):1541-7.

CHAPTER II

NITRIC OXIDE PROMOTES CANCER CELL DEDIFFERENTIATION BY DISRUPTING AN OCT4:CAVEOLIN-1 COMPLEX : A NEW REGULATORY MECHANISM FOR CANCER STEM CELL FORMATION

This research had been published in Journal of Biological Chemistry by year 2018 volume 293 issue 35 page13534 - 13552 on the topic namely: Nitric oxide promotes cancer cell dedifferentiation by disrupting an Oct4:caveolin-1 complex: A new regulatory mechanism for cancer stem cell formation (doi: 10.1074/jbc.RA117.000287).

The web link of this article as follow: <https://www.ncbi.nlm.nih.gov/pubmed/29986880>

Ph.D. student

Arnatchai Maiuthed

Affiliation

1. Department of Pharmacology and Physiology, Faculty of Pharmaceutical Sciences, Chulalongkorn University, Bangkok 10300
2. Cell-based Drug and Health Products Development Research Unit, Faculty of Pharmaceutical Sciences, Chulalongkorn University, Bangkok 10300

Advisor

Associate Professor Pithi Chanvorachote, Ph.D.

Affiliation

1. Department of Pharmacology and Physiology, Faculty of Pharmaceutical Sciences, Chulalongkorn University, Bangkok 10300
2. Cell-based Drug and Health Products Development Research Unit, Faculty of Pharmaceutical Sciences, Chulalongkorn University, Bangkok 10300

Approval of the co-authors on the use of publication material in the dissertation of Arnatchai Maiuthed


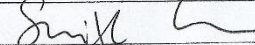

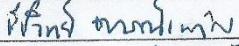

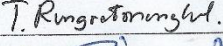

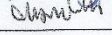
Approval of the co-authors on the use of publication material in
the dissertation of Arnatchai Maiuthed

Concerns publication:

"Nitric oxide promotes cancer cell dedifferentiation by disrupting an Oct4:caveolin-1 complex: A new regulatory mechanism for cancer stem cell formation"

Arnatchai Maiuthed, Narumol Bhummaphan, Sudjit Luanpitpong, Apiwat Mutirangura, Chatchawit Apornthewan, Arthitaya Meeprasert, Thanyada Rungrotmongkol, Yon Rojanasakul, and Pithi Chanvorachote, Journal of Biological Chemistry 2018, 293(35), 13534 –13552,
doi:10.1074/jbc.RA117.000287

With this I agree that Arnatchai Maiuthed uses the publication in text format and pictorial form for his cumulative dissertation "NOVEL REGULATORY MECHANISMS OF PROTEIN KINASE B ON APOPTOSIS SUSCEPTIBILITY AND CANCER DEDIFFERENTIATION" (working title).

Full name	Signature
Narumol Bhummaphan	
Sudjit Luanpitpong	
Apiwat Mutirangura	
Chatchawit Apornthewan	
Arthitaya Meeprasert	
Thanyada Rungrotmongkol	
Yon Rojanasakul	
Pithi Chanvorachote	

Abstract

Cancer stem cells (CSCs) are unique populations of cells that can self-renew and generate different cancer cell lineages. Although CSCs are believed to be a promising target for novel therapies, the specific mechanisms by which these putative therapeutics could intervene are less clear. Nitric oxide (NO) is a biological mediator frequently up-regulated in tumors and has been linked to cancer aggressiveness. Here, we search for targets of NO that could explain its activity. We find that it directly affects the stability and function of octamer-binding transcription factor 4 (Oct4), known to drive the stemness of lung cancer cells. We demonstrated that NO promotes the CSC-regulatory activity of Oct4 through a mechanism that involves complex formation between Oct4 and the scaffolding protein caveolin-1 (Cav-1). In the absence of NO, Oct4 forms a molecular complex with Cav-1, which promotes the ubiquitin-mediated proteasomal degradation of Oct4. NO promotes Akt-dependent phosphorylation of Cav-1 at tyrosine 14, disrupting the Cav-1:Oct4 complex. Site-directed mutagenesis and computational modeling studies revealed that the hydroxyl moiety at tyrosine 14 of Cav-1 is crucial for its interaction with Oct4. Both removal of the hydroxyl via mutation to phenylalanine and phosphorylation lead to an increase in binding free energy (ΔG_{bind}) between Oct4 and Cav-1, destabilizing the complex. Together, these results unveiled a novel mechanism of CSC regulation through NO-mediated stabilization of Oct4, a key stem cell transcription factor, and point to new opportunities to design CSC-related therapeutics.



Introduction

Cancer stem cells (CSCs) or cancer stem-like cells are specific cell populations that can differentiate and generate cancer cells in various types of cancer, including lung cancer (1, 2). These cells have characteristics similar to those of normal stem cells, in particular, an ability to self-renew and generate different cell lineages (3). Such ability is believed to facilitate the progression of cancers and their aggressive behaviors (4). Increasing evidence also suggests that CSCs possess several virulent features that make them invasive and resistant to chemo/radiotherapy (5).

The successful establishment of induced pluripotent stem cells that form fully differentiated cells has revealed that the differentiated cells retain the capacity to revert to stem cells, and certain regulatory transcription factors, such as octamerbinding transcription factor 4 (Oct4), Nanog, c-Myc, Klf4, Sox2, and Lin28, are essential for somatic cell reprogramming (6, 7). Likewise, cancer dedifferentiation is evident and has been linked to cancer progression and aggressive behaviors (8, 9). Similar to somatic cell reprogramming, tumor dedifferentiation is a reversal of cell development to a more immature state. Such discovery has led to an interest in uncovering the origin of CSCs and targeting these cells for therapy. In cancer, Oct4, Sox2, and Nanog have been shown to associate with the stemness of cells by sustaining the level of stem cell-related proteins, such as CD133, ALDH1A1, and ABCG2 (10). Induced expression of the Oct4 gene and transmembrane delivery of the Oct4 protein were shown to induce the dedifferentiation of melanoma cells to CSC-like cells with a strong reduction in melanocytic markers and acquisition of spheroid-forming ability (11). In lung cancer, the expression of Oct4 correlates with aggressive behaviors and CSC properties (12–14). Moreover, in various cancers, the overexpression of Oct4 and its downstream targets is associated with CSCs and the progression of disease (15–17), although the underlying mechanisms remain obscure.

In recent years, the role of the microenvironment in cancer progression has increasingly been recognized (18). Nitric oxide (NO) is a key mediator frequently up-regulated in lung cancer microenvironment (19). It is also known to play a pivotal role in controlling several cellular processes in both normal and pathological conditions (20). In lung cancer, NO and its producing enzymes, nitric-oxide synthases (NOSs), are highly up-regulated (19, 21). NO has also been shown to promote anoikis or cell survival after detachment (22), motility (23), CSC-like phenotypes (24), and chemotherapeutic resistance (25, 26).

Caveolin-1 (Cav-1) is a 21-kDa scaffolding protein found in caveolae (27). Cav-1 is required for the formation of caveolae as well as its function, including endocytosis, lipid homeostasis, and signal transduction (28). The tumor suppressor function and scaffolding capacity of Cav-1 have been extensively studied in various cancers (29–32), but its role in the regulation of

CSCs remains obscure. Furthermore, the co-expression of Cav-1 and NOS in certain cancers has been reported (33). In addition, the caveolin-scaffolding domain of Cav-1 exhibits protein–protein interactions with NOS, which resulted in a decrease of the cellular function of NOS (34, 35). These findings suggest that Cav-1 and NO may play an opposite role in regulating CSCs. However, detailed mechanisms and their cross-talk remain to be investigated.

Oct4 is a key CSC mediator that promotes the expression of other CSC factors, and its introduction into cancer cells induces cancer stemness (36). We found that Oct4 interacts with Cav-1 and that such interaction is under the regulation of NO. In this study, we hypothesized that Cav-1 regulates the cellular level of Oct4, and therefore it influences CSCs in lung cancer via a NO-dependent mechanism. Using molecular techniques and computer modeling approaches, we demonstrated for the first time that Cav-1 forms a molecular complex with Oct4 and regulates its expression through ubiquitin–proteasome-mediated degradation. We also investigated the roles of NO in complex formation and stem properties of lung cancer cells, and unveiled a novel mechanism of CSC regulation that may lead to a better understanding of cancer cell biology under nitrosative oxidative stress conditions, which may be exploited for CSC-targeted therapy.

Results

Nitric oxide increases CSC-like phenotypes of human lung cancer cells.

To study the potential regulation of CSCs by NO, we first characterized the optimal dose response to NO in human lung cancer cells. Sub-confluent monolayers of human lung cancer H460 cells were exposed to various concentrations of DPTA NONOate, a well-established NO donor, for 24 h, and cell viability was determined by MTT assay. At the concentration range of 0–40 μM , the NO donor was found to have no significant effect on cell viability; however, at 80 μM or higher, a significant decrease in cell viability was observed in the treated cells (Fig. 1A). Apoptosis and necrosis studies by Hoechst 33342/propidium iodide (PI) assays also showed that the low dose (40 μM) DPTA NONOate had no significant effect on DNA condensation/fragmentation or nuclear PI fluorescence (Fig. 1, B and C), indicating the lack of apoptotic and necrotic cell death under the test conditions.

To determine the effect of NO on the spheroid-forming ability of lung cancer cells under nonattachment conditions, H460, H23, and H292 cells were treated with 0–40 μM DPTA NONOate for 5 days, and their spheroid-forming capacity was evaluated by seeding them at low density on ultralow attached plates. Time courses of spheroid formation for H460, H23, and H292 cells at 10, 20, and 40 days post-seeding are depicted in Fig. 1, D, G, and J, whereas quantitative analyses of the spheroid number and size are shown in Fig. 1, E/F, H/I, and K/L, respectively. A significant increase in the number of spheroids formed at 20 days was recorded for the H460 and H292 cells

treated with 10 μM or higher concentrations of DPTA NONOate, whereas a similar increase was observed for H23 cells at 5 μM or higher concentrations. At 40 days post-seeding, a significant increase in spheroid number was observed in H460, H23, and H292 cells treated with 5 μM or higher concentrations of NONOate. However, none of the treated cells showed a significant change in the spheroid number at 10 days. Fig. 1, *F*, *I*, and *L*, shows the relative spheroid size of the treated and untreated H460, H23, and H292 cells, respectively. Although the spheroid size of the treated cells was smaller than that of the control cells at 10 days, a significant increase in the spheroid size was observed at 20 and 40 days for all cell lines tested. At 20 days post-seeding, the increase in spheroid size was observed at the treatment dose of 10 μM or higher concentration for H460 and H292 cells and at 5 μM or higher concentration for H23 cells. At 40 days post seeding, all cell lines exhibited a significant increase in spheroid size at the treatment dose of 5 μM or higher concentration. These results indicate that nontoxic concentrations of DPTA NONOate promote spheroid formation of lung cancer H460, H23, and H292 cells.



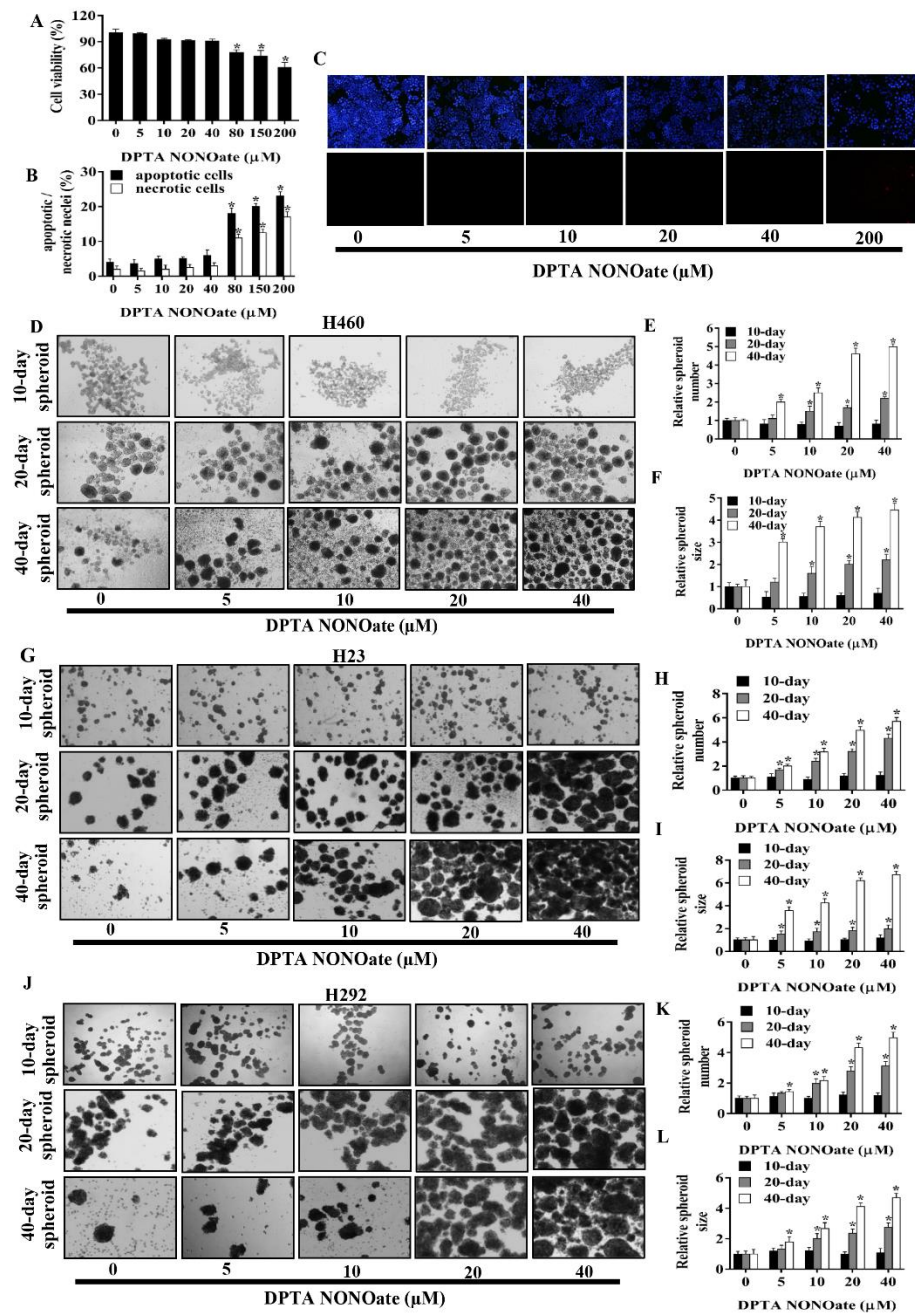


Figure 1. NO donor promotes human lung CSC-like phenotypes.

A, H460 cells were treated with NO donor (DPTA NONOate) for 24 h and analyzed for cell viability by MTT assay. Apoptotic and necrotic cell death after the treatment was analyzed by Hoechst 33342/PI co-staining assays. B, percentages of apoptotic and necrotic nuclei in NO-treated cells were analyzed and calculated as relative to the control cells. C, 10 immunofluorescence images of the treated and nontreated cells stained with Hoechst 33342/PI. After being treated with DPTA NONOate (0–40 μM) for 5 days, H460 (D), H23 (G), and H292 (J) cells were suspended and subjected to spheroid formation assay. Spheroid number H460 (E), H23 (H), H292 (K), and size H460 (F), H23 (I), H292 (L) were analyzed and calculated as relative to the control after 10, 20, and 40 days. Plots are means \pm S.D. ($n = 3$). *, $p < 0.05$ versus nontreated cells.

Nitric oxide increases the expression of stemness-related proteins

Stem cell markers such as CD133, ALDH1A1, and ABCG2 and stemness transcription factors such as Oct4, Sox2, and Nanog are commonly accepted as key drivers or markers of CSCs (10). We used these proteins to verify the CSC-inducing effect of NO in the tested lung cells. H460 cells were cultivated in the presence or absence of DPTA NONOate (5–40 μ M) for 1, 3, and 5 days, and the expression level of these markers was assessed by Western blotting. Fig. 2, A–C, shows a dose- and time-dependent expression of CD133, ABCG2, ALDH1A1, and Oct4 in response to the NO treatment. No significant changes in the expression level of these proteins were observed 1 day after the treatment (Fig. 2D). At 3 days, an increased expression of Oct4 was seen at the treatment dose of 10 M, whereas CD133 expression was up-regulated at 20 and 40 μ M (Fig. 2E). Surprisingly, we observed a reduction in Sox2 expression at 3 days after the treatment with 20 and 40 μ M DPTA NONOate. Fig. 2F further shows the up-regulation of CD133, ALDH1A1 and Oct4 at 5 days post-treatment with 10 μ M or higher concentrations of DPTA NONOate and a decrease in Sox2 expression at the dose of 10 μ M or higher.

To confirm the above finding, we performed immunofluorescence experiments assessing the expression of CSC markers CD133 and Oct4 in H460 cells following NO exposure. The cells were treated with 40 M DPTA NONOate for 5 days and analyzed for CD133 and Oct4 expression by immunofluorescence staining. Consistent with the Western blotting results, the immunofluorescence results indicate the up-regulation of CD133 and Oct4 expression in the treated lung cancer cell (Fig. 2G)

The expression levels of stemness-associated proteins in response to the NO donor treatment were also assessed in H23 and H292 cells. Fig. 2, H and J, shows that treatment of H23 cells with DPTA NONOate for 5 days induced an up-regulation of CD133 and ABCG2 at the treatment dose of 5 M or higher, whereas an increase in Oct4 and ALDH1A1 was observed at the dose of 20 M or higher. Fig. 2, I and K, shows the results of NO treatment in H292 cells. A significant increase in Oct4 expression was seen at the treatment dose of 5 M or higher and at 20 M or higher for CD133, ABCG2, and ALDH1A1. These results along with the spheroid formation results support the regulatory role of NO in controlling the stemness of lung cancer cells.

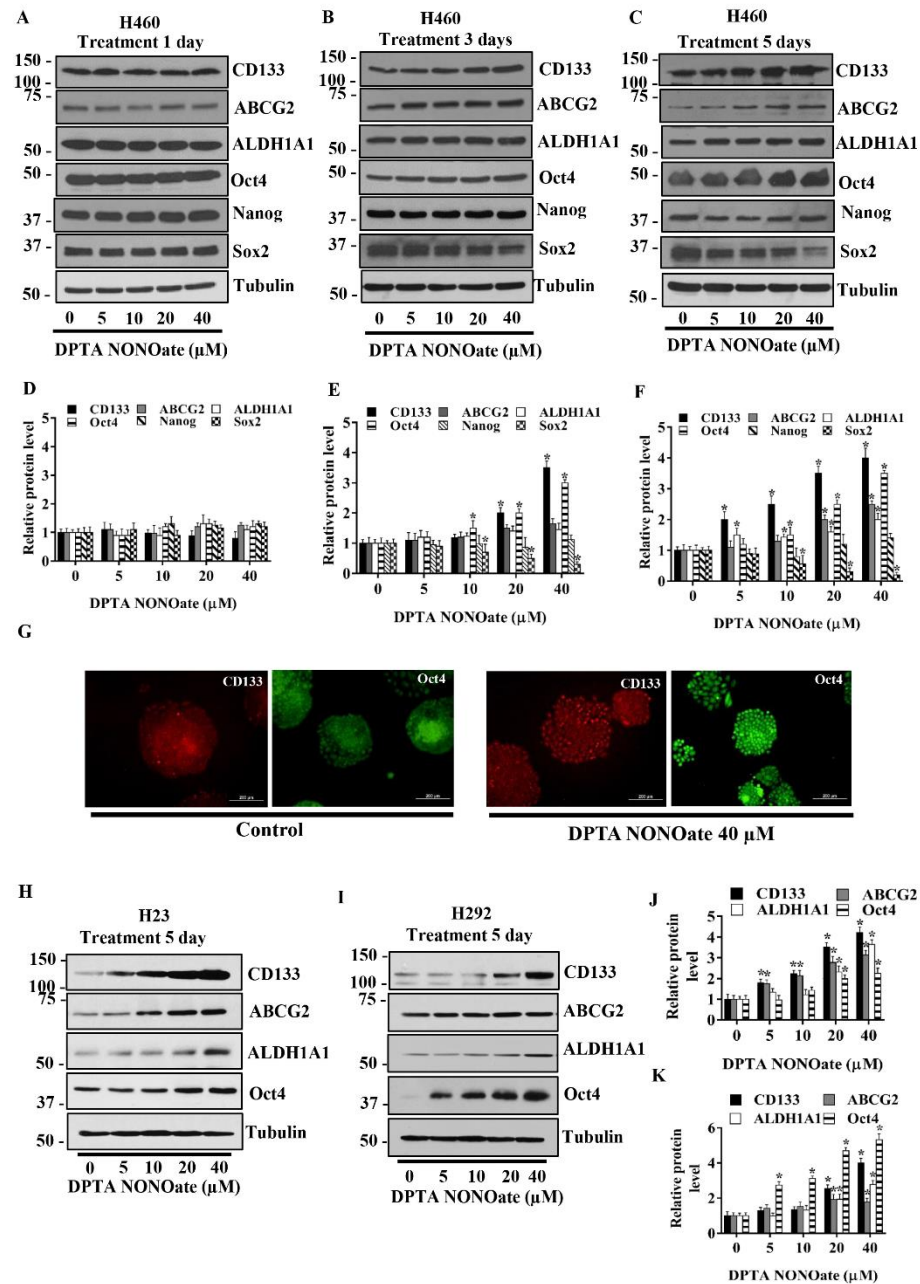


Figure 2. NO donor increases CSC markers in NSCLC cell lines.

H460 cells were treated with DPTA NONOate for 1 day (A), 3 days (B), and 5 days (C) after which they were analyzed for CSC markers (CD133, ALDH1A1, and ABCG2) and CSC transcription factors (Oct4, Nanog, and Sox2) by Western blotting. The blots were reprobed with tubulin to confirm equal loading of the protein samples. The immunoblot signals at 1 day (D), 3 days (E), and 5 days (F) after the treatment were quantified by densitometry, and mean data from independent experiments were normalized and presented. The bars are means \pm S.D. ($n = 3$). *, $p < 0.05$ versus nontreated cells. G, expression of CD133 and Oct4 in H460 cells treated with DPTA NONOate (40 μM) for 5 days were analyzed by fluorescence microscopy (10). Immunofluorescence was performed using mouse anti-CD133 mAb followed by Alexa-Fluor568-labeled secondary antibody to visualize

CD133 expression and using mouse anti-Oct4 mAb followed by Alexa-Fluor488-labeled secondary antibody to visualize Oct4 expression in separated experiments. Cells were stained with Hoechst 33342 dye to aid visualization of the cell nucleus. The CD133 and Oct4 proteins were appeared as red and green fluorescence, respectively. H23 (H) and H292 (I) were treated with DPTA NONOate for 5 days and then were analyzed for CSC markers (CD133, ABCG2, and ALDH1A1) and Oct4. The blots were reprobated with tubulin to confirm equal loading of the protein samples. The immunoblot signals of H23 (J) and H292 (K) were quantified by densitometry, and mean data from independent experiments were normalized and presented. The bars are means \pm S.D. ($n = 3$). *, $p < 0.05$ versus nontreated cells.

Microarray gene profiles of nitric oxide-mediated gene expression.

Two different passages of H460 cells treated with DPTA NONOate and their nontreated counterparts were subjected to microarray analysis as mentioned under “Experimental procedures.” The gene probe list of the chip is shown in Table S1. The CU-DREAM (37) program was used to analyze the raw data, and gene probes with significant differences ($p < 0.05$) were chosen for further evaluation using the Bioconductor R statistic program. The heat map generated from the Bioconductor R statistics program (Fig. 3A) illustrates the intensity detected for different gene probes. H460 control cell samples were labeled control 1 and control 2, and the DPTA NONOate-treated cells were labeled as DPTA NONOate 1 and DPTA NONOate 2. The high-resolution microarray heat map image is available in Fig. S1. The computer program bracket links two samples that have similar genotypes. As expected, control 1 and control 2 displayed expression profiles distinct from those of NO-treated 1 and 2. The probed gene with significant differences ($p < 0.01$) (Table S2) was selected as the next interpretation. Although the mRNA level of Oct4 analyzed by microarray in NO-treated cells was not significantly altered (Table S2), the Oct4 protein expression was significantly up-regulated (Fig. 2), suggesting that the NO may not regulate Oct4 up-regulation via transcriptional means but may affect the protein stability.

The genes displayed significant differences ($p < 0.01$) (Table S2) between treatments, and control groups were subjected for Gene Ontology (GO) using Enrichr (an integrative web-based and mobile software application; <http://amp.pharm.mssm.edu/Enrichr/>) (38, 39), providing the gene set enrichment analysis. We used the Enrichr-EhEA-2016 feature (39), which analyzed and indicated the responsible transcription factors (TFs) for the set of gene expression changed with ChIP databases (PMID: 20709693) (40). Fig. 3B shows the analyzed results by EnrichrEhEA-2016 indicating the TF names and PubMed IDs of ChIP-seq experiments; a list of NO-mediated gene expression changes that matched the gene list in each ChIP-seq; and the p value calculated from matched and unmatched genes in each ChIP-seq. The results showed that genes altered by NO treatment are the regulated target genes of various TFs, including Ap2-alpha, Ets1, Jar1d1A, Oct4,

Myc, Sall4, Klf4, E2A, Top2B, Maf, and Stat3 (Fig. 3B). To verify the effect of NO in regulation of CSCs through Oct4 activity, the Oct4-targeted genes were analyzed by RT-PCR (Fig. 3C). The mRNA expression of COLEC12, LAMP1, MYH3, PER3, ROS26, and UBE2S genes were up-regulated after treatment with NO in a concentration dependent manner. The RT-PCR results were consistent with the results from the microarray analysis. Fig. 3D indicates the selected NO-mediated gene alteration (only genes of which their mRNA expression is controlled by Oct4) and its primer sequences.

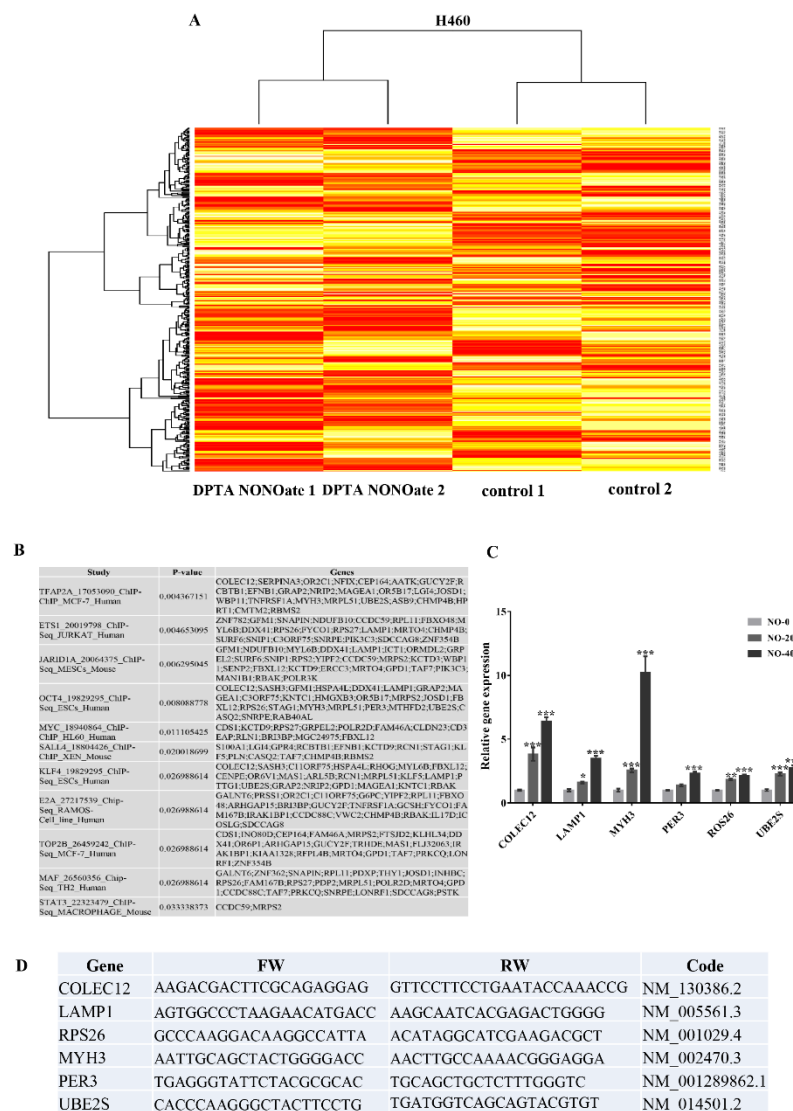


Figure 3. Microarray analysis of the effect of nitric oxide on H460 cells.

H460 cells treated with DPTA NONOate and untreated control were subjected to analyzing the mRNA expression profile by Affymetrix chips as per the manufacturer's procedure. A, gene probes with a significant

difference ($p < 0.05$) between DPTA NONOate-treated and the control group analyzed by CU-DREAM program generated heat maps of genes by the Bioconductor R statistic program. B, results from Enrichr-EhEA-2016 demonstrated the gene list of nitric oxide-mediated gene expression matched with targeted genes of transcription factors evaluated by ChIP-seq assay. C, qRT-PCR was used to verify the microarray results. The mRNA expression of Oct4 downstream targets, including COLEC12, LAMP1, MYH3, PER3, ROS26, and UBE2S, were subjected to RT-PCR analysis. The bars are means \pm S.D. ($n = 3$). *, $p < 0.05$ versus nontreated cells; **, $p < 0.001-0.01$; and ***, $p < 0.001$. D, NO-inducing gene alteration (only from Oct4 axis) and its primer sequences for RT-PCR.

Nitric oxide suppresses the degradation of Oct4 by diminishing its ubiquitin proteasomal degradation.

Based on previous studies showing the role of Oct4 in controlling stem cell properties and expression of CSC markers CD133 and ALDH1A1 (41, 42), our finding demonstrates that the effects of NO on Oct4 were not involved in the transcription process of Oct4. Thus, we investigated the potential regulation of NO on Oct4 post-translational modifications. Because NO has previously been shown to promote the stability of various proteins (43, 44), we tested whether NO could stabilize Oct4, which may contribute to its up-regulation after the NO donor treatment.

The cells were treated with 40 μ M DPTA NONOate at various times in the presence or absence of cycloheximide (CHX), a protein synthesis inhibitor, and the expression of Oct4 was monitored by Western blotting (Fig. 4A). The results showed that treatment of the cells with DPTA NONOate significantly increased the expression of Oct4 over time as compared with the untreated control (Fig. 4B), suggesting the stabilizing effect of NO on Oct4.

Because previous studies have shown that the cellular level of Oct4 is regulated by the ubiquitin-proteasomal degradation pathway (45), we next investigated whether Oct4 up-regulation by NO may occur through this pathway. Immunoprecipitation studies were carried out to evaluate the effect of NO on Oct4 ubiquitination. H460 cells were treated with various concentrations of DPTA NONOate in the presence of lactacystin, a highly specific proteasome inhibitor, for 12 h, after which cell lysates were prepared and immunoprecipitated using an anti-Oct4 antibody. The resulting immune complexes were then analyzed for protein ubiquitination by Western blotting using an antiubiquitin antibody. The results showed that Oct4 ubiquitination was dose-dependently reduced by the NO donor treatment (Fig. 4, C and D). This study indicates that NO exerts a promoting effect on Oct4 expression by inhibiting its ubiquitin-proteasomal degradation.

Nitric oxide increases phosphorylated Akt (Ser-473) and caveolin-1 levels

Phosphorylation of Oct4 by cellular kinases is crucial to its biological activity (46). We next tested whether NO could alter the activity of key cellular kinases, including Akt, Src, and Erk in lung cancer H460, H23, and H292 cells. The cells were cultivated in the presence or absence of various concentrations of DPTA NONOate, and the expression levels of these proteins as well as their phosphorylated forms were determined by Western blotting. The results showed that NO treatment significantly increased the expression ratio of p-Akt (Ser-473) to Akt in a dose-dependent manner in H460 (Fig. 4, E and H), H23 (Fig. 4, F and I), and H292 (Fig. 4, G and J) cells.

We further investigated whether the effect of NO-mediated Oct4 up-regulation is an Akt-dependent mechanism, and H460 cells were treated with 40 M DPTA NONOate in the presence or absence of 2.5 M perifosine (selective Akt inhibitor) for 5 days. As control, cells were treated with 2.5 M perifosine alone for 5 days and analyzed for Oct4 expression by Western blotting (Fig. 4, K and L). Treatment of the cells with DPTA NONOate strongly up-regulated the Oct4 level, whereas the perifosine treatment alone dramatically down-regulated the Oct4 level. In addition, the up-regulation of Oct4 by DPTA NONOate could be blocked by the perifosine treatment, suggesting that the upregulation of Oct4 by NO occurs through an Akt-dependent pathway.

Cav-1 was shown to exhibit an inhibitory effect on inducible NO synthases (34, 35). We therefore investigated whether NO could affect Cav-1 expression. H460, H23, and H292 cells were cultivated in the presence or absence of various concentrations of DPTA NONOate, and the expression level of Cav-1 was examined by Western blotting. The results showed that Cav-1 expression was strongly up-regulated in the NO-treated cells in a dose-dependent manner in H460 (Fig. 4, E and H), H23 (Fig. 4, F and I), and H292 (Fig. 4, G and J) cells.

Caveolin-1 enhances the degradation of Oct4 via ubiquitin-proteasome pathway.

Cav-1 is known to regulate several cancer cell behaviors, including migration (47), invasion (48), and anoikis resistance (49). Because Cav-1 is up-regulated by NO, we tested whether Cav-1 could be involved in the regulation of lung CSCs. Cav-1 expression was ectopically expressed or knocked down by FLAG-Cav-1 or shRNA-Cav-1, respectively, and their effects on spheroid formation and CSC marker expression were examined in H460 cells. Fig. 5 A shows microscopic images of the spheroids formed by the genetically modified and control cells. Quantitative analyses of the spheroid number and size showed a significant increase in the spheroid number in shRNA-Cav-1 cells and a decrease in FLAG-Cav-1 cells as compared with controls (Fig. 5 B). Spheroid size was also found to decrease in FLAG-Cav-1 cells; however, no significant change was observed in shRNA-Cav-1 cells. These results indicate that Cav-1 is a negative regulator of CSCs in the tested cell system. Western blot analysis of CSC-related

proteins, including CD133, ALDH1A1, and Oct4, showed that the expression of these proteins was inversely correlated with Cav-1 expression (Fig. 5, C and D), thus supporting the suppressive role of Cav-1 in CSC regulation. These results also suggest that certain downstream targets of Cav-1, such as Oct4, may be involved in the regulation of CSCs by Cav-1. For verification, the data were provided in Fig. S2. The expression of Cav-1 protein in nontreated H460 cells was comparable with mock control transfectants (Fig. S2A). The effect of shRNA–Cav-1 plasmid on the alteration of Cav-1, Oct4, and CD133 proteins was verified with two other shRNA–Cav-1 sequences, and the results were consistent (Fig. S2B).

Cav-1 is known to regulate several targeted proteins by controlling their stability post-translationally (50, 51). To test whether Cav-1 could down-regulate Oct4 (Fig. 5, C and D) in a post-translational modification manner, we performed a CHX protein synthesis inhibition study in which Cav-1 knockdown and overexpressing cells were treated with 50 μ g/ml CHX, a protein synthesis inhibitor, over time and analyzed for Oct4 expression by Western blotting. The results showed that Oct4 protein levels were significantly reduced in the Cav-1-overexpressing cells as compared with the knockdown cells at 24 and 36 h post-treatment (Fig. 5, E and F). This result suggests that Cav-1 regulates the stability of Oct4 post-translationally.

Oct4 was previously shown to be degraded via the ubiquitin–proteasomal pathway (52, 53). To test whether Cav-1 could regulate ubiquitination of Oct4, the ubiquitination level of Oct4 in Cav-1–overexpressing and knockdown cells was determined. Cells were treated with lactacystin, a proteasome inhibitor, and analyzed for Oct4 ubiquitination by immunoprecipitation and Western blotting (Fig. 5G). The results showed that Oct4 ubiquitination substantially increased in the Cav-1–overexpressing cells but decreased in the knockdown cells relative to controls (Fig. 4, G and H). Together, these results suggest Cav-1 mediated down-regulation of Oct4 via ubiquitin–proteasomal degradation as a mechanism of CSC regulation by Cav-1.

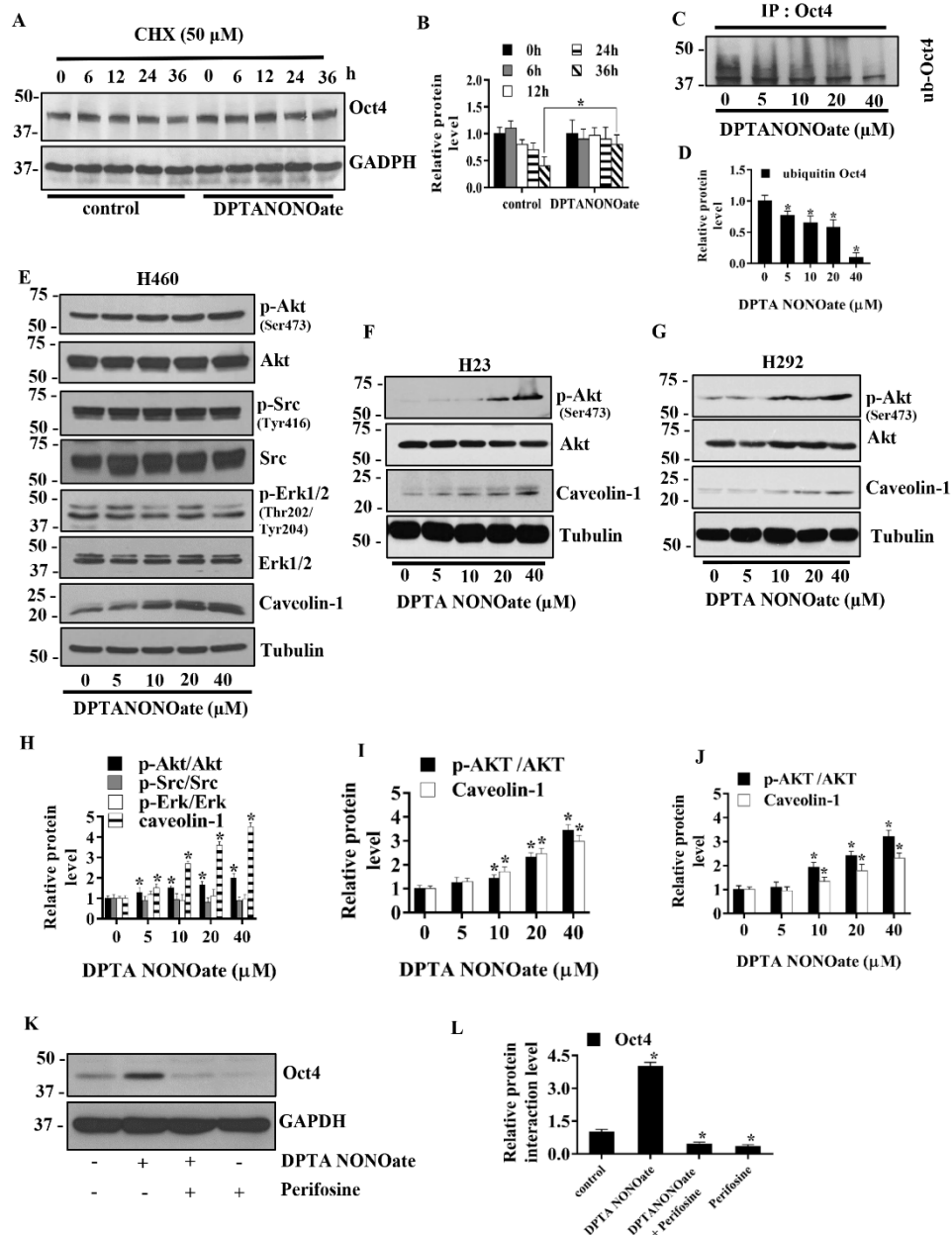


Figure 4. NO donor increases Oct4 stability through Akt-dependent mechanisms.

A, H460 cells were treated with 40 μ M DPTANONOate and 50 μ g/ml CHX for the indicated times and analyzed for Oct4 levels by Western blotting. The blots were re-probed with GAPDH to confirm equal loading of the samples. B, immunoblot signals of Oct4 were quantified by densitometry, and mean data from independent experiments were normalized and presented. The bars are means \pm S.D. (n = 3). *, p < 0.05 versus nontreated cells. C, H460 cells were treated with DPTANONOate (0–40 μ M) and lactacystin (10 μ M) for 12 h and subjected to immunoprecipitation (IP) of Oct4. The immunoprecipitation complexes were analyzed for ubiquitin level by Western blotting. D, immunoblot signals of ubiquitin were quantified by densitometry, and mean data from independent experiments were normalized and presented. The bars are means \pm S.D. (n = 3). *, p < 0.05 versus nontreated cells. E, H460 cells were treated with DPTANONOate (0–40 μ M) for 5 days and analyzed for phosphorylated Akt (Ser-473), Akt, p-Src (Tyr-416), Src, p-Erk1/2 (Thr-202/Tyr-204), Erk1/2, and Caveolin-1 levels by Western blotting. Tubulin was used as a loading control. F, H23 cells were treated with DPTANONOate (0–40 μ M) for 5 days and analyzed for phosphorylated Akt (Ser-473), Akt, and Caveolin-1 levels by Western blotting. Tubulin was used as a loading control. G, H292 cells were treated with DPTANONOate (0–40 μ M) for 5 days and analyzed for phosphorylated Akt (Ser-473), Akt, and Caveolin-1 levels by Western blotting. Tubulin was used as a loading control. H, H460 cells were treated with DPTANONOate (0–40 μ M) for 5 days and analyzed for phosphorylated Akt (Ser-473), p-Src (Tyr-416), p-Erk1/2 (Thr-202/Tyr-204), and Caveolin-1 levels by Western blotting. The bars are means \pm S.D. (n = 3). *, p < 0.05 versus nontreated cells. I, H23 cells were treated with DPTANONOate (0–40 μ M) for 5 days and analyzed for phosphorylated Akt (Ser-473) and Caveolin-1 levels by Western blotting. The bars are means \pm S.D. (n = 3). *, p < 0.05 versus nontreated cells. J, H292 cells were treated with DPTANONOate (0–40 μ M) for 5 days and analyzed for phosphorylated Akt (Ser-473) and Caveolin-1 levels by Western blotting. The bars are means \pm S.D. (n = 3). *, p < 0.05 versus nontreated cells. K, H460 cells were treated with DPTANONOate and Perifosine for 5 days and analyzed for Oct4 levels by Western blotting. GAPDH was used as a loading control. L, H460 cells were treated with control, DPTANONOate, DPTANONOate + Perifosine, and Perifosine for 5 days and analyzed for Oct4 levels by Western blotting. The bars are means \pm S.D. (n = 3). *, p < 0.05 versus control.

phosphorylated Src (Tyr-416), Src, phosphorylated ERK1/2, Eek (1/2), and Cav-1 by Western blotting. The blots were reprobbed with tubulin to confirm equal loading of the samples. H23(F) and H292 (G) were treated with DPTA NONOate (0–40 M) for 5 days and analyzed for phosphorylated Akt (Ser-473), Akt, and Cav-1 by Western blotting. The blots were reprobbed with tubulin to confirm equal loading of the samples. The immunoblot signals H460 (H), H23 (I), and H292 (J) were quantified by densitometry, and mean data from independent experiments were normalized and presented. The bars are means \pm S.D. (n = 3). *, p < 0.05 versus nontreated cells. K, H460 cells were treated with 40 M DPTA NONOate, 40 M NONOate + 2.5 M perifosine (specific Akt inhibitor), or 2.5 M perifosine for 5 days and subjected to Western blot analysis for Oct4 detection. L, Western blotting bands of Oct4 were quantified by densitometry, and mean data from independent experiments were normalized and presented. The bars are means \pm S.D. (n = 3). *, p < 0.05 versus control cells

Caveolin-1 interacts with Oct-4

The scaffolding function of Cav-1 has been shown to be important in the stability and function of several proteins (35, 51, 54). To test whether Cav-1 could interact and form a molecular complex with Oct4, H460 cells were immunoprecipitated with an anti-Oct4 or anti-Cav-1 antibody and analyzed for specific protein-binding partners by Western blotting. Fig. 6A shows that when Oct4 was immunoprecipitated with anti-Oct4 antibody, the resulting immune complexes were positive with anti-Cav-1 antibody but not with anti-p-Cav-1 (Tyr-14) antibody, indicating that Oct4 forms a molecular complex with Cav-1 but not with p-Cav-1 (Tyr-14). To confirm, Akt activity in the cells was enhanced by SC79, a specific Akt activator, and the alteration in level of p-Cav-1 (Tyr-14) and its interaction with Oct4 were analyzed (Fig. S2C). Under active Akt status (10 M SC79 treatment), we observed the significant up-regulation of p-Cav-1 (Tyr-14) and the decrease of the Oct4:Cav-1 complex (Fig. S2C).

The results showed that Cav-1 was immunoprecipitated with anti-Cav-1 antibody, and the immune complexes were similarly positive for anti-Oct4 antibody (Fig. 6B). A previous study (46) showed that Akt activity could facilitate phosphorylation of Oct4 and subsequently promoted proliferation of CSCs. To test whether phosphorylated Oct4 could bind with Cav-1, anti-pOct4 antibody was used for immunoprecipitation, and the immunoprecipitation complexes were subjected to evaluation for Cav-1 expression. Fig. 6C shows that p-Oct4 (Ser-236) formed complexes only with the Cav-1-

form (21 kDa mass). As expected, p-Cav-1(Tyr-14) formed no immune complexes with Oct4 (Fig. 6D). Taken together, we found the Cav-1:Oct4 protein:protein complex can be inhibited by the phosphorylation of Cav-1 at tyrosine 14.

To substantiate the Oct4:Cav-1 interaction, in-cell co-localization experiments were conducted using proximity ligation assay. In this study, cells were treated with anti-Oct4 and anti-Cav-1, followed by an addition of plus and minus proximity ligation assay (PLA) probes with

attached specific DNA strands. The two DNA strands in proximity were ligated, amplified, and visualized under a fluorescence microscope. Fig. 6E shows the in-cell Oct4:Cav-1 protein:protein complexes (green fluorescence) with Hoechst 33342 (blue fluorescence) serving as a nuclear stain. These results support the immunoprecipitation results and indicate the direct interaction between Oct4 and Cav-1 in the tested lung cancer cells.

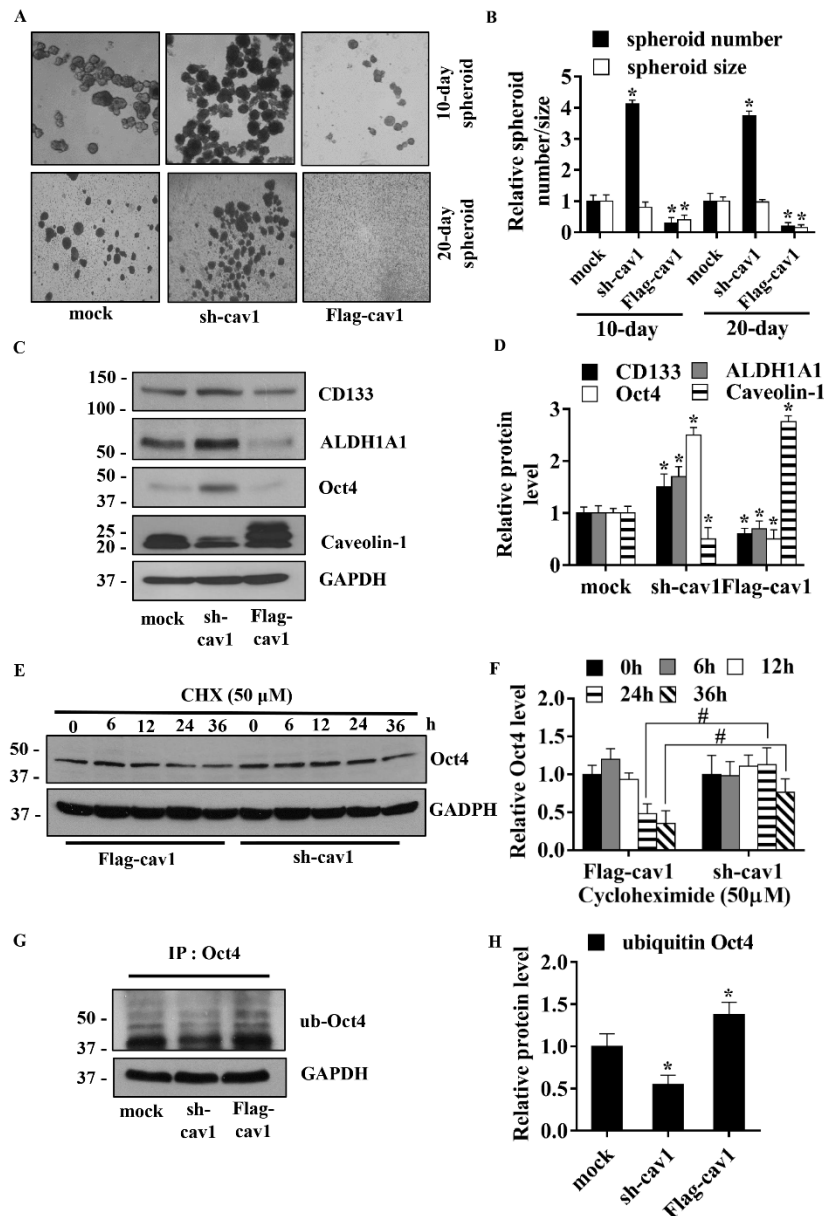


Figure 5. Caveolin-1 diminishes human lung CSC-like phenotypes.

A, stable transfection of H460 with short hairpin plasmid (sh-cav1), Cav-1–overexpressing plasmid (FLAG-cav1), and control were suspended and subjected to spheroid formation assay. B, relative spheroid number and size were analyzed and calculated as relative to mock-transfected cells on days 10 and 20 of the assay. All plots are means \pm S.D. (n = 3). *, p < 0.05 versus mock cells. C, stable transfections of H460 cells with sh-cav1, FLAG-cav1,

or control were analyzed for Cav-1, CSC markers (CD133 and ALDH1A), and CSC transcription factor (Oct4) by Western blotting. Blots were re-probed with GAPDH as a loading control. D, immunoblot signals were quantified by densitometry, and mean data from independent experiments were normalized and presented. The bars are means S.D. (n = 3). *, p < 0.05 versus mock cells. E, stable transfections of H460 cell with sh-cav1 and FLAG-cav1 were treated with 50 μ g/ml CHX at indicated times and analyzed for Oct4 level by Western blotting. The blots were re-probed with GAPDH to confirm equal loading of the samples. F, immunoblot signals were quantified by densitometry, and mean data from independent experiments were normalized and presented. The bars are means S.D. (n = 3). #, p < 0.05 versus FLAG-cav1-transfected cells. G, stable transfected H460 cells were treated with 10 μ M lactacystin for 12 h and subjected to Oct4 immunoprecipitation (IP) of Oct4. The immune complexes were analyzed for ubiquitin by Western blotting. H, immunoblot signals were quantified by densitometry, and mean data from independent experiments were normalized and presented. The bars are means S.D. (n = 3). *, p < 0.05 versus mock cells.

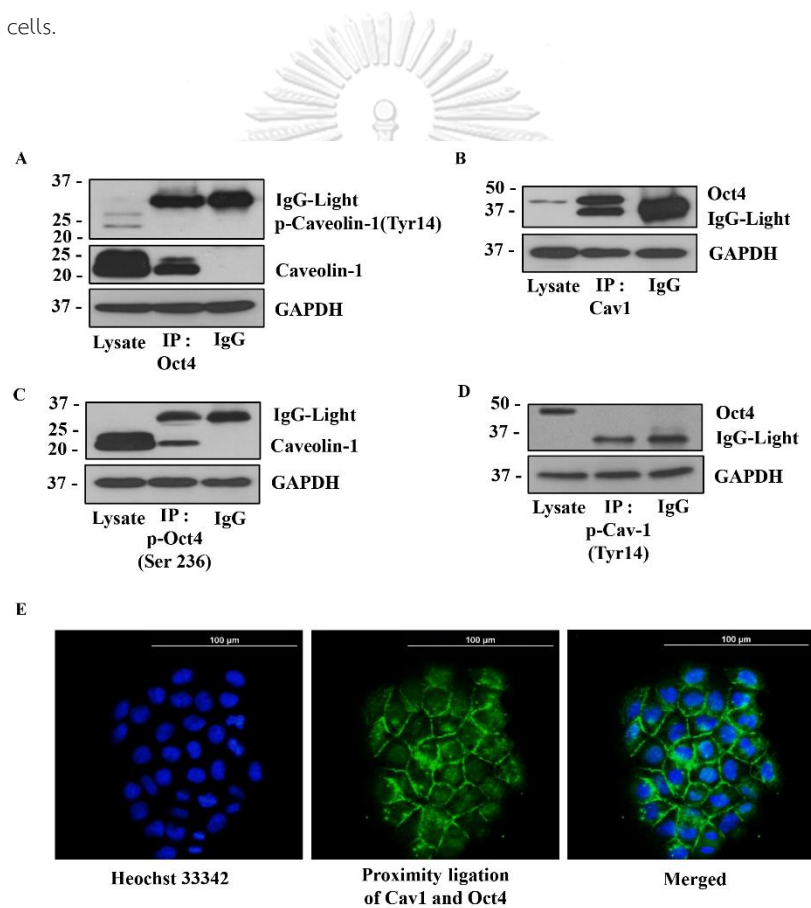


Figure 6. Caveolin-1 exhibits direct protein-protein interaction with Oct4.

A, H460 cell lysates were prepared and immunoprecipitated (IP) with anti-Oct4 antibody or control IgG and then analyzed Cav-1 and phosphorylated Cav-1 (Tyr-14) by Western blotting assay. B, H460 cell lysates were prepared and immunoprecipitated with anti-Cav-1 antibody or control IgG and then analyzed Oct4 with Western blotting assay. C, H460 cell lysates were prepared and immunoprecipitated with anti-phosphorylated Oct4 (Ser-236) antibody or control IgG and then analyzed the Cav-1 expression by Western blotting assay. D, H460 cell lysates were prepared and immunoprecipitated with anti-phosphorylated Cav-1(Tyr-14) antibody or control IgG,

then evaluated Oct4 protein level by Western blotting. In all experiments, immunoblots were performed on cell lysates used as input for immunoprecipitation (IP) using GAPDH antibody to confirm equal loading of the samples. E, protein-protein interaction of Cav-1 and Oct4 was confirmed by PLA in H460 cells. After plating H460 cells for 24 h, the cells were permeabilized and stained with rabbit anti-Cav-1 and mouse anti-Oct4 for 24 h. The stained cells were subjected to PLA following the manufacturer's instruction. The interaction between Cav-1 and Oct4 was visualized by fluorescence microscopy (20). Cells were stained with Hoechst 33342 dye to aid visualization of the cell nucleus. The Cav-1:Oct4 complexes appear as green fluorescence.

NO-mediated phosphorylation of Akt promotes Oct4 expression by dissociating it from caveolin-1 complex

To investigate the effect of NO on the binding interaction between Oct4 and Cav-1, immunoprecipitation studies were conducted in cells treated with DPTA NONOate. After the treatment, cell lysates were prepared and immunoprecipitated with an anti-Oct4 antibody. The immune complexes were then analyzed for Cav-1 by Western blotting. Fig. 7, A and B, shows that as compared with the untreated control, the NO donor treatment dramatically decreased the binding interaction between Oct4 and Cav-1. We also investigated the potential role of Akt in regulating the Oct4:Cav-1 complex formation because Akt is a known target of NO (22) and is involved in many cancer cell behaviors, including cell invasiveness, anoikis, chemotherapy resistance, and tumorigenesis (56). In this study, H460 cells were treated with DPTA NONOate in the presence or absence of perifosine, a specific Akt inhibitor, and after the treatment, cells lysates were prepared and immunoprecipitated with an anti-Oct4 antibody. The resulting immune complexes were then probed for Cav-1 by Western blotting. The results showed that the Akt inhibitor (perifosine) significantly increased the Cav-1:Oct4 complex formation, whereas the NO donor decreased the complex formation (Fig. 7, C and D). These results indicate that the complex formed by Cav-1 and Oct4 is regulated by NO through an Akt-dependent process. Together with the results from Fig. 4, NO increased stability of Oct4 by inducing Akt phosphorylation (Ser-473), which diminished the interaction of Oct4 to Cav-1.

Cav-1 was earlier shown to decrease the cellular level of Oct4 by forming a repression complex. To investigate whether Cav-1 diminishes the activity of NO on Oct4, Cav-1 knockdown (shRNA-Cav-1) or overexpressing (FLAG-Cav-1) cells were treated with DPTA NONOate, and the expression level of Oct4 in these cells was determined by Western blotting. Fig. 7, E and F, shows that the NO treatment significantly increased Oct4 levels in the both Cav-1 knockdown and overexpressing cells. As expected, the difference in Oct4 expression between the treated and untreated cells was significantly higher in the knockdown cells compared with the overexpressing cells. These results suggest that Cav-1 not only decreases the Oct4 level but also diminishes the efficacy of NO to up-regulate Oct4.

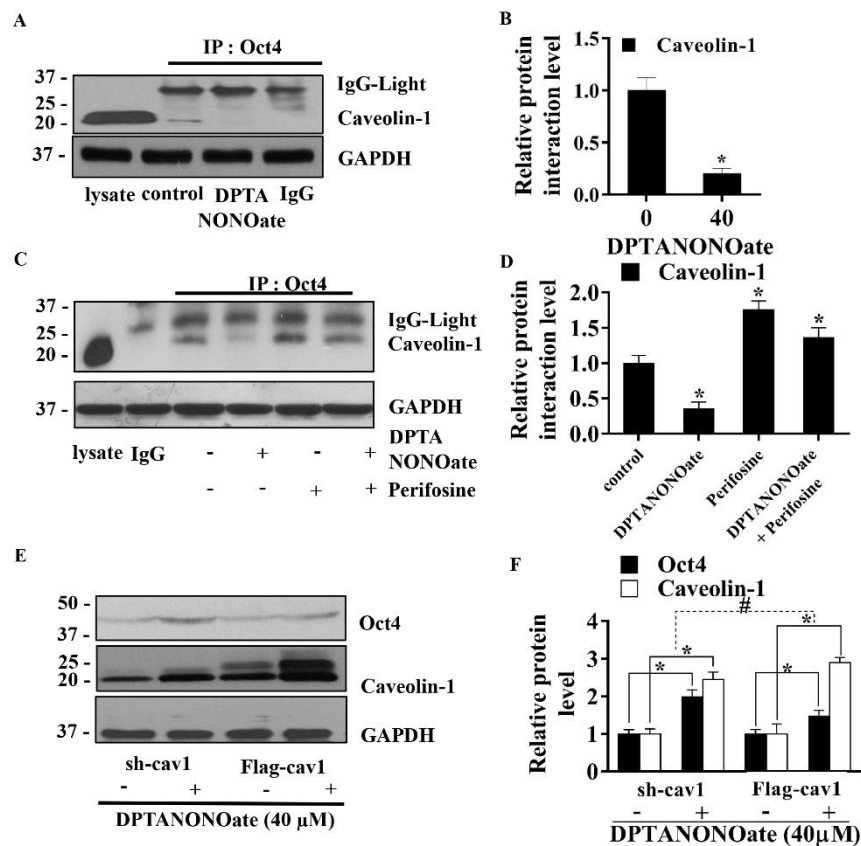


Figure 7. NO-mediated Akt diminishes the interaction between Cav-1 and Oct4.

A, after treating with DPTA NONOate (40 M) for 12 h, the H460 cell lysates were prepared and subjected to immunoprecipitation (IP) with antiOct4 antibody or control IgG and then analyzed the Cav-1 level by Western blotting. B, interaction signals were quantified by densitometry, and mean data from independent experiments were normalized and presented. The bars are means S.D. (n = 3). *, p < 0.05 versus control cells. C, H460 cells were treated with 40 M DPTA NONOate, 2.5 M perifosine (specific Akt inhibitor), or 40 M NONOate + 2.5 M perifosine for 12 h, subjected to immunoprecipitation with anti-Oct4 antibody or control IgG, and then evaluated the Cav-1 protein level by Western blotting. D, interaction signals were quantified by densitometry, and mean data from independent experiments were normalized and presented. The bars are means S.D. (n = 3). *, p < 0.05 versus control cells. In all experiments, the immunoblots were performed on cell lysates used as input for immunoprecipitation using GAPDH antibody to confirm equal loading of the samples. E, stable transfections of H460 cells with sh-cav1 or FLAG-cav1 were treated with 40 M NONOate for 5 days, and cell lysates were performed, and measurement of Oct4 and Cav-1 levels was by Western blotting. F, immunoblot signals were quantified by densitometry, and mean data from independent experiments were normalized and presented. The bars are means S.D. (n = 3). *, p < 0.05 versus nontreated cells. #, p < 0.05 versus the sh-cav1 means difference of nontreated and treated cells.

Tyrosine 14 of caveolin-1 is required for its interaction with Oct4.

Our immunoprecipitation study demonstrated that phosphorylated Cav-1 (Tyr-14) was unable to form a complex with Oct4 (Fig. 6, A and D). To determine whether tyrosine 14 of Cav-1 is essential for the complex formation, site-directed mutation of tyrosine to phenylalanine at position 14 of Cav-1 (Y14F) was performed in pcDNA3.1 His-Myc plasmid. The mutated plasmid was transfected into H460 cells, and its effect on Cav-1:Oct4 complex formation was determined compared with WT FLAG-Cav-1 transfection. Cell lysates of His-Myc-Cav-1 (Y14F)-transfected cells and control FLAG-Cav-1-transfected cells were prepared and immunoprecipitated with anti-His and anti-FLAG antibody, respectively. The immune complexes were analyzed for Oct4 expression by Western blotting. As expected, the tyrosine to phenylalanine mutation at position 14 of Cav-1 prevented its interaction with Oct4 (Fig. 8A). These results clearly indicate that tyrosine 14 of Cav-1 is essential for the complex formation with Oct4 and suggest that phosphorylation of the tyrosine residue may interrupt the complex formation.

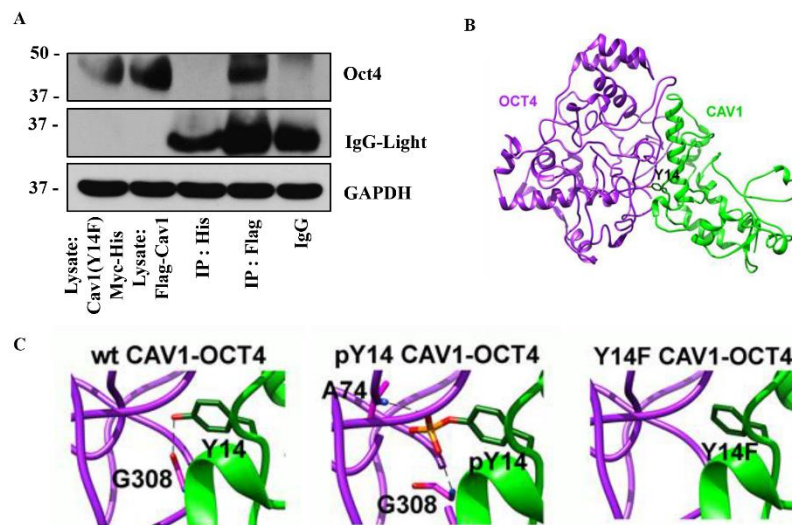


Figure 8. Effect of Cav-1 (Y14F) mutation on the interaction between Cav-1 and Oct4.

A, H460 cells were transfected with Cav1-(Y14F)-Myc-His or FLAG-Cav1. The transfected cells were subjected to co-immunoprecipitation by pulling down the tagged proteins (IP:His for Cav1(Y14F)Myc-His and IP:FLAG for FLAG Cav1) and measuring the level of Oct4 by Western blotting. B, 3D model of WT Cav-1 (wtCav1) (green) bound with Oct4 (purple), where the Tyr-14 residue is presented as a green stick. C, close-up of the Cav-1 residue 14 on intermolecular hydrogen bond interaction with the Oct4 residues (Gly-308) (dashed line) for the WT, pTyr-14, and Y14F Cav-1:Oct4 complexes.

Cav-1:Oct4 complex models

Most Cav-1-interacting proteins contain a caveolin-binding motif (CBM) comprising XXXXX, XXXXXX, or XXXXXXXX, where is an aromatic amino acid, and X is any amino acid (50), but Oct4 does not contain this domain (42). To investigate how Cav-1 interacts with Oct4 and what specific amino acid residue(s) may be responsible for this interaction, we conducted a computational modeling study of the Cav-1:Oct4 complex. The optimized structures of all model complexes are depicted in Fig. 8, B and C, and the intermolecular hydrogen binding (H-bond) interactions formed between the two proteins are summarized in Table 1. Note that the H-bond was defined by the following criteria: (i) the distance between the H-bond donor (D) and acceptor (A) atoms is less than 3.5 Å, and (ii) the angle between D-H-A is larger than 120°. From Table 1, it appears that most H-bonds between Cav-1 and Oct4 proteins are conserved, even though Tyr-14 is either phosphorylated or mutated to phenylalanine. Interestingly, the Y14F substitution in Cav-1 introduced a loss of H-bond at the mutated residue, whereas an additional H-bond between the Cav-1 pTyr-14 residue and the Oct4 Ala-74 residue was detected (see also Fig. 8C).

The effect of phosphorylation (pTyr-14) and single mutation (Y14F) of Cav-1 on its binding interaction with Oct4 was investigated using the molecular modeling/Poisson-Boltzmann surface area (MM/PBSA) method. The binding free energy (G_{bind}) and its energetic components on the minimized structures of the WT, pTyr-14, and Y14F Cav-1 complexed with Oct4 are summarized in Table 2. The overall structures of the three complexes are relatively similar, and thus the entropic term can be ignored. Table 2 shows that both pTyr-14 and Y14FCav-1 induce an increase in G_{bind} 30 and 3 kcal/mol respectively. Although the negative charge of pTyr-14 leads to a more favorable electrostatic interaction (by 78 kcal/mol), the large positive polar solvation free energy ($\Delta G_{\text{sol-ele}}$ of 602.4 kcal/mol) reduces the binding efficiency between pTyr-14 Cav-1 and Oct4 proteins. Meanwhile, both van der Waals and electrostatic contributions are slightly reduced in the case of Y14F Cav-1 mutant. These computational models are consistent with our experimental data that could indicate that NO-mediated Akt liberates Oct4 from the Cav-1:Oct4 complex through Tyr-14 phosphorylation of Cav-1. The released Oct4 is accumulated in the cells and promotes the expression of stemness-related genes as depicted in Fig. 9, A and B.

Table 1

Hydrogen bond pairs detected at the Cav-1–Oct4 interface for the three studied systems.

@ means “at” the specific functional group

CAV1	OCT4	WT CAV1-OCT4	pY14 CAV1-OCT4	Y14F CAV1-OCT4
Y6@OH	D20@O	✓	✓	-
Y6@N		-	-	✓
H12@ND1	S12@OG	✓	✓	✓
H12@N		✓	✓	✓
Y14@OH	G308@O	✓	-	-
pY14@O1P	A74@N	-	✓	-
pY14@O3P	G308@N	-	✓	-
V41@O	Y325@OH	✓	-	-
	Y325@N	-	✓	✓
H45@NE2	G17@N	-	-	✓
H45@O	H329@NE2	✓	✓	✓
T46@OG	G18@N	✓	✓	✓
V52@O	K254@NZ	✓	✓	✓
N53@O		✓	✓	✓
R54@O		✓	✓	✓
N53@OD1	R282@NE	✓	✓	✓
	R282@NH2	✓	✓	✓
D61@OD1	Y292@N	✓	-	✓
	Y292@OH	-	✓	-
F68@O	R295@NH1	✓	✓	✓
E69@OE2	Q294@N	✓	✓	✓

Table 2

The binding free energy and its components (kcal/mol) calculated from MM/PBSA method.

	WT CAV1-OCT4	pY14 CAV1-OCT4	Y14F CAV1-OCT4
MM			
ΔE_{ele}	-372.8	-450.9	-362.9
ΔE_{vdW}	-161.4	-156.0	-160.6
ΔE_{MM}	-534.2	-610.9	-523.5
PBSA			
$\Delta G_{sol-ele}$	494.8	602.4	487.0
ΔG_{sol-np}	-25.4	-26.2	-25.4
ΔG_{sol}	469.4	576.2	461.6
$\Delta E_{ele} + \Delta G_{sol-ele}$	122.0	151.5	124.1
$\Delta E_{vdW} + \Delta G_{sol-np}$	-186.8	-182.2	-186.0
ΔG_{bind}	-64.8	-34.8	-62.0

Discussion

In this study, we provided new evidence showing that NO promotes CSC-like phenotypes in lung cancer cells in part through its stabilizing effect on Oct4. CSCs are the specific population of cancer cells that resides in solid tumors and in leukemia (1, 2). The regulation of CSCs is believed to control the aggressiveness of cancers (4). Various intrinsic and extrinsic stimuli and their cross-talk were documented as the important factors controlling the stemness of cancer cells (57, 58). The intrinsic factors include tumor suppressor proteins, oncoproteins, and epigenetic regulators, whereas the extrinsic factors include microenvironmental mediators, cytokines, and paracrine factors in the circulating system. NO is a microenvironmental mediator that is elevated in several types of cancer, including lung cancer, colon cancer, and breast cancer (19, 59, 60). An aberrantly high expression of NO was also shown to be correlated with poor prognosis of several cancers. These clinical data are consistent with previous experimental data by our groups and others showing the stimulating effect of NO on cancer cell aggressiveness (22–26).

Oct-4 is recognized as a key transcription factor controlling the stemness of both normal and cancer cells. In lung cancer cells, the expression of Oct4 is highly correlated with the aggressiveness and stemness of the cells (12, 13, 41). Moreover, in various cancer types, an increased expression of Oct4 was found to be highly correlated with CSC level and disease progression (16, 61). The level of Oct4 is primarily regulated by post-translational modifications that control both the expression and activity of Oct4 (52). Alterations in this process could result in Oct4 dysregulation and malfunctions. The stability of Oct4 is largely controlled by its degradation that occurs mainly through the ubiquitin–proteasome degradation pathway (52). We found that NO exerts its effect on Oct4 by interfering with this degradation process, thereby increasing its cellular level. In conformity with this finding, we also observed an increase in stem cell marker expression and CSC-like behaviors in the treated cells with elevated Oct4 levels.

In addition, Sox2 dramatically decreased in dose- and time-dependent manners after NO treatment. The up-regulation of Oct4 with down-regulation of Sox2 were also found in cervical cancer, and such a pattern was found to be strongly associated with a poor prognosis (62). Besides, a previous study found that the concomitant increase of Oct4, Klf4, and MYC with activated status of Akt can deplete endogenous Sox2 (63). Likewise, our microarray analysis revealed that NO promoting transcriptional signaling of Oct4, Klf4, and Myc cascades and Akt activity may negatively influence Sox2 expression in our system. Previous studies indicated that Sox2 functions as a differentiation enhancer in several cells, including lung cells (64–67), suggesting that NO not only increased stem cell transcription factor Oct4, but also decreased differentiation signals by decreasing the expression of Sox2.

Akt has been reported to regulate Oct4 (46), and its activation due to genetic instability is frequently observed in lung cancer (68). Enhanced Akt activation has also been shown to be correlated with chemo- and radiotherapy resistance (69) and metastasis (70), and both are key characteristics of CSCs. Moreover, the levels of Akt and Oct4 are correlated with poor prognosis of patients. In this study, we found that NO regulates CSC-like phenotypes of lung cancer cells by increasing the stability of Oct4 in an Akt-dependent manner.

We demonstrated that Cav-1 has a negative regulatory effect on Oct4 stability through its scaffolding property. Indeed, the Cav-1:Oct4 complex facilitates Oct4 degradation via the ubiquitin–proteasome pathway. The disruption of such a complex diminishes the degradation of Oct4 and increases its cellular level, thus promoting the CSC-like behaviors. Moreover, we found that Oct4, which lacks the CBM (42), can form a molecular complex with Cav-1 through H-bonding. To our knowledge, this is the first demonstration of the protein–protein interaction of Cav-1 and its binding partner that does not occur through the interaction between CBM and caveolin-scaffolding domain (50). We further found that the tyrosine residue at position 14 of Cav-1 is required for its interaction with Oct4, i.e. via H-bonding possibly between the H-bond donor OH-tyrosine 14 and H-bond acceptor that resides in Oct4. Such binding interaction is disrupted when the Tyr-14 of Cav-1 is phosphorylated or mutated.

Although Cav-1 is highly co-expressed with NOS in cancer (33), it can negatively regulate NOS. For example, Cav-1 was shown to inhibit the function of NO synthases that produce NO by interacting via its caveolin-scaffolding domain (34, 35). This suggests that Cav-1 and NO may play an opposite role in the regulation of CSCs. We found that Cav-1 forming the complex with Oct-4 and facilitate Oct4 degradation. Together with results from Fig. 4 indicated that NO contradicts the role of Cav-1 through Akt-dependent manner by Akt-mediated diminish the interaction of Oct4 to Cav-1.

Surprisingly, we found that treatment of the cells with NO also increased the Cav-1 level. Although there is no clear explanation, in our opinion such a phenomenon may be due to the compensation mechanism of the cells for balancing control of Oct4. Besides, we previously showed that NO could increase the Cav-1 level by directly inhibiting its degradation through S-nitrosylation (71).

As Oct4 (72–74) and Cav-1 (75–78) were found in various types of normal and cancerous cells, and the function of Oct4 in the regulation of stem cell properties was widely demonstrated in both CSC and noncancerous stem cells (72–74), it is interesting to investigate for the Cav-1:Oct4 suppressor complex in normal stem cells. Also, the abundance of Oct4 in cancer cells

may be enhanced by the fact that the cancer cells frequently reside in a high NO concentration environment (19) or gain of Akt function (79).

In summary, our data demonstrated that NO positively regulates CSC markers, including CD133, ALDH1A1, and ABCG2, and promotes tumor spheroid formation, a key feature of CSCs, through its stabilizing effect on Oct4. Such up-regulation depends on Akt activation and complex formation between Oct4 and Cav-1. By forming a molecular complex with Oct4, Cav-1 facilitates ubiquitin–proteasome-mediated degradation of Oct4, which lowers its cellular level and thus bioactivity. NO promotes the release of Oct4 from the complex, decreasing its degradation and enhancing its activity on CSCs. In forming the complex, the tyrosine 14 residue of Cav-1 is crucial for its interaction with Oct4. Mutation or phosphorylation of this residue, i.e. by tyrosine to phenylalanine substitution or by NO-mediated Akt activation, diminishes the interaction. Together, our findings unveil a novel mechanism of CSC regulation, which could be important in understanding the aggressive behaviors of cancer cells and in identifying potential drug targets for CSC therapy.

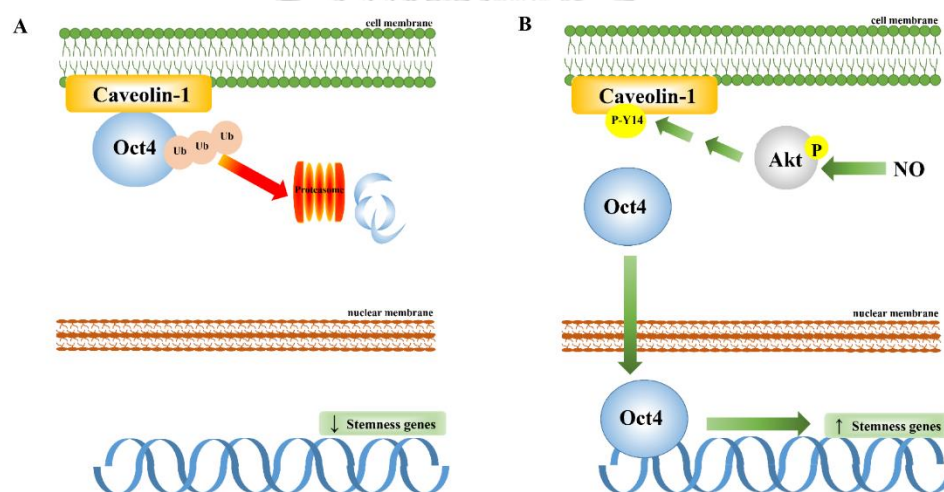


Figure 9. Schematic overview of NO-promoted CSC-like phenotypes through stabilization of Oct4 cellular level by dissociating it from the Cav-1:Oct4 degradation complex.

A, in the absence of NO, Cav-1 binds to Oct4 and enhances its degradation through the ubiquitin–proteasome pathway. The reduction of cellular Oct4 level by Cav-1 leads to a decrease in stemness-related gene expression, which diminishes CSC-like phenotypes. B, in the presence of NO, NO promotes phosphorylation of Cav-1 (tyrosine 14) through the activation of Akt signaling. Because Cav-1 is phosphorylated, Oct4 is dissociated from the Cav-1 complex. The liberated Oct4 accumulates in the nucleus and enhances the expression of stemness-related genes, which promote CSC-like phenotypes.

Experimental procedures

Cells and reagents

Human nonsmall cell lung cancer (NSCLC)-derived cell lines H460, H23, and H292 were obtained from the American Type Culture Collection ATCC (Manassas, VA). The cells were cultured in RPMI 1640 medium supplemented with 10% fetal bovine serum (FBS), 2 mM L-glutamine, and 100 units/ml each of penicillin and streptomycin (Gibco) at 37 °C in a 5% CO₂-humidified incubator. Cells were routinely passaged at preconfluent density using a 0.25% trypsin solution with 0.53 mM EDTA.

RPMI 1640 medium, FBS, L-glutamine, penicillin/streptomycin, phosphate-buffered saline (PBS), trypsin, and EDTA were purchased from Gibco. NO donor dipropyleneetriamine (DPTA) NONOate was purchased from Santa Cruz Biotechnology (Santa Cruz, CA). MTT, dimethyl sulfoxide (DMSO), Hoechst 33342, PI, and bovine serum albumin (BSA) were purchased from Sigma. Perifosine (Akt inhibitor), antibodies for Akt (catalog no. 9272), phosphorylated Akt (Ser-473) (catalog no. 4060), ERK (catalog no. 4695), phosphorylated ERK (Thr- 202/Tyr-204) (catalog no. 4370), Src (catalog no. 2109), phosphorylated Src (Tyr-416) (catalog no. 6943), ABCG2 (catalog no. 42078), ALDH1A1 (catalog no. 54135), Oct4 (catalog no. 4286), Sox2 (catalog no. 3579), Nanog (catalog no. 8822), Caveolin-1 (Cav-1) (catalog no. 3267), phosphorylated Cav-1 (Tyr-14) (catalog no. 3251), -actin (catalog no. 3700), -tubulin (catalog no. 2125), GAPDH (catalog no. 2118), and secondary antibodies conjugated with horseradish peroxidase (HRP) were purchased from Cell Signaling (Danvers, MA). Antibody for CD133 (catalog no. 130-090-422) was purchased from NewEast Bioscience (Miltenyi Biotec GmbH, Germany). Antibody for ubiquitin (catalog no. u0508) was purchased from Sigma. Protein G-agarose bead was purchased from GE Healthcare (Uppsala, Sweden).

Cytotoxicity assay

For cytotoxicity assay, cells were seeded onto 96-well plates at a density of 1x 10⁴ cells/well and were allowed to incubate overnight. Cells were then treated with various concentrations of NO donor (DPTA NONOate 0–200 M) and analyzed for cell viability using MTT assay according to the manufacturer's protocol (Sigma). In brief, the medium was replaced, and the treated cells were treated with MTT (500 g/ml) for 4 h at 37 °C. After that, the supernatant was removed, and 100 μ l of DMSO was added to solubilized crystal formazan product. The intensity of the formazan product was determined by spectrophotometry at 570 nm using a microplate reader (Anthros, Durham, NC). The cytotoxicity index was calculated by dividing the absorbance of the treated cells by that of the control cells.

Cell death assay

H460 cells were plated on 96-well plates at a density of 1×10^4 cells/well and allowed to attach overnight, after which they were subjected to treatment with DPTA NONOate (0–200 M) for 24 h. After treatment, the cells were washed with PBS and incubated with 10 g/ml Hoechst 33342 and 5 g/ml PI for 30 min at 37 °C. Nuclear condensation or DNA fragmentation of apoptotic cells and PI-positive necrotic cells was visualized and scored under a fluorescence microscope (Olympus IX51 with DP70 digital camera system, Tokyo, Japan).

Spheroid formation assay

After treatment, the cells were trypsinized with 2.5% trypsin/EDTA and seeded into a 24-well ultralow attachment plate at the density of 2.5×10^3 cells/well in RPMI 1640 serum-free medium. Phase-contrast images of formed spheroids were taken at days 10, 20 and 40 post-seeding using an inverted phase-contrast microscope (Olympus IX51 with DP70).

Microarray analysis

After specific treatment, the cells were harvested; mRNA was collected, and cRNA was prepared as per Affymetrix's protocol. The gene probes list is shown in Table S1. Gene expression profiles of two independent experiments were analyzed by the CU-DREAM program (37). The gene probes with significant differences ($p < 0.05$) between control and treatment groups were chosen to evaluate and generate a heat map by using the Bioconductor R statistic programs. The gene probes with a strongly significant difference ($p < 0.01$) (Table S2) between control and treatment groups were enriched (<http://amp.pharm.mssm.edu/Enrichr/>) (38, 39) for analyzing gene set enrichment.

RNA isolation and RT-PCR

Total RNA was prepared using TRIzol reagent (Invitrogen), and cDNA was prepared using SuperScript III first-strand synthesis system and oligo(dT) primer (First BASE Laboratories Sdn Bhd) (primer sequences shown in Fig. 3). Quantitative PCR analysis was performed on a 7500 Fast real-time PCR using a Power SYBR Green PCR master mix (Applied Biosystems). 95 °C for 10 min was used for initial enzyme activation and was followed by 40 cycles of denaturation at 95 °C for 15 s and then at 60 °C for 1 min for annealing and extension processes. Relative expression of each gene was normalized with GAPDH gene product.

Plasmid construction and transfection

Plasmid construction

Cav-1 shRNA (sc-29241-SH) was purchased from Santa Cruz Biotechnology, Inc. A full-length WT Cav-1 expression vector was generated by subcloning a pGex-Cav1 (a gift from

Ambra Pozzi (Addgene plasmid catalog no. 33364) into pCANw-FLAG to generate the pCANwFLAG-Cav-1. The plasmid containing site-directed mutation of Cav-1 (Y14F) was purchased as pcDNA3.1()myc-His- Cav-1(Y14F) and verified by GeneArt gene synthesis (quality assurance documentation 16AAX3YC).

Plasmid transfection

Subconfluent (70%) monolayers of cells were transfected with pCANw-FLAG-cav-1 or Cav-1 shRNA or pcDNA3.1()myc-His- cav(Y14F) plasmid in OptiMEM reduced serum media (Gibco, Life Technology, Inc.) using Lipofectamine 3000 reagent, according to the manufacture's protocol (Invitrogen). After 48 h, the medium was replaced with RPMI 1460 medium containing 10% FBS, and the transfected cells were used as transient transfection. For stable transfection, the transfected cells were further cultured and selected for antibiotic resistance for 30 days. The expression of the targeted protein or tagged protein were verified by Western blotting. The cells were cultured in antibiotic-free RPMI 1640 medium for at least two passages before further study.

Co-immunoprecipitation

After specific treatments, cells were washed with PBS and lysed with lysis buffer (20 mM Tris-HCl, 1 mM MgCl₂, 150 mM NaCl, 1% Nonidet P-40, 10% glycerol, supplemented with protease inhibitor mixture (Merck, Calbiochem)) and phosphatase inhibitor mixture (Sigma) at 4 °C for 20 min. The lysate was pre-cleared by incubating with beads at 4 °C for 1 h and then centrifuged at 12,000 g for 20 min at 4 °C. Cell supernatant was determined for protein content using the Bradford method (Pierce™, BCA protein assay kit, ThermoFisher Scientific). Cell lysates (500 µg of protein) were incubated with specific antibody at 4 °C overnight. After that, the lysate:immune complexes were incubated with protein G-conjugated agarose beads for 4 h at 4 °C. The immune:protein:bead complexes were washed five times with cold lysis buffer and suspended in 6Laemmli sample buffer. The protein complexes were separated by SDS-PAGE and analyzed for protein expression by immunoblotting assay.

Western blot analysis

After specific treatments, cells were incubated with lysis buffer containing 20 mM Tris-HCl (pH 7.5), 1% Triton X-100, 150 mM NaCl, 1 mM Na₂EDTA, 1 mM EGTA, 2.5 mM sodium pyrophosphate, 1 mM -glycerophosphate, 1 mM sodium orthovanadate, 50 mM sodium fluoride, 1 g/ml leupeptin, 100 mM phenylmethylsulfonyl fluoride, and protease inhibitor mixture (Roche Applied Science) for 30 min on ice. Cellular lysates were collected and determined for protein content using BCA protein assay kit (Pierce). Equal amounts of protein from each sample were resolved by SDS-PAGE. After separation, proteins were transferred onto 0.45-m nitrocellulose

membranes (BioRad). The blots were blocked for 1 h in 5% nonfat dry milk in TBST (Tris-buffered saline with 0.1% Tween containing 25 mM Tris-HCl (pH 7.5), 125 mM NaCl, and 0.1% Tween 20) and incubated with appropriate primary antibodies at 4 °C overnight. After three washes with TBST, the membrane blots were incubated with HRP-conjugated secondary antibodies for 2 h at room temperature. The immune blots were detected by enhanced chemiluminescence (Supersignal West Pico; Pierce) and quantified using ImageJ software.

Immunofluorescence

Cells were washed with PBS, fixed with 4% paraformaldehyde in PBS at room temperature for 10 min, and permeabilized with 0.1% Triton X-100 in PBS for 5 min. They were then washed with PBS and blocked for nonspecific binding by incubation with 3% BSA in PBS for 30 min. The blocked cells were incubated with specific antibody overnight, and after washing with PBS, they were incubated with species-specific AlexaFluor488-conjugated antibody or AlexaFluor569-conjugated antibody for 2 h. The stained cells were washed and mounted with an antifade mounting medium. Hoechst 33342 was used to stain the cell nucleus. The cells were visualized by fluorescence imaging (Olympus IX5).

Proximity ligation assay

Cells were fixed with 4% paraformaldehyde in PBS at room temperature for 10 min and permeabilized with 0.1% Triton X-100 in PBS for 5 min. Then the fixed cells were incubated with primary antibodies (against Cav-1 and Oct4) for 24 h at 4 °C. Excess primary antibodies were removed by washing the cells with cold PBS, and oligonucleotide-conjugated secondary antibodies (PLA probe MINUS and PLA probe PLUS) were added to the cells and allowed to be incubated for 1 h at 37 °C.

The samples were washed with a buffer containing 0.01 M Tris (pH 7.4), 0.15 M NaCl, and 0.05% Tween 20 and treated with a ligation solution for 30 min at 37 °C. After that, the ligate nucleotides were amplified and labeled with a fluorescence probe by added amplification solution (fluorescently labeled oligonucleotides) and polymerase solution in pre-heated humidity 37 °C incubator for 100 min. After washing and drying at room temperature in the dark, the samples were mounted using an antifade mounting medium containing 4,6-diamidino-2-phenylindole. Specific protein-protein interactions were analyzed by fluorescence microscopy (Olympus IX5).

Computational method

To date, the three-dimensional structures of both CAV1 and OCT4 have yet to be resolved; therefore, in this study, homology modeling, a promising tool to predict protein structure based on a template containing a similar sequence, was applied using Phyre2 (80). The

sequences of CAV1 and OCT4 were taken from Uniprot entry codes Q03135 (81) and Q01860 (82), respectively. According to the sequence alignment by BLAST (83, 84), the crystal structure of lipoprotein MtsA (PDB code 3HH8 (52) with 27% similarity) was used as a template for CAV1 WT, whereas OCT4 was built from POU protein (PDB code 3L1P (85) with 88% similarity) and OTX2 homeobox protein (PDB code 2DMS with 23% similarity).

Each modeled protein was performed in an aqueous solution by all-atom molecular dynamics (MD) simulations using AMBER14 package with standard procedures (86–88) as summarized below. The two predicted structures were individually minimized using steepest descent and conjugated gradient based on the AMBER ff12SB force fields (89) to reduce the steric hindrance. Next, the 10-ns MD simulation with the NPT ensemble at 300 K and 1 atm was carried out by the PMEMD module. To restrain the covalent bond involved with hydrogen atoms, the SHAKE algorithm was applied (90). The particle mesh Ewald summation was used to treat the long-range electrostatic interactions, whereas 10 Å of a cutoff value was defined for nonbonded interactions (91). The last snapshot of the CAV1- and OCT4-simulated systems was further used for structure prediction of the WT CAV1:OCT4 complex.

Molecular protein–protein docking was performed using ZDOCK 3.0.2 (92) to predict the complex structure of OCT4 binding to WT CAV1 based on the parameters used in previous studies (55, 93). From the 2000 docked structures, the WT CAV1:OCT4 complex with the highest ZDOCK score was retrieved and subsequently used to construct the phosphorylated Tyr-14 CAV1 (pTyr-14 CAV1) and Y14F CAV1 mutant in complex with OCT4. To reduce the bad contact, all complexes were then minimized by steepest descent and conjugated gradient approaches using AMBER14 with the AMBER ff12SB force fields (91). Furthermore, the intermolecular hydrogen bonding interaction and MM/PBSA binding free energy of CAV1:OCT4 complexes were analyzed to investigate the effect of the phosphorylation and the single mutation at Tyr-14 position using MMPBSA.py module.

Statistical analysis

The data from three or more independent experiments are presented as the mean S.D. Multiple comparisons were examined for significant difference of multiple groups, using analysis of variance (ANOVA), followed by individual comparisons with Scheffe's post hoc test. Statistical significance was considered at $p < 0.05$.

Author contributions

A. Maiuthed and P. C. data curation; A. Maiuthed, A. Meeprasert, and P. C. formal analysis; A. Maiuthed, N. B., S. L., A. Mutirangura, C. A., A. Meeprasert, T. R., and P. C. investigation; A. Maiuthed, T. R., and P. C. methodology; A. Maiuthed and P. C. writing-original draft; Y. R. and P. C.

conceptualization; Y. R. and P. C. supervision; Y. R. and P. C. writing-review and editing; P. C. resources; P. C. funding acquisition; P. C. validation; P. C. project administration.

Grants

This work was supported by Grant PHD/0063/2557 from Thailand Research Fund through The Royal Golden Jubilee Ph.D. program and Grant RSA6180036 from the Thailand Research Fund. The authors declare that they have no conflicts of interest with the contents of this article.

Supplement data

Supplement table 1: Probe ID and reference sequence of the microarray chip.

This data is available on

<http://www.jbc.org/content/early/2018/07/09/jbc.RA117.000287/suppl/DC1>

Supplement table 2: Genes upregulated/downregulated after treatment with NO in H460 cell

Up-regulation	Probe ID	Gene Symbol
NM_016831	7897378	PER3
NM_016183	7898549	MRT04
NM_032648	7899750	FAM167B
NM_152493	7899870	ZNF362
NM_001408	7903632	CELSR2
NM_006271	7905581	S100A1
NM_012437	7905598	SNAPIN
NM_003094	7908988	SNRPE
NM_024700	7915008	SNIP1
NM_001232	7918878	CASQ2
NM_001160325	7921362	OR6P1
NM_004483	7922104	GCSH
NM_002901	7939120	RCN1
NM_001665	7945944	RHOG
NM_001005489	7948322	OR5B17
NM_020179	7951004	C11orf75
NM_006288	7952268	THY1
NM_005276	7955348	GPD1
NM_001029	7956114	RPS26
NM_002475	7956200	MYL6B
NM_005538	7956423	INHBC
NM_013381	7957221	TRHDE
NM_001065	7960518	TNFRSF1A
NM_016497	7960553	MRPL51
NM_007210	7963313	GALNT6
NM_138284	7967969	IL17D
NM_001730	7969414	KLF5
NM_005561	7970287	LAMP1
NM_001005466	7977771	OR10G2
NM_144673	7996313	CMTM2
NM_000151	8007429	G6PC
NM_002470	8012787	MYH3
NM_014501	8012958	UBE2S
NM_001080395	8019090	AATK
NM_130386	8021946	COLEC12
NM_006339	8024660	HMG20B
NM_002501	8026139	NFIX
NM_012099	8029688	CD3EAP
NM_001134316	8033023	MGIC24975
NM_017703	8033813	FBXL12
NM_139284	8036055	LG34
NM_015265	8047257	FLJ32063

NM_001024690	8052742	FBXO48
NM_001099219	8069976	KRTAP19-8
NM_144659	8069987	C21orf77
NM_005867	8070296	DSCR4
NM_015259	8070720	ICOSLG
NM_020315	8072870	PDXP
NM_001012659	8081989	ARGFX
NM_153264	8082585	COL29A1
NM_001031703	8086784	C3orf75
NM_080927	8089082	DCBLD2
NM_005862	8090898	STAG1
NM_002159	8095435	HTN1
NM_001263	8096130	CDS1
NM_014278	8097335	HSPA4L
NM_002704	8100971	PPBP
NM_001813	8102076	CENPE
NM_173667	8105517	FLJ37543
NM_004219	8109639	PTTG1
NM_005642	8114653	TAF7
NM_015050	8119198	FTSJD2
NM_001013734	8121553	RFPL4B
NM_002667	8121729	PLN
NM_001013623	8122452	FAM164B
NM_002377	8123176	MAS1
NM_030651	8125321	PRRT1
NM_198570	8132805	VWC2
NM_004445	8136811	EPHB6
NM_001135914	8142821	CRBM2
NM_024815	8149646	NUDT18
NM_003012	8150428	SFRP1
NM_006753	8164862	SURF6
NM_001031834	8169006	RAB40AL
NM_000194	8169984	HPR1
NM_018666	8170076	SAGE1
NM_153270	8171796	KLHL34
NM_001522	8174448	GUCY2F
NM_004988	8175775	MAGEA1
NM_001006120	8176753	RBMY1B
NM_001006118	8176753	RBMY1B
NM_005058	8176742	RBMY1B
NM_152585	8176742	RBMY1B
NM_001006117	8176742	RBMY1B
NM_001006121	8176742	RBMY1B

Table Supplement2: Genes downregulated after treatment with nitric oxide in H460 cell

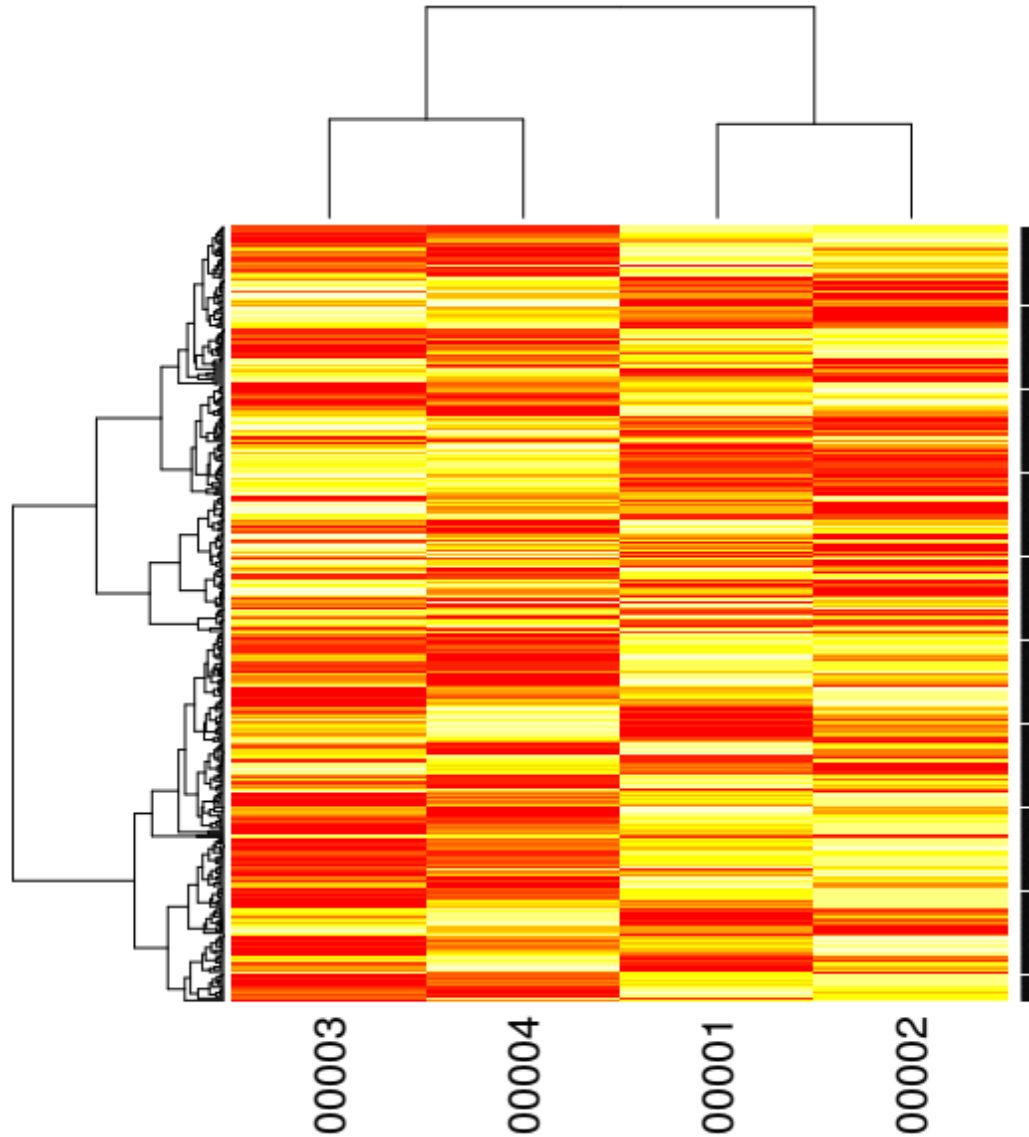
Down-regulation	Probe ID	Gene Symbol
NM_000975	7898875	RPL11
NM_001030	7900157	RPS27
NM_016121	7909745	KCTD3
NM_006642	7911017	SDCCAG8
NM_178815	7926531	ARL5B
NM_153336	7931159	PSTK
NM_006257	7931930	PRKCCQ
NM_173801	7940210	PLACL1
NM_001031739	8171392	ASB9
NM_014956	7944113	CEP164
NM_014182	7956031	ORMDL2
NM_002896	7956261	RBMS2
NM_152318	7958211	C12orf45
NM_014708	7959408	KNTC1
NM_080626	7959777	BRJ3BP
NM_031474	7960331	NRIP2
NM_016312	7961489	WBP11
NM_014167	7965200	CCDC59
NM_018191	7971602	RCBTB1
NM_001085	7976496	SERPINA3
NM_001080414	7980773	CCDC89C
NM_001031723	7989885	LOC646358
NM_004548	7992402	NDUFB10
NM_012368	7992889	OR2C1
NM_020786	7996341	PDP2
NM_016310	7998129	POLR3K
NM_002952	7998655	RPS2
NM_001545	8009727	ICT1
NM_020776	8021001	KIAA1328
NM_002647	8021015	PKC3
NM_024029	8034108	YIPF2
NM_005282	8037614	GPR4
NM_006636	8042830	MTHFD2
NM_018460	8045563	ARHGAP15
NM_032788	8053775	ZNF514
NM_000122	8054978	ERCC3
NM_004805	8055089	POLR2D
NM_013450	8056060	BAZ2B
NM_017759	8058415	INCB0D
NM_176812	8061958	CHMP4B
NM_001145206	8071981	CTA-221G9.4
NM_004810	8073194	GRAP2

NM 014876	8076128	JOSD1
NM 024996	8083630	GFM1
NM 021627	8084607	SENP2
NM 024513	8086572	FYCO1
NM 000055	8091867	BCHE
NM 171828	8092241	KCNMB3
NM 001074	8095395	UGT2B7
NM 152407	8109141	GRPEL2
NM 014983	8109201	HMGXB3
NM 058230	8110463	ZNF354B
NM 016222	8116096	DDX41
NM 001010844	8120826	RBAK1BP1
NM 017633	8127778	FAM46A
NM 080743	8128079	SRtp35
NM 021163	8131292	RBAK
NM 203397	8134737	LOC255374
NM 002769	8136795	PRSSI
NM 001001667	8136837	OR6V1
NM 194284	8144505	CLDN23
NM 005526	8148824	HSF1
NM 152271	8149399	LONRF1
NM 017634	8149857	KCTD9
NM 016034	8159249	MRPS2
NM 016219	8159566	MAN1B1
NM 006911	8159981	RLN1
NM 001001662	8162639	ZNF782
NM 002668	8167449	PLP2
NM 004429	8168045	EFNB1
NM 018990	8169859	SASH3



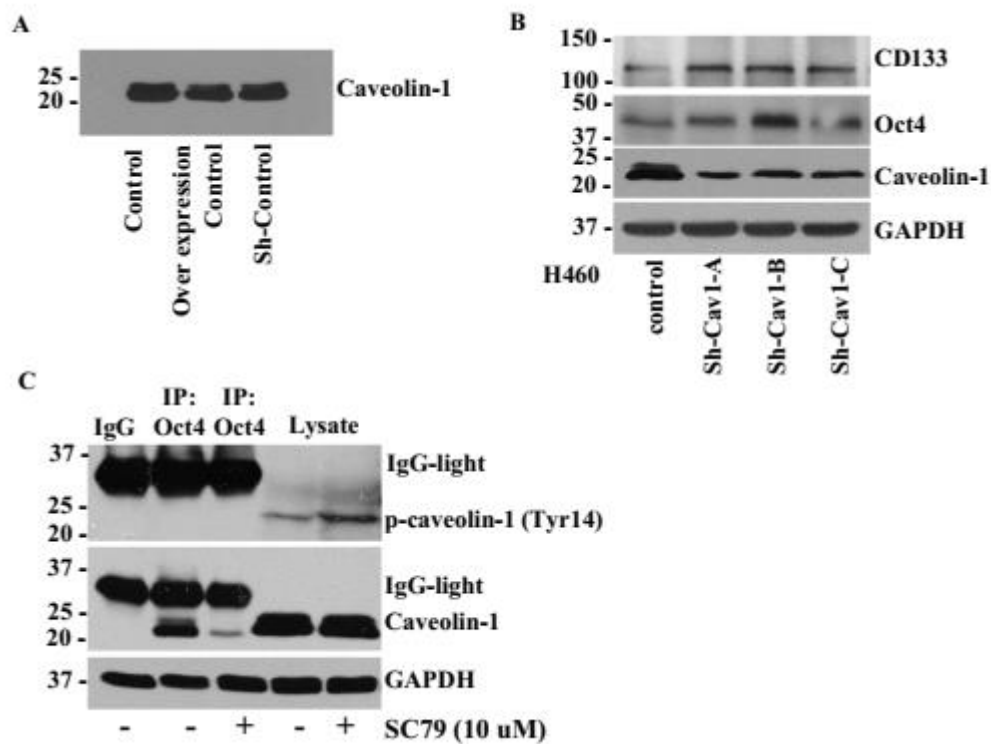
จุฬาลงกรณ์มหาวิทยาลัย
CHULALONGKORN UNIVERSITY

Supplement Figure 1: the high resolution of microarray heat map image



The gene probes with significant difference ($P < 0.05$) between DPTA NONOate-treated (0003 and 0004) and control group (0001 and 0002) analyzed by CU-DREAM program were generated Heat map of genes by the Bioconductor R statistic program. These image is also available on <http://www.jbc.org/content/early/2018/07/09/jbc.RA117.000287/suppl/DC1>

Supplement Figure 2



(A) Plasmid backbones have no un-specific effect on the Cav-1 expression. H460 cells were transfected with pCANw-Flag (over expression control) or sh-scramble plasmid (Sh-control) and subjected to Western blot analysis for Cav-1 detection.

(B) Oct4 expression in the cells transfected with plasmids of different Sh-Cav-1 sequences. H460 cell were transfection with Sh-Cav1 sequence A, Sh-Cav1 sequence B, or Sh-Cav1 sequence C (Origene Cat. No. TG314183). The expression level of Cav-1, Oct4, and CD133 were then evaluated.

(C) p-Cav-1 (tyr14) and its interaction with Oct4 under activated Akt induced by a specific Akt activator SC79. H460 cells were treated with 10 μ M SC79 for 24h. Cell lysates were prepared for immunoprecipitation assay. The protein-immune complexes were pulled down by anti-Oct4 antibody and investigated for p-Cav-1(Tyr14) and Cav-1 by Western blot analysis.

References

1. Bonnet, D., and Dick, J. E. (1997) Human acute myeloid leukemia is organized as a hierarchy that originates from a primitive hematopoietic cell. *Nat. Med.* 3, 730–737
2. Salcido, C. D., Larochelle, A., Taylor, B. J., Dunbar, C. E., and Varticovski, L. (2010) Molecular characterisation of side population cells with cancer stem cell-like characteristics in small-cell lung cancer. *Br. J. Cancer* 102,1636–1644
3. Shackleton, M. (2010) Normal stem cells and cancer stem cells: similar and different. *Semin. Cancer Biol.* 20, 85–92
4. Lobo, N. A., Shimono, Y., Qian, D., and Clarke, M. F. (2007) The biology of cancer stem cells. *Annu. Rev. Cell Dev. Biol.* 23, 675–699
5. Chang, J. C. (2016) Cancer stem cells: Role in tumor growth, recurrence, metastasis, and treatment resistance. *Medicine* 95, S20–25
6. Takahashi, K., Tanabe, K., Ohnuki, M., Narita, M., Ichisaka, T., Tomoda, K., and Yamanaka, S. (2007) Induction of pluripotent stem cells from adult human fibroblasts by defined factors. *Cell* 131, 861–872
7. Yu, J., Hu, K., Smuga-Otto, K., Tian, S., Stewart, R., Slukvin, I. I., and Thomson, J. A. (2009) Human induced pluripotent stem cells free of vector and transgene sequences. *Science* 324, 797–801
8. Gabbert, H., Wagner, R., Moll, R., and Gerharz, C.-D. (1985) Tumor dedifferentiation: An important step in tumor invasion. *Clin. Exp. Metastasis* 3, 257–279
9. Friedmann-Morvinski, D., and Verma, I. M. (2014) Dedifferentiation and reprogramming: origins of cancer stem cells. *EMBO Rep.* 15, 244–253
10. Liu, A., Yu, X., and Liu, S. (2013) Pluripotency transcription factors and cancer stem cells: small genes make a big difference. *Chin. J. Cancer* 32, 483–487
11. Kumar, S. M., Liu, S., Lu, H., Zhang, H., Zhang, P. J., Gimotty, P. A., Guerra, M., Guo, W., and Xu, X. (2012) Acquired cancer stem cell phenotypes through Oct4-mediated dedifferentiation. *Oncogene* 31, 4898–4911
12. Karoubi, G., Gugger, M., Schmid, R., and Dutly, A. (2009) OCT4 expression in human non-small cell lung cancer: implications for therapeutic intervention. *Interact. Cardiovasc. Thorac. Surg.* 8, 393–397
13. Kobayashi, I., Takahashi, F., Nurwidya, F., Nara, T., Hashimoto, M., Murakami, A., Yagishita, S., Tajima, K., Hidayat, M., Shimada, N., Suina, K., Yoshioka, Y., Sasaki, S., Moriyama, M., Moriyama, H., and Takahashi, K. (2016) Oct4 plays a crucial role in the maintenance of gefitinib-resistant lung cancer stem cells. *Biochem. Biophys. Res. Commun.* 473, 125–132

14. Chen, Y.-C., Hsu, H.-S., Chen, Y.-W., Tsai, T.-H., How, C.-K., Wang, C.-Y., Hung, S.-C., Chang, Y.-L., Tsai, M.-L., Lee, Y.-Y., Ku, H.-H., and Chiou, S.-H. (2008) Oct-4 expression maintained cancer stem-like properties in lung cancer-derived CD133-positive cells. *PLoS ONE* 3, e2637
15. Liu, C. G., Lu, Y., Wang, B. B., Zhang, Y. J., Zhang, R. S., Lu, Y., Chen, B., Xu, H., Jin, F., and Lu, P. (2011) Clinical implications of stem cell gene Oct-4 expression in breast cancer. *Ann. Surg.* 253, 1165–1171
16. Hatefi, N., Nouraei, N., Parvin, M., Ziaee, S.-A., and Mowlana, S. J. (2012) Evaluating the expression of Oct4 as a prognostic tumor marker in bladder cancer. *Iran. J. Basic Med. Sci.* 15, 1154–1161
17. Kosaka, T., Mikami, S., Yoshimine, S., Miyazaki, Y., Daimon, T., Kikuchi, E., Miyajima, A., and Oya, M. (2016) The prognostic significance of OCT4 expression in patients with prostate cancer. *Hum. Pathol.* 51, 1–8
18. Quail, D. F., and Joyce, J. A. (2013) Microenvironmental regulation of tumor progression and metastasis. *Nat. Med.* 19, 1423–1437
19. Liu, P. F., Zhao, D. H., Qi, Y., Wang, J. G., Zhao, M., Xiao, K., and Xie, L. X. (2018) The clinical value of exhaled nitric oxide in patients with lung cancer. *Clin. Respir. J.* 12, 23–30
20. Hirst, D. G., and Robson, T. (2011) Nitric oxide physiology and pathology. *Methods Mol. Biol.* 704, 1–13
21. Masri, F. (2010) Role of nitric oxide and its metabolites as potential markers in lung cancer. *Ann. Thorac. Med.* 5, 123–127
22. Powan, P., and Chanvorachote, P. (2014) Nitric oxide mediates cell aggregation and mesenchymal to epithelial transition in anoikis-resistant lung cancer cells. *Mol. Cell. Biochem.* 393, 237–245
23. Saisongkorh, V., Maiuthed, A., and Chanvorachote, P. (2016) Nitric oxide increases the migratory activity of non-small cell lung cancer cells via AKT-mediated integrin α 5 and 1 upregulation. *Cell Oncol.* 39, 449–462
24. Yongsanguanchai, N., Pongrakhananon, V., Mutirangura, A., Rojanasakul, Y., and Chanvorachote, P. (2015) Nitric oxide induces cancer stem cell-like phenotypes in human lung cancer cells. *Am. J. Physiol. Cell Physiol.* 308, C89–C100
25. Chanvorachote, P., Nimmannit, U., Stehlik, C., Wang, L., Jiang, B. H., Ongpipatanakul, B., and Rojanasakul, Y. (2006) Nitric oxide regulates cell sensitivity to cisplatin-induced apoptosis through S-nitrosylation and inhibition of Bcl-2 ubiquitination. *Cancer Res.* 66, 6353–6360
26. Matsunaga, T., Yamaji, Y., Tomokuni, T., Morita, H., Morikawa, Y., Suzuki, A., Yonezawa, A., Endo, S., Ikari, A., Iguchi, K., El-Kabbani, O., Tajima, K., and Hara, A. (2014) Nitric oxide confers

- cisplatin resistance in human lung cancer cells through upregulation of aldo-keto reductase 1B10 and proteasome. *Free Radic. Res.* 48, 1371–1385
27. Williams, T. M., and Lisanti, M. P. (2004) The caveolin proteins. *Genome Biol.* 5, 214–214
 28. Liu, P., Rudick, M., and Anderson, R. G. (2002) Multiple functions of caveolin-1. *J. Biol. Chem.* 277, 41295–41298
 29. Bélanger, M. M., Roussel É., Couet, J. (2004) Caveolin-1 is down-regulated in human lung carcinoma and acts as a candidate tumor suppressor gene. *Chest* 125, 106S–107S
 30. Wiechen, K., Diatchenko, L., Agoulnik, A., Scharff, K. M., Schober, H., Arlt, K., Zhumabayeva, B., Siebert, P. D., Dietel, M., Schäfer, R., and Sers, C. (2001) Caveolin-1 is down-regulated in human ovarian carcinoma and acts as a candidate tumor suppressor gene. *Am. J. Pathol.* 159, 1635–1643
 31. Shyamsunder, P., Vidyasekar, P., Shukla, A. R., Mohan, S., and Verma, R. S. (2013) Lowered expression levels of a tumor suppressor gene– caveolin-1 within dysregulated gene networks of Fanconi anemia. *Gene* 527, 521–528
 32. Sun, M.-Z., Guan, Z., Liu, S., Zhou, X., Wang, N., Shao, S., and Lin, D. (2012) Caveolin-1 interferes cell growth of lung cancer NCI-H446 cell through the interactions with phospho-ERK1/2, estrogen receptor and progesterin receptor. *Biomed. Pharmacother.* 66, 242–248
 33. Yokomori, H., Oda, M., Yoshimura, K., Nomura, M., Wakabayashi, G., Kitajima, M., and Ishii, H. (2003) Elevated expression of caveolin-1 at protein and mRNA level in human cirrhotic liver: relation with nitric oxide. *J. Gastroenterol.* 38, 854–860
 34. Ju, H., Zou, R., Venema, V. J., and Venema, R. C. (1997) Direct interaction of endothelial nitric-oxide synthase and caveolin-1 inhibits synthase activity. *J. Biol. Chem.* 272, 18522–18525
 35. Felley-Bosco, E., Bender, F. C., Courjault-Gautier, F., Bron, C., and Quest, A. F. (2000) Caveolin-1 down-regulates inducible nitric oxide synthase via the proteasome pathway in human colon carcinoma cells. *Proc. Natl. Acad. Sci. U.S.A.* 97, 14334–14339
 36. Chen, Y. C., Hsu, H. S., Chen, Y. W., Tsai, T. H., How, C. K., Wang, C. Y., Hung, S. C., Chang, Y. L., Tsai, M. L., Lee, Y. Y., Ku, H. H., and Chiou, S. H. (2008) Oct-4 expression maintained cancer stem-like properties in lung cancer-derived CD133-positive cells. *PLoS ONE* 3, e2637
 37. Aporn Dewan, C., and Mutirangura, A. (2011) Connection up- and downregulation expression analysis of microarrays (CU-DREAM): a physiogenomic discovery tool. *Asian Biomed.* 5, 257–262
 38. Chen, E. Y., Tan, C. M., Kou, Y., Duan, Q., Wang, Z., Meirelles, G. V., Clark, N. R., and Ma'ayan, A. (2013) Enrichr: interactive and collaborative HTML5 gene list enrichment analysis tool. *BMC Bioinformatics* 14, 128

39. Kuleshov, M. V., Jones, M. R., Rouillard, A. D., Fernandez, N. F., Duan, Q., Wang, Z., Koplev, S., Jenkins, S. L., Jagodnik, K. M., Lachmann, A., McDermott, M. G., Monteiro, C. D., Gundersen, G. W., and Ma'ayan, A. (2016) Enrichr: a comprehensive gene set enrichment analysis web server 2016 update. *Nucleic Acids Res.* 44, W90–W97
40. Lachmann, A., Xu, H., Krishnan, J., Berger, S. I., Mazloom, A. R., and Ma'ayan, A. (2010) ChEA: transcription factor regulation inferred from integrating genome-wide ChIP-X experiments. *Bioinformatics* 26, 2438–2444
41. Jin, G. P., Chang, Z. Y., Schöler, H. R., and Pei, D. (2002) Stem cell pluripotency and transcription factor Oct4. *Cell Res.* 12, 321–329
42. Zeineddine, D., Hammoud, A. A., Mortada, M., and Boeuf, H. (2014) The Oct4 protein: more than a magic stemness marker. *Am. J. Stem Cells* 3, 74–82
43. Li, F., Sonveaux, P., Rabbani, Z. N., Liu, S., Yan, B., Huang, Q., Vujaskovic, Z., Dewhirst, M. W., and Li, C.-Y. (2007) Regulation of HIF-1 stability through S-nitrosylation. *Mol. Cell* 26, 63–74
44. Matsumoto, A., Comatas, K. E., Liu, L., and Stamler, J. S. (2003) Screening for nitric oxide-dependent protein–protein interactions. *Science* 301, 657–661
45. Xu, H., Wang, W., Li, C., Yu, H., Yang, A., Wang, B., and Jin, Y. (2009) WWP2 promotes degradation of transcription factor OCT4 in human embryonic stem cells. *Cell Res.* 19, 561–573
46. Zhao, Q.-W., Zhou, Y.-W., Li, W.-X., Kang, B., Zhang, X.-Q., Yang, Y., Cheng, J., Yin, S.-Y., Tong, Y., He, J.-Q., Yao, H.-P., Zheng, M., and Wang, Y.-J. (2015) Akt-mediated phosphorylation of Oct4 is associated with the proliferation of stem-like cancer cells. *Oncol. Rep.* 33, 1621–1629
47. Chanvorachote, P., Chunchacha, P., and Pongrakhananon, V. (2014) Caveolin-1 induces lamellipodia formation via an Akt-dependent pathway. *Cancer Cell Int.* 14, 52–52
48. Diaz-Valdivia, N., Bravo, D., Huerta, H., Henriquez, S., Gabler, F., Vega, M., Romero, C., Calderon, C., Owen, G. I., Leyton, L., and Quest, A. F. (2015) Enhanced caveolin-1 expression increases migration, anchorage independent growth and invasion of endometrial adenocarcinoma cells. *BMC Cancer* 15, 463
49. Chanvorachote, P., Pongrakhananon, V., and Chunchacha, P. (2014) Prolonged nitric oxide exposure enhances anoikis resistance and migration through epithelial-mesenchymal transition and caveolin-1 upregulation. *BioMed Res. Int.* 2014, 941359
50. Byrne, D. P., Dart, C., and Rigden, D. J. (2012) Evaluating caveolin interactions: do proteins interact with the caveolin scaffolding domain through a widespread aromatic residue-rich motif? *PLoS ONE* 7, e44879

51. Galbiati, F., Volonte, D., Brown, A. M., Weinstein, D. E., Ben-Ze'ev, A., Pestell, R. G., and Lisanti, M. P. (2000) Caveolin-1 expression inhibits Wnt/-catenin/Lef-1 signaling by recruiting-catenin to caveolae membrane domains. *J. Biol. Chem.* 275, 23368–23377
52. Xu, H. M., Liao, B., Zhang, Q. J., Wang, B. B., Li, H., Zhong, X. M., Sheng, H. Z., Zhao, Y. X., Zhao, Y. M., and Jin, Y. (2004) Wwp2, an E3 ubiquitin ligase that targets transcription factor Oct-4 for ubiquitination. *J. Biol. Chem.* 279, 23495–23503
53. Liao, B., and Jin, Y. (2010) Wwp2 mediates Oct4 ubiquitination and its own auto-ubiquitination in a dosage-dependent manner. *Cell Res.* 20, 332–344
54. Chen, S. F., Liou, J. Y., Huang, T. Y., Lin, Y. S., Yeh, A. L., Tam, K., Tsai, T. H., Wu, K. K., and Shyue, S. K. (2010) Caveolin-1 facilitates cyclooxygenase-2 protein degradation. *J. Cell. Biochem.* 109, 356–362
55. Tantong, S., Pringsulaka, O., Weerawanich, K., Meeprasert, A., Rungrotmongkol, T., Sarnthima, R., Roytrakul, S., and Sirikantaramas, S. (2016) Two novel antimicrobial defensins from rice identified by gene coexpression network analyses. *Peptides* 84, 7–16
56. Altomare, D. A., and Testa, J. R. (2005) Perturbations of the AKT signaling pathway in human cancer. *Oncogene* 24, 7455–7464
57. Zon, L. I. (2008) Intrinsic and extrinsic control of haematopoietic stemcell self-renewal. *Nature* 453, 306–313
58. de Haan, G., and Van Zant, G. (1997) Intrinsic and extrinsic control of hemopoietic stem cell numbers: mapping of a stem cell gene. *J. Exp. Med.* 186, 529–536
59. Rao, C. V. (2004) Nitric oxide signaling in colon cancer chemoprevention. *Mutat. Res.* 555, 107–119
60. Ridnour, L. A., Barasch, K. M., Windhausen, A. N., Dorsey, T. H., Lizardo, M. M., Yfantis, H. G., Lee, D. H., Switzer, C. H., Cheng, R. Y., Heinecke, J. L., Brueggemann, E., Hines, H. B., Khanna, C., Glynn, S. A., Ambs, S., and Wink, D. A. (2012) Nitric oxide synthase and breast cancer: role of TIMP-1 in NO-mediated Akt activation. *PLoS ONE* 7, e44081
61. Hayashi, H., Arao, T., Togashi, Y., Kato, H., Fujita, Y., De Velasco, M. A., Kimura, H., Matsumoto, K., Tanaka, K., Okamoto, I., Ito, A., Yamada, Y., Nakagawa, K., and Nishio, K. (2015) The OCT4 pseudogene POU5F1B is amplified and promotes an aggressive phenotype in gastric cancer. *Oncogene* 34, 199–208
62. Kim, B. W., Cho, H., Choi, C. H., Ylaya, K., Chung, J.-Y., Kim, J.-H., and Hewitt, S. M. (2015) Clinical significance of OCT4 and SOX2 protein expression in cervical cancer. *BMC Cancer* 15, 1015

63. Ormsbee Golden, B. D., Wuebben, E. L., and Rizzino, A. (2013) Sox2 expression is regulated by a negative feedback loop in embryonic stem cells that involves AKT signaling and FoxO1. *PLoS ONE* 8, e76345
64. Kempfle, J. S., Turban, J. L., and Edge, A. S. (2016) Sox2 in the differentiation of cochlear progenitor cells. *Sci. Rep.* 6, 23293
65. Gontan, C., de Munck, A., Vermeij, M., Grosveld, F., Tibboel, D., and Rottier, R. (2008) Sox2 is important for two crucial processes in lung development: branching morphogenesis and epithelial cell differentiation. *Dev. Biol.* 317, 296–309
66. Tompkins, D. H., Besnard, V., Lange, A. W., Keiser, A. R., Wert, S. E., Bruno, M. D., and Whitsett, J. A. (2011) Sox2 activates cell proliferation and differentiation in the respiratory epithelium. *Am. J. Respir. Cell Mol. Biol.* 45, 101–110
67. Tompkins, D. H., Besnard, V., Lange, A. W., Wert, S. E., Keiser, A. R., Smith, A. N., Lang, R., and Whitsett, J. A. (2009) Sox2 is required for maintenance and differentiation of bronchiolar Clara, ciliated, and goblet cells. *PLoS ONE* 4, e8248
68. Tang, J. M., He, Q. Y., Guo, R. X., and Chang, X. J. (2006) Phosphorylated Akt overexpression and loss of PTEN expression in non-small cell lung cancer confers poor prognosis. *Lung Cancer* 51, 181–191
69. Cassinelli, G., Zuco, V., Gatti, L., Lanzi, C., Zaffaroni, N., Colombo, D., and Perego, P. (2013) Targeting the Akt kinase to modulate survival, invasiveness and drug resistance of cancer cells. *Curr. Med. Chem.* 20, 1923–1945
70. Qiao, M., Sheng, S., and Pardee, A. B. (2008) Metastasis and AKT activation. *Cell Cycle* 7, 2991–2996
71. Chanvorachote, P., Nimmannit, U., Lu, Y., Talbott, S., Jiang, B. H., and Rojanasakul, Y. (2009) Nitric oxide regulates lung carcinoma cell anoikis through inhibition of ubiquitin–proteasomal degradation of caveolin-1. *J. Biol. Chem.* 284, 28476–28484
72. Villodre, E. S., Kipper, F. C., Pereira, M. B., and Lenz, G. (2016) Roles of OCT4 in tumorigenesis, cancer therapy resistance and prognosis. *Cancer Treat. Rev.* 51, 1–9
73. Trosko, J. E. (2006) From adult stem cells to cancer stem cells: Oct-4 Gene, cell-cell communication, and hormones during tumor promotion. *Ann. N.Y. Acad. Sci.* 1089, 36–58
74. Shi, G., and Jin, Y. (2010) Role of Oct4 in maintaining and regaining stem cell pluripotency. *Stem Cell Res. Ther.* 1, 39
75. Cohen, A. W., Schubert, W., Brasaemle, D. L., Scherer, P. E., and Lisanti, M. P. (2005) Caveolin-1 expression is essential for proper nonshivering thermogenesis in brown adipose tissue. *Diabetes* 54, 679–686

76. Wang, H., Wang, A. X., and Barrett, E. J. (2011) Caveolin-1 is required for vascular endothelial insulin uptake. *Am. J. Physiol. Endocrinol. Metab.* 300, E134–E144
77. Kogo, H., Aiba, T., and Fujimoto, T. (2004) Cell type-specific occurrence of caveolin-1 and -1 in the lung caused by expression of distinct mRNAs. *J. Biol. Chem.* 279, 25574–25581
78. Kato, T., Miyamoto, M., Kato, K., Cho, Y., Itoh, T., Morikawa, T., Okushiba, S., Kondo, S., Ohbuchi, T., and Katoh, H. (2004) Difference of caveolin-1 expression pattern in human lung neoplastic tissue. Atypical adenomatous hyperplasia, adenocarcinoma and squamous cell carcinoma. *Cancer Lett.* 214, 121–128
79. Carnero, A. (2010) The PKB/AKT pathway in cancer. *Curr. Pharm. Des.* 16, 34–44
80. Kelley, L. A., Mezulis, S., Yates, C. M., Wass, M. N., and Sternberg, M. J. (2015) The Phyre2 web portal for protein modeling, prediction and analysis. *Nat. Protoc.* 10, 845–858
81. Glenney, J. R., Jr. (1992) The sequence of human caveolin reveals identity with VIP21, a component of transport vesicles. *FEBS Lett.* 314, 45–48
82. Takeda, J., Seino, S., and Bell, G. I. (1992) Human Oct3 gene family: cDNA sequences, alternative splicing, gene organization, chromosomal location, and expression at low levels in adult tissues. *Nucleic Acids Res.* 20, 4613–4620
83. Boratyn, G. M., Camacho, C., Cooper, P. S., Coulouris, G., Fong, A., Ma, N., Madden, T. L., Matten, W. T., McGinnis, S. D., Merezuk, Y., Raytselis, Y., Sayers, E. W., Tao, T., Ye, J., and Zaretskaya, I. (2013) BLAST: a more efficient report with usability improvements. *Nucleic Acids Res.* 41, W29–W33
84. Johnson, M., Zaretskaya, I., Raytselis, Y., Merezuk, Y., McGinnis, S., and Madden, T. L. (2008) NCBI BLAST: a better web interface. *Nucleic Acids Res.* 36, W5–W9
85. Esch, D., Vahokoski, J., Groves, M. R., Pogenberg, V., Cojocar, V., Vom Bruch, H., Han, D., Drexler, H. C., Araúzo-Bravo, M. J., Ng, C. K., Jauch, R., Wilmanns, M., and Schöler, H. R. (2013) A unique Oct4 interface is crucial for reprogramming to pluripotency. *Nat. Cell Biol.* 15, 295–301
86. Kaiyawet, N., Rungrotmongkol, T., and Hannongbua, S. (2013) Effect of halogen substitutions on dUMP to stability of thymidylate synthase/ dUMP/mTHF ternary complex using molecular dynamics simulation. *J. Chem. Inf. Model.* 53, 1315–1323
87. Meeprasert, A., Khuntawee, W., Kamlungsua, K., Nunthaboot, N., Rungrotmongkol, T., and Hannongbua, S. (2012) Binding pattern of the long acting neuraminidase inhibitor laninamivir towards influenza A subtypes H5N1 and pandemic H1N1. *J. Mol. Graph. Model.* 38, 148–154
88. Meeprasert, A., Hannongbua, S., and Rungrotmongkol, T. (2014) Key binding and susceptibility of NS3/4A serine protease inhibitors against hepatitis C virus. *J. Chem. Inf. Model.* 54, 1208–1217

89. Maier, J. A., Martinez, C., Kasavajhala, K., Wickstrom, L., Hauser, K. E., and Simmerling, C. (2015) ff14SB: improving the accuracy of protein side chain and backbone parameters from ff99SB. *J. Chem. Theory Comput.* 11, 3696–3713
90. Ryckaert, J.-P., Ciccotti, G., and Berendsen, H. J. C. (1977) Numerical integration of the cartesian equations of motion of a system with constraints: molecular dynamics of n-alkanes. *J. Comput. Physics* 23, 327–341
91. York, D. M., Darden, T. A., and Pedersen, L. G. (1993) The effect of longrange electrostatic interactions in simulations of macromolecular crystals: a comparison of the Ewald and truncated list methods. *J. Chem. Physics* 99, 8345–8348
92. Pierce, B. G., Wiehe, K., Hwang, H., Kim, B. H., Vreven, T., and Weng, Z. (2014) ZDOCK server: interactive docking prediction of protein–protein complexes and symmetric multimers. *Bioinformatics* 30, 1771–1773
93. Kongsune, P., Rungrotmongkol, T., Nunthaboot, N., Yotmanee, P., Sompornpisut, P., Poovorawan, Y., Wolschann, P., and Hannongbua, S. (2012) Molecular insights into the binding affinity and specificity of the hemagglutinin cleavage loop from four highly pathogenic H5N1 isolates towards the proprotein convertase furin. *Monatshefte für Chemie Chemical Monthly* 143, 853–860

CHAPTER III

CYTOPLASMIC p21 MEDIATES 5-FLUOROURACIL RESISTANCE BY
INHIBITING PRO-APOPTOTIC CHK2

This research had been published in Cancers in October 9, 2018 with the topic namely: Cytoplasmic p21 mediates 5-fluorouracil resistance by inhibiting pro-apoptotic Chk2 (doi: 10.3390/cancers10100373)

The web link of this article as following: <https://www.mdpi.com/2072-6694/10/10/373/htm>

Ph.D. student

Arnatchai Maiuthed

Affiliation

1. Department of Pharmacology and Physiology, Faculty of Pharmaceutical Sciences, Chulalongkorn University, Bangkok 10300
2. Cell-based Drug and Health Products Development Research Unit, Faculty of Pharmaceutical Sciences, Chulalongkorn University, Bangkok 10300

Advisor

Associate Professor Pithi Chanvorachote, Ph.D.

Affiliation

1. Department of Pharmacology and Physiology, Faculty of Pharmaceutical Sciences, Chulalongkorn University, Bangkok 10300
2. Cell-based Drug and Health Products Development Research Unit, Faculty of Pharmaceutical Sciences, Chulalongkorn University, Bangkok 10300

Co-advisor

Professor Regine Schneider-Stock, Ph.D.

Affiliation

1. Experimental Tumor Pathology, University Hospital, Friedrich-Alexander University Erlangen-Nürnberg (FAU), Erlangen, Germany
2. Institute of Pathology, University Hospital, Friedrich-Alexander University Erlangen-Nürnberg (FAU), Erlangen, Germany

Approval of the co-authors on the use of publication material in the dissertation of Arnatchai Maiuthed

Approval of the co-authors on the use of publication material in the dissertation of Arnatchai Maiuthed

Concerns publication:

"Cytoplasmic p21 mediates 5-fluorouracil resistance by inhibiting pro-apoptotic Chk2"

Arnatchai Maiuthed, Chuanpit Ninsontia, Katharina Erlenbach-Wuensch, Benardina Ndreshkjana, Julienne K. Muenzner, Aylin Caliskan, Husayn Ahmed P., Chatchai Chaotham, Arndt Hartmann, Adriana Vial Roehe, Vijayalakshmi Mahadevan, Pithi Chanvorachote, and Regine Schneider-Stock, Cancers 2018, 10,373; doi:10.3390/cancers10100373

With this I agree that Arnatchai Maiuthed uses the publication in text format and pictorial form for his cumulative dissertation "NOVEL REGULATORY MECHANISMS OF PROTEIN KINASE B ON APOPTOSIS SUSCEPTIBILITY AND CANCER DEDIFFERENTIATION" (working title).

Full name	Signature
Chuanpit Ninsontia	
Katharina Erlenbach-Wuensch	
Benardina Ndreshkjana	
Julienne K. Muenzner	
Aylin Caliskan	
Husayn Ahmed P.	
Chatchai Chaotham	
Arndt Hartmann	
Adriana Vial Roehe	
Vijayalakshmi Mahadevan	
Pithi Chanvorachote	
Regine Schneider-Stock	

Approval of the co-authors on the use of publication material in
the dissertation of Arnatchai Maiuthed

Concerns publication:

"Cytoplasmic p21 mediates 5-fluorouracil resistance by inhibiting pro-apoptotic Chk2"

Arnatchai Maiuthed, Chuanpit Ninsontia, Katharina Erlenbach-Wuensch, Bernardina Ndreshkjana, Julienne K. Muenzner, Aylin Caliskan, Husayn Ahmed P., Chatchai Chaotham, Arndt Hartmann, Adriana Vial Roehe, Vijayalakshmi Mahadevan, Pithi Chanvorachote, and Regine Schneider-Stock, *Cancers* 2018, 10,373; doi:10.3390/cancers10100373

With this I agree that Arnatchai Maiuthed uses the publication in text format and pictorial form for his cumulative dissertation "NOVEL REGULATORY MECHANISMS OF PROTEIN KINASE B ON APOPTOSIS SUSCEPTIBILITY AND CANCER DEDIFFERENTIATION" (working title).

Full name	Signature
Chuanpit Ninsontia	<i>Chuanpit</i>
Katharina Erlenbach-Wuensch	
Bernardina Ndreshkjana	
Julienne K. Muenzner	
Aylin Caliskan	
Husayn Ahmed P.	
Chatchai Chaotham	<i>ch</i>
Arndt Hartmann	
Adriana Vial Roehe	
Vijayalakshmi Mahadevan	
Pithi Chanvorachote	<i>Chanvorachote</i>
Regine Schneider-Stock	



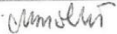
Approval of the co-authors on the use of publication material in
the dissertation of Arnatchai Maiuthed

Concerns publication:

"Cytoplasmic p21 mediates 5-fluorouracil resistance by inhibiting pro-apoptotic Chk2"

Arnatchai Maiuthed, Chuanpit Ninsontia, Katharina Erlenbach-Wuensch, Bernardina Ndreshkjana, Julienne K. Muenzner, Aylin Caliskan, Husayn Ahmed P., Chatchai Chaotham, Arndt Hartmann, Adriana Vial Roehe, Vijayalakshmi Mahadevan, Pithi Chanvorachote, and Regine Schneider-Stock. *Cancers* 2018, 10,373; doi:10.3390/cancers10100373

With this I agree that Arnatchai Maiuthed uses the publication in text format and pictorial form for his cumulative dissertation "NOVEL REGULATORY MECHANISMS OF PROTEIN KINASE B ON APOPTOSIS SUSCEPTIBILITY AND CANCER DEDIFFERENTIATION" (working title).

Full name	Signature
Chuanpit Ninsontia	
Katharina Erlenbach-Wuensch	
Bernardina Ndreshkjana	
Julienne K. Muenzner	
Aylin Caliskan	
Husayn Ahmed P.	
Chatchai Chaotham	
Arndt Hartmann	
Adriana Vial Roehe	
Vijayalakshmi Mahadevan	
Pithi Chanvorachote	
Regine Schneider-Stock	



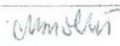
Approval of the co-authors on the use of publication material in
the dissertation of Arnatchai Maiuthed

Concerns publication:

"Cytoplasmic p21 mediates 5-fluorouracil resistance by inhibiting pro-apoptotic Chk2"

Arnatchai Maiuthed, Chuanpit Ninsontia, Katharina Erlenbach-Wuensch, Bernardina Ndreshkjana, Julienne K. Muenzner, Aylin Caliskan, Husayn Ahmed P., Chatchai Chaotham, Arndt Hartmann, Adriana Vial Roehe, Vijayalakshmi Mahadevan, Pithi Chanvorachote, and Regine Schneider-Stock, *Cancers* 2018, 10,373; doi:10.3390/cancers10100373

With this I agree that Arnatchai Maiuthed uses the publication in text format and pictorial form for his cumulative dissertation "NOVEL REGULATORY MECHANISMS OF PROTEIN KINASE B ON APOPTOSIS SUSCEPTIBILITY AND CANCER DEDIFFERENTIATION" (working title).

Full name	Signature
Chuanpit Ninsontia	
Katharina Erlenbach-Wuensch	
Bernardina Ndreshkjana	
Julienne K. Muenzner	
Aylin Caliskan	
Husayn Ahmed P.	
Chatchai Chaotham	
Arndt Hartmann	
Adriana Vial Roehe	
Vijayalakshmi Mahadevan	
Pithi Chanvorachote	
Regine Schneider-Stock	

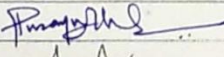

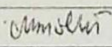
Approval of the co-authors on the use of publication material in
the dissertation of Arnatchai Maiuthed

Concerns publication:

"Cytoplasmic p21 mediates 5-fluorouracil resistance by inhibiting pro-apoptotic Chk2"

Arnatchai Maiuthed, Chuanpit Ninsontia, Katharina Erlenbach-Wuensch, Bernardina Ndreshkjana, Julienne K. Muenzner, Aylin Caliskan, Husayn Ahmed P., Chatchai Chaotham, Arndt Hartmann, Adriana Vial Roehe, Vijayalakshmi Mahadevan, Pithi Chanvorachote, and Regine Schneider-Stock, Cancers 2018, 10,373; doi:10.3390/cancers10100373

With this I agree that Arnatchai Maiuthed uses the publication in text format and pictorial form for his cumulative dissertation "NOVEL REGULATORY MECHANISMS OF PROTEIN KINASE B ON APOPTOSIS SUSCEPTIBILITY AND CANCER DEDIFFERENTIATION" (working title).

Full name	Signature
Chuanpit Ninsontia	
Katharina Erlenbach-Wuensch	
Bernardina Ndreshkjana	
Julienne K. Muenzner	
Aylin Caliskan	
Husayn Ahmed P.	
Chatchai Chaotham	
Arndt Hartmann	
Adriana Vial Roehe	
Vijayalakshmi Mahadevan	
Pithi Chanvorachote	
Regine Schneider-Stock	

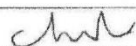
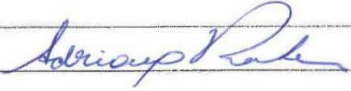
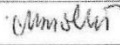
Approval of the co-authors on the use of publication material in
the dissertation of Arnatchai Maiuthed

Concerns publication:

"Cytoplasmic p21 mediates 5-fluorouracil resistance by inhibiting pro-apoptotic Chk2"

Arnatchai Maiuthed, Chuanpit Ninsontia, Katharina Erlenbach-Wuensch, Bernardina Ndreshkjana, Julienne K. Muenzner, Aylin Caliskan, Husayn Ahmed P., Chatchai Chaotham, Arndt Hartmann, Adriana Vial Roehe, Vijayalakshmi Mahadevan, Pithi Chanvorachote, and Regine Schneider-Stock, *Cancers* 2018, 10,373; doi:10.3390/cancers10100373

With this I agree that Arnatchai Maiuthed uses the publication in text format and pictorial form for his cumulative dissertation "NOVEL REGULATORY MECHANISMS OF PROTEIN KINASE B ON APOPTOSIS SUSCEPTIBILITY AND CANCER DEDIFFERENTIATION" (working title).

Full name	Signature
Chuanpit Ninsontia	
Katharina Erlenbach-Wuensch	
Bernardina Ndreshkjana	
Julienne K. Muenzner	
Aylin Caliskan	
Husayn Ahmed P.	
Chatchai Chaotham	
Arndt Hartmann	
Adriana Vial Roehe	
Vijayalakshmi Mahadevan	
Pithi Chanvorachote	
Regine Schneider-Stock	

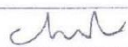
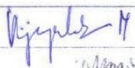
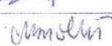
Approval of the co-authors on the use of publication material in
the dissertation of Arnatchai Maiuthed

Concerns publication:

"Cytoplasmic p21 mediates 5-fluorouracil resistance by inhibiting pro-apoptotic Chk2"

Arnatchai Maiuthed, Chuanpit Ninsontia, Katharina Erlenbach-Wuensch, Bernardina Nreleshkjana, Julienne K. Muenzner, Aylin Caliskan, Husayn Ahmed P., Chatchai Chaotham, Arndt Hartmann, Adriana Vial Roehe, Vijayalakshmi Mahadevan, Pithi Chanvorachote, and Regine Schneider-Stock, *Cancers* 2018, 10,373; doi:10.3390/cancers10100373

With this I agree that Arnatchai Maiuthed uses the publication in text format and pictorial form for his cumulative dissertation "NOVEL REGULATORY MECHANISMS OF PROTEIN KINASE B ON APOPTOSIS SUSCEPTIBILITY AND CANCER DEDIFFERENTIATION" (working title).

Full name	Signature
Chuanpit Ninsontia	
Katharina Erlenbach-Wuensch	
Bernardina Nreleshkjana	
Julienne K. Muenzner	
Aylin Caliskan	
Husayn Ahmed P.	
Chatchai Chaotham	
Arndt Hartmann	
Adriana Vial Roehe	
Vijayalakshmi Mahadevan	
Pithi Chanvorachote	
Regine Schneider-Stock	

Abstract

The oncogenic cytoplasmic p21 contributes to cancer aggressiveness and chemotherapeutic failure. However, the molecular mechanisms remain obscure. Here, we show for the first time that cytoplasmic p21 mediates 5-Fluorouracil (5FU) resistance by shuttling p-Chk2 out of the nucleus to protect the tumor cells from its pro-apoptotic functions. We observed that cytoplasmic p21 levels were up-regulated in 5FU-resistant colorectal cancer cells in vitro and the in vivo Chorioallantoic membrane (CAM) model. Kinase array analysis revealed that p-Chk2 is a key target of cytoplasmic p21. Importantly, cytoplasmic form of p21 mediated by p21T145D transfection diminished p-Chk2-mediated activation of E2F1 and apoptosis induction. Co-immunoprecipitation, immunofluorescence, and proximity ligation assay showed that p21 forms a complex with p-Chk2 under 5FU exposure. Using in silico computer modeling, we suggest that the p21/p-Chk2 interaction hindered the nuclear localization signal of p-Chk2, and therefore, the complex is exported out of the nucleus. These findings unravel a novel mechanism regarding an oncogenic role of p21 in regulation of resistance to 5FU-based chemotherapy. We suggest a possible value of cytoplasmic p21 as a prognosis marker and a therapeutic target in colorectal cancer patients.

Keywords: 5-fluorouracil resistance; p21; cytoplasmic p21; Chk2; colorectal cancer; protein interaction

Introduction

5-Fluorouracil (5FU) is one of the most commonly prescribed drugs for treatment of various solid tumors, especially colorectal cancer (CRC) [1,2]. However, 5FU resistance is known to be a major obstacle for efficient 5FU-based chemotherapy in cancer patients [1–3]. The response rates of metastatic CRC for 5FU single treatment and combinations with other agents are about 15% and 50%, respectively [1,3]. Therefore, new strategies of cancer treatment are urgently needed.

The p21 protein (also known as WAF1 or CIP1) was initially documented to be a tumor suppressor protein due to its ability to inhibit cyclin-dependent kinase (CDK) and proliferating cell nuclear antigen (PCNA) functions, finally contributing to cell cycle arrest [4–6]. However, accumulating evidence has suggested that p21 may also play an oncogenic role. In this regard, high expression levels of p21 in many cancer types are correlated with tumor progression [7–11]. A phase I clinical study showed that the potentiation of irinotecan by flavopiridol is due to the reduction of p21 [12]. Likewise, the induction of p21 in rectal carcinoma is associated with resistance to many therapeutic regimens [13]. So far, there is no distinct mechanism that sufficiently explains the dual functions of p21. It was suggested that the role of p21 on cell function control may depend on its sub-cellular localization. Tumor-suppressive functions of p21 are rather associated with a nuclear localization, while more oncogenic activities are found when p21 is localized in the cytoplasm [4,14]. Dependent on its subcellular localization, p21 promotes apoptosis in response to different stimuli [4,14–16] or rather triggers pro-survival signaling [17–22], which might then contribute to cancer progression and chemotherapeutic resistance. As an example, cytoplasmic p21 has been shown to mediate cisplatin and paclitaxel resistance in various cancers [23–25].

Only a few reports describe potential mechanisms of cytoplasmic retention of p21. In general, the nuclear localization signal (NLS) and the nuclear export signal (NES) motifs are responsible for the active shuttling of proteins between the nucleus and the cytoplasm. Thus, the accessibility of the NLS and NES regions under different stress conditions could determine the final localization of p21. Moreover, since the NLS of p21 is localized in close proximity of phosphorylation sites, it is suggested that kinases are responsible for the compartment switch of p21. For example, activated AKT is able to phosphorylate p21 at threonine 145 (T145), which results in a cytoplasmic localization of p21 [26]. Indeed, an overactivation of AKT kinase signaling has been shown in 5FU-resistant colon cancer cells [27]. Cytoplasmic p21 also interacts with Rho kinase 2, an inhibitor of stress fiber formation and ASK1 to differentiate myofibroblasts into fibroblasts and to protect them from apoptosis [28]. Thus, altered nuclear export mechanisms or inhibition of nuclear translocation of p21 could be responsible for cytoplasmic localization of p21

under drug exposure. Meanwhile, the general importance of the cytoplasmic–nuclear transport machinery for cancer has been accepted and it was recently proposed as a promising target for anticancer therapy [29]. Nevertheless, the exact mechanism, by which cytoplasmic p21 mediates chemoresistance and which interaction partners are involved, remains majorly unknown. Especially the role of cytoplasmic p21 in controlling 5FU resistance of CRC has never been addressed. Our present study has identified pChk2 T68 as a novel interaction partner of cytoplasmic p21 that seems to confer to 5FU resistance in CRC. We could verify interplay between p21 and pChk2T68 not only *in vitro*, but also *in vivo* and *in silico*.

Results

Cytotoxic effect of 5FU on colorectal cancer cell lines

To define a suitable experimental model for investigation of the role of p21 for 5FU resistance, we evaluated the susceptibility to 5FU treatment in three different colorectal tumor cell lines (HCT116, HT29 and SW837). MTT assay showed the reduction of cell viability in a dose-dependent manner after 48 h of 5FU treatment in all investigated cell lines. IC₅₀ values were 10 μ M for HCT116 and SW837 cells (Figure 1a,b) and 20 μ M for HT29 cells (Figure 1c). Consistently, Annexin-PI flow cytometric analysis indicated that the number of apoptotic cells was also increased in a dose-dependent manner for HCT116 and SW837 cells, but not for the rather resistant HT29 cells (Figure 1d–f). Although the endogenous p21 level differed between the three cell lines, there was a remarkable increase in p21 in adherent resistant HCT116 and SW837 cells, whereas the resistant HT29 cells increased their p21 expression to a much lower extent after 5FU exposure, possibly due to their mutant p53 status (Figure 1g). Thus, our results suggest a potential involvement of p21 in reduced response to 5FU in CRC cells remarkable increase in p21 in adherent resistant HCT116 and SW837 cells, whereas the resistant HT29 cells increased their p21 expression to a much lower extent after 5FU exposure, possibly due to their mutant p53 status (Figure 1g). Thus, our results suggest a potential involvement of p21 in reduced response to 5FU in CRC cells.

Cytoplasmic localization of p21 in 5FU-resistant cells *in vitro* and *in vivo*

Next, we investigated the subcellular localization of p21 in CRC cells exposed to 5FU by immunofluorescence. After 48 h of 5FU treatment, dead cells were removed by washing with PBS and the remaining adherent (mainly resistant) cells were stained with a p21 antibody. Figure 2a clearly indicates that p21 was mainly expressed in the cytoplasm of HCT116 cells and this cytoplasmic p21 increased in a dose-dependent manner. Some studies have reported that AKT-

driven phosphorylation of p21 (p-p21T145) is majorly responsible for p21 accumulating in the cytoplasm [25,26]. However, as the applied p-p21T145 antibody produced a high number of unspecific bands in Western Blots (Figure S1, Supplementary Materials), it could not be used for immunofluorescence analysis. Nevertheless, in Western Blot experiments, the correct band of p-p21T145 could be identified by loading a sample of HCT116 p21^{-/-} cells (Figure S1, Supplementary Materials). Here, we found a dose-dependent increase in expression of p-p21T145 in 5FU-treated cells (Figure 2b). Consistently, similar results were obtained for HT29 and SW837 cells (Figure S2, Supplementary Materials) and the more resistant HT29 cells exhibited the highest endogenous p-p21T145 expression level. Next, we performed *in vivo* xenograft experiments using the CAM assay. HCT116 cells were treated with 5FU for 48 h, the supernatant with apoptotic dead cells was removed, and 1×10^6 cells were then transplanted onto the CAM, and tumor xenografts were harvested after 5 days of inoculation (13 \times control and 11 \times 5FU pre-treated specimens, Figure 2c). 5FU treatment led to remarkable reductions in tumor size (22 mm³ to 9.4 mm³) and vital tumor cell area (86.2% to 11%), and an increase in necrotic areas (4.2% to 23%) (Figure 2d: representative images are shown). In the vital cells of the micro-tumors, which were expected to represent the 5FU-resistant cell population, we could observe an increase in p21 expression in the nucleus and cytoplasm after 5FU treatment (Figure 2d,e).

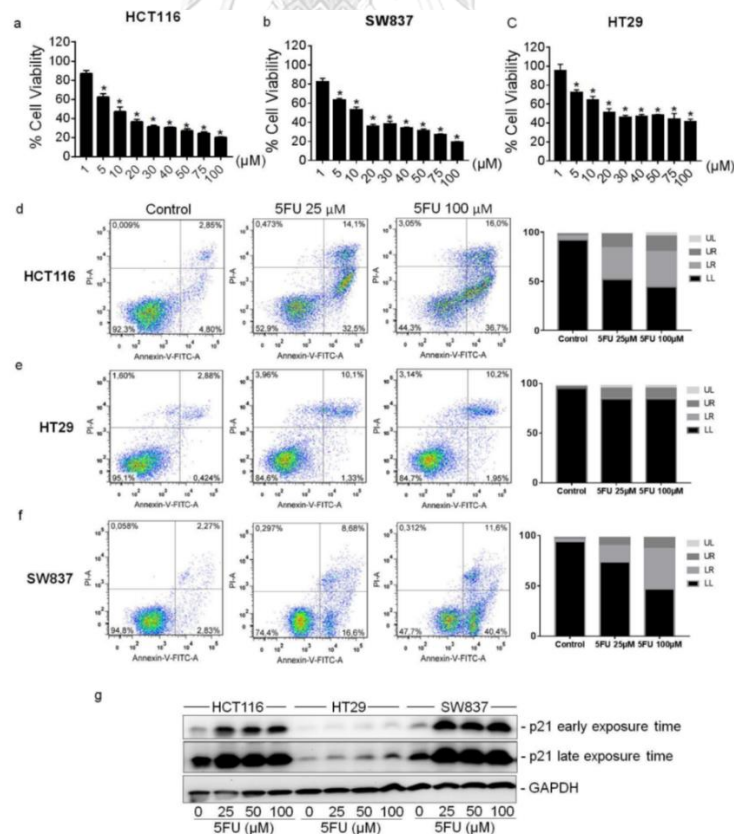


Fig. 1 Susceptibility of colorectal cancer cell lines towards 5FU treatment and p21 expression in 5FU-resistant cells.

Effects of 5FU on cell viability of (a) HCT116 (b) SW837 and (c) HT29 cells. Cells were treated with various concentrations of 5FU (0–100 μ M) for 48 h. The percentage of cell viability was determined by the MTT assay. Values represent means \pm SD of three independent experiments. * $p < 0.05$ versus non-treated control. Effects of 5FU on cell apoptosis of (d) HCT116 (e) HT29 and (f) SW837 cells. Cells were treated with 25 μ M or 100 μ M of 5FU for 48 h. Apoptotic cell death was determined by Annexin-PI co-staining and fluorescent signals were analyzed by flow cytometry. UL: upper left (necrosis), LL: lower left (vital), LR: lower right (apoptosis), UR: upper right (late apoptosis). (g) The expression level of p21 in 5FU-resistant cells was determined by Western Blot analysis in three colorectal cancer cell lines. Cells were treated with various concentrations of 5FU for 48 h. After incubation, dead cells were discarded by washing the plates 3 times with PBS, and the remaining resistant cells were collected to prepare protein lysates as mentioned in the Material and Methods section. The blots were re-probed with GAPDH to confirm equal loading of the samples.



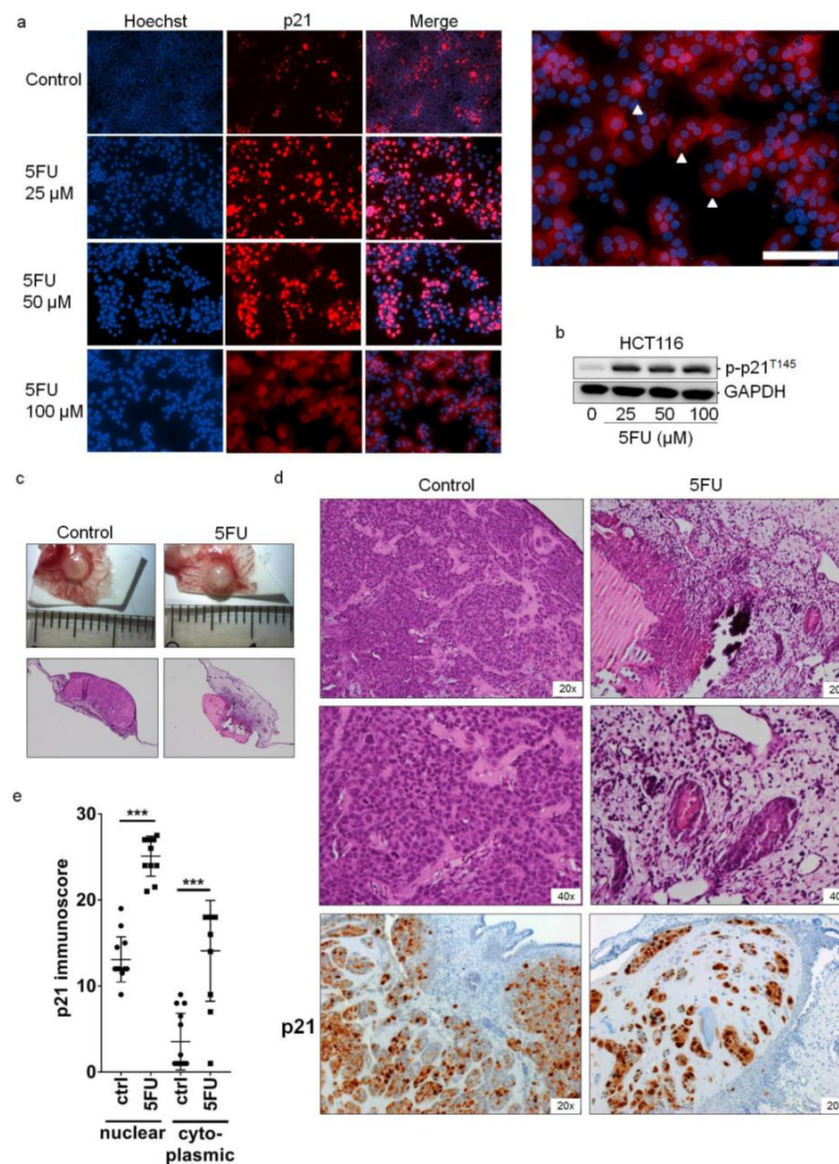


Fig. 2 Localization of p21 in 5FU-resistant HCT116 cells.

(a) HCT116 cells were treated with various concentrations of 5FU for 48 h and the expression of p21 was determined by immunofluorescence staining using mouse anti-p21 monoclonal antibodies followed by an Alexa Fluor 555-labeled secondary antibody to visualize p21 expression (red) and the nuclei (Hoechst 33342, blue). Scale bar: 50 μm. (b) The expression level of phosphorylated-p21 (p-p21^{T145}) in 5FU-resistant HCT116 cells was determined by Western Blot analysis. Cells were treated with various concentrations of 5FU for 48 h. After incubation, dead cells were discarded by washing the plates 3 times with PBS and the remaining resistant cells were collected to prepare protein lysates as mentioned in the Material and Methods section. The blots were re-probed with GAPDH to confirm equal loading of the samples. (c) Ex ovo images and overviews of H&E-stained sections of CAM micro-tumors. For this, HCT116 cells were treated with 15 μM of 5FU for 48 h. Then the 5FU-resistant HCT116 cells were subjected to the CAM. After 5 days, tumor tissues were collected, tumor size was measured, and xenografts were subjected to standard histological and immunohistochemical procedures. (d) H&E

staining and immunohistochemical staining of p21 protein in vital areas of tumor slices. (e) Immunoscore of p21 regarding its cytoplasmic and nuclear localization in xenografts of 5FU-treated HCT116 and control cells. *** $p < 0.001$ versus non-treated control.

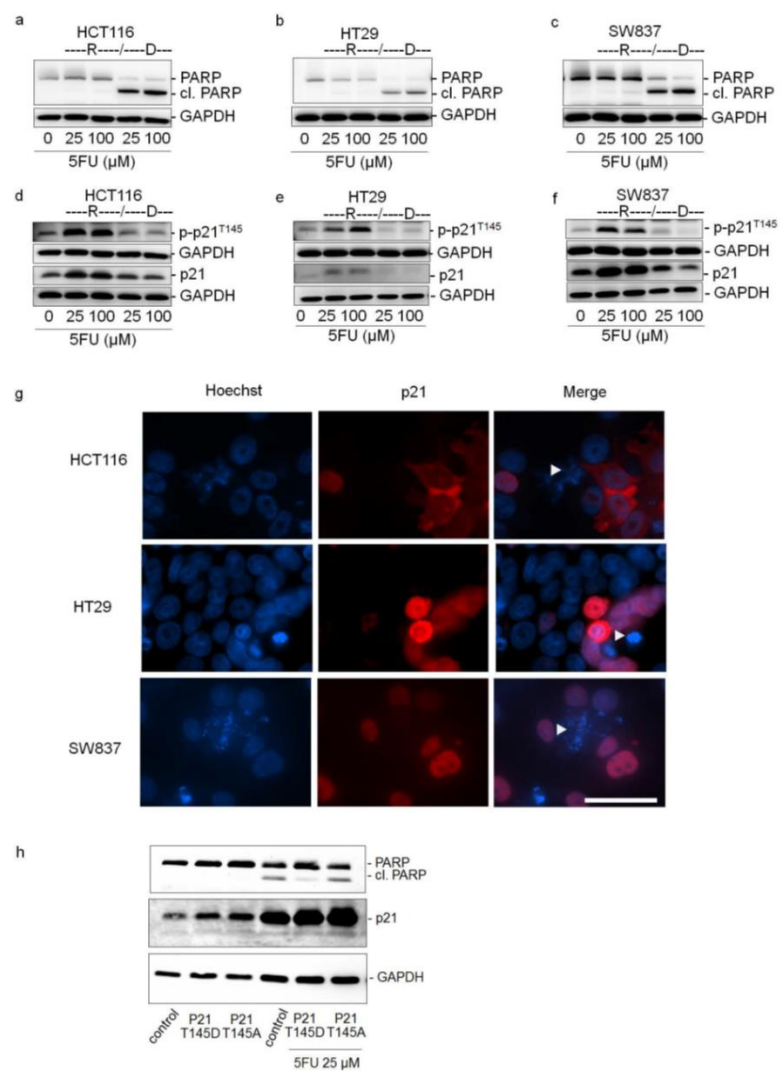
Cytoplasmic p21 induces apoptosis resistance after 5FU treatment

To further evaluate the role of cytoplasmic p21 in 5FU resistance, control as well as separately collected resistant (R, adherent) and dead (D, detached) cells after 5FU exposure for 48 h were analyzed for PARP cleavage, p21, and p-p21T145 protein expression by Western Blot analysis. PARP is known to be one of the major targets of caspase-3 and PARP cleavage is a commonly applied marker of apoptotic cell death [30,31]. The nearly complete absence of cleaved PARP in resistant adherent cells (R) indicated that low or no apoptotic signaling was activated in these cells. In contrast, high PARP cleavage could be observed in apoptotic floating cells (D) (Figure 3a–c). As anticipated from the CAM experiments, there was a remarkable increase in both total p21 and p p21T145 levels for vital cells (R) of all three cell lines. While the total p21 protein expression decreased to the corresponding control levels in apoptotic cells (D), the p-p21T145 protein expression was even reduced below the control levels (Figure 3d–f). Immunofluorescence images of 5FU-treated HCT116, HT29 and SW837 cells confirmed these findings, showing a cytoplasmic enrichment of p21 in viable adherent cells. Interestingly, the few apoptotic cells with signs of chromatin condensation did not show p21 at all (Figure 3g).

Since there was a remarkable cytoplasmic p21 increase under 5FU treatment in the resistant cells in vitro and in vivo, we transfected HCT116 cells with the hyperphosphorylated p21T145D or the non-phosphorylatable p21T145A form of p21. In general, transfection without 5FU treatment did not induce PARP cleavage. However, 5FU treatment led to a strong increase in p21 without PARP cleavage in p21T145D-transfected cells, while in control cells and cells transfected with the p21T145A form, PARP cleavage was induced (Figure 3h). Moreover, nuclear and cytoplasmic localizations of p21 after p21T145D transfection were verified by immunofluorescence, whereas p21 after p21T145A transfection was found mostly in the nucleus (Figure S3a, Supplementary Materials). Successful transfection after 24 h is shown in Figure S3b (Supplementary Materials). It should be noted that transient transfection led to a normalization of p21 level after 72 h (Figure 3h, left panel), but cells were treated with 5FU at the time point of maximal p21 expression (Figure S3b, Supplementary Materials).

At this point, from our experimental data obtained from the three CRC cell lines (HCT116, HT29 and SW837) described above, we would expect that HCT116 cells without p21 should be more sensitive to 5FU. To test this, we treated HCT116 p21^{-/-} cells with 10 μ M 5FU and performed

an Annexin-PI-FACS analysis (48 h, Figure 4a,b) and crystal violet assay (24 h and 48 h, Figure 4c) to determine the viability of cells. Interestingly, p21^{-/-} cells were even more resistant to the 5FU treatment, suggesting that cells without p21 paradoxically take another pathway to develop a resistance to 5FU treatment.



Cytoplasmic p21 mediates 5FU resistance in colorectal cancer cells.

(a–f) The expression levels of PARP, cleaved PARP (cl. PARP), phosphorylated-p21 (p-p21^{T145}) and p21 in resistant cells (R) and dead cells (D) were determined by Western Blot analysis after 48 h of treatment with 5FU. For this, HCT116, HT29, and SW837 cells were treated with various concentrations of 5FU. After 48 h, resistant cells (R) and dead cells (D) were collected separately and protein lysates were prepared. The blots were re-probed with GAPDH to confirm equal loading of the samples. (g) Expression of p21 in viable and dead cells after 48 h of 5FU treatment. HCT116, HT29, and SW837 cells were treated with various concentrations of 5FU for 48 h and the expression levels of p21 were determined by immunofluorescence staining for p21 (red) and the cell nuclei (Hoechst 33342, blue). White arrow indicates apoptotic cells having condensed chromatin and/or fragmented nuclei. Scale bar: 50 μ m. (h) 5FU susceptibility of HCT116 cells transfected with hyperphosphorylated p21^{T145D}

and unphosphorylatable p21T145A. After 24 h of transfection, cells were treated with 5FU (25 μ M) for further 48 h. Untreated cells were used as controls. The expression levels of PARP, cleaved PARP (cl. PARP), and p21 were determined by Western Blot analysis. The blots were re-probed with GAPDH to confirm equal loading of the samples.

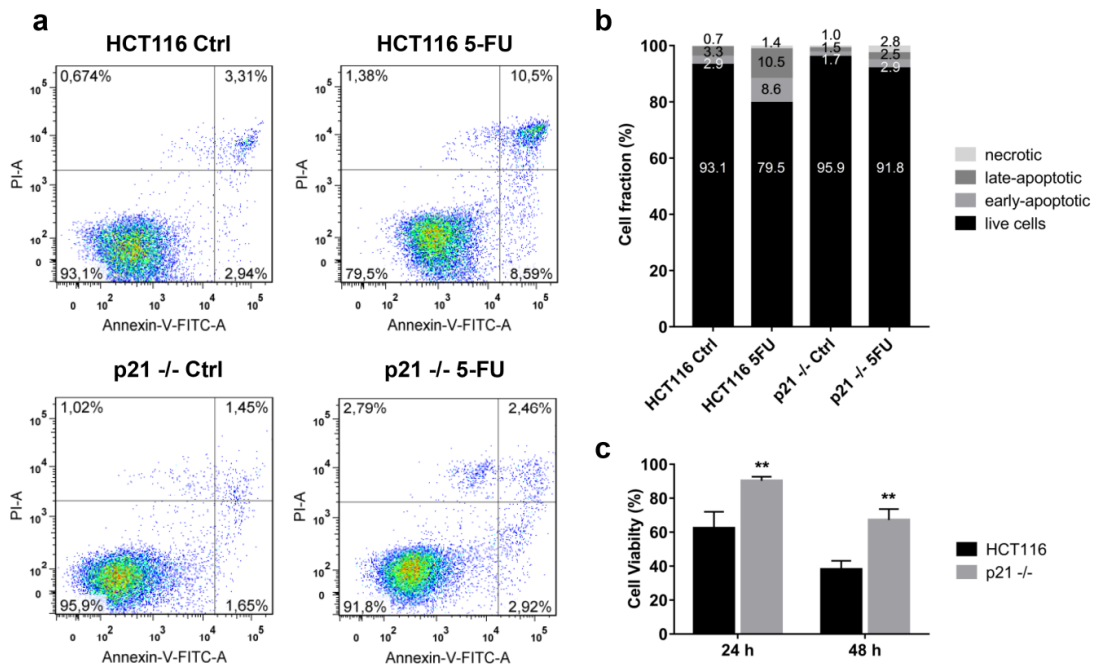


Fig. 4 Susceptibility of HCT116 wildtype (HCT116) and HCT116 p21 knockout (p21^{-/-}) colorectal cancer cell lines towards 5FU treatment.

(a) Effects of 5FU (10 μ M) on the induction of apoptosis and necrosis in HCT116 and p21^{-/-} cells after 48 h of incubation as assessed by the Annexin-PI assay. The experiment was carried out in technical and biological duplicate. One representative experiment is shown. (b) Fractions of live, early-apoptotic, late-apoptotic and necrotic cells in 5FU-treated and control HCT116 and p21^{-/-} cell populations as determined from the Annexin-PI assay after 48 h of incubation. Values of one representative experiment are shown. (c) Cell viability of HCT116 and p21^{-/-} cells after treatment with 5FU (10 μ M) for 24 h and 48 h with respect to DMSO controls. Values represent means \pm SD of three independent experiments. ** $p < 0.01$.

Cytoplasmic p21 activates cell survival signals and attenuates the pro-apoptotic effect of Chk2 in vitro and in vivo

To identify which kinase could be a crucial interaction partner of p21 for 5FU resistance, we quantified the expression of a phospho-kinase panel in control and the hyperphosphorylated p21T145D-transfected cells using an antibody-based array. Figure 5a,b shows that there was an increase in phosphorylation of Chk2 (T68), FAK (Y397), Lck (Y394), ERK 1/2 (T202/Y204,

T185/Y187), and AMPK α 1 (T183) in the hyperphosphorylated p21T145D-transfected cells when compared to the control cells. In addition, as it is known that phosphorylation of p21 at threonine 145 is mediated by the activity of AKT, hyperphosphorylated AKTT308D,S473D was used to investigate the expression of human kinase profile after transfection of HCT116 cells with hyperphosphorylated AKTT308D,S473D plasmid. As expected, transfection with hyperphosphorylated AKTT308D,S473D provided the same pattern of up-regulated kinases as transfection with hyperphosphorylated p21T145D (Figure S4, Supplementary Materials)

Thus, for the first time, we identified possible targets of p-p21 that could be involved in mediating 5FU resistance. We further focused on the interplay of p-p21 with the stress-responsive protein Chk2. This protein seemed to be promising since a few studies already indicated a role of p-Chk2T68 for the regulation of apoptosis in response to stress signals [32,33]. Moreover, its forkhead-associated (FHA) domain, which typically binds to phospho-threonine residues [34], might interact with threonine 145 of p21. Therefore, we suggest that p-p21T145 might interfere with the pro-apoptotic function of p-Chk2T68. To study the interaction between p21 and Chk2 in more detail, we first investigated the expression level of p-Chk2T68 and its total form in 5FU-resistant cells (vital adherent cells after 5FU treatment). The results indicated that in all three investigated cell lines, an increased protein expression of p-Chk2T68 was found in viable 5FU-resistant cells, while the total Chk2 protein level remained mainly unaffected by 5FU treatment (Figure 5c–e).

To clarify if the increase in p-Chk2T68 levels is correlated with an increase in phosphorylation of its major target, p-E2F1 [33], we transfected HCT116 cells with hyperphosphorylated p21T145D or the non-phosphorylatable p21T145A and then studied the p-E2F1 levels by Western Blot after 5FU exposure. While the damage sensor p-Chk2T68 was commonly induced after 5FU treatment, transfection with the non-phosphorylatable p21T145A form interestingly resulted in a higher p-E2F1 level than transfection with the hyperphosphorylated p-p21T145D (Figure 5f), suggesting that non-phosphorylatable p21T145A form cannot interact with pChk2 to inhibit its signaling.

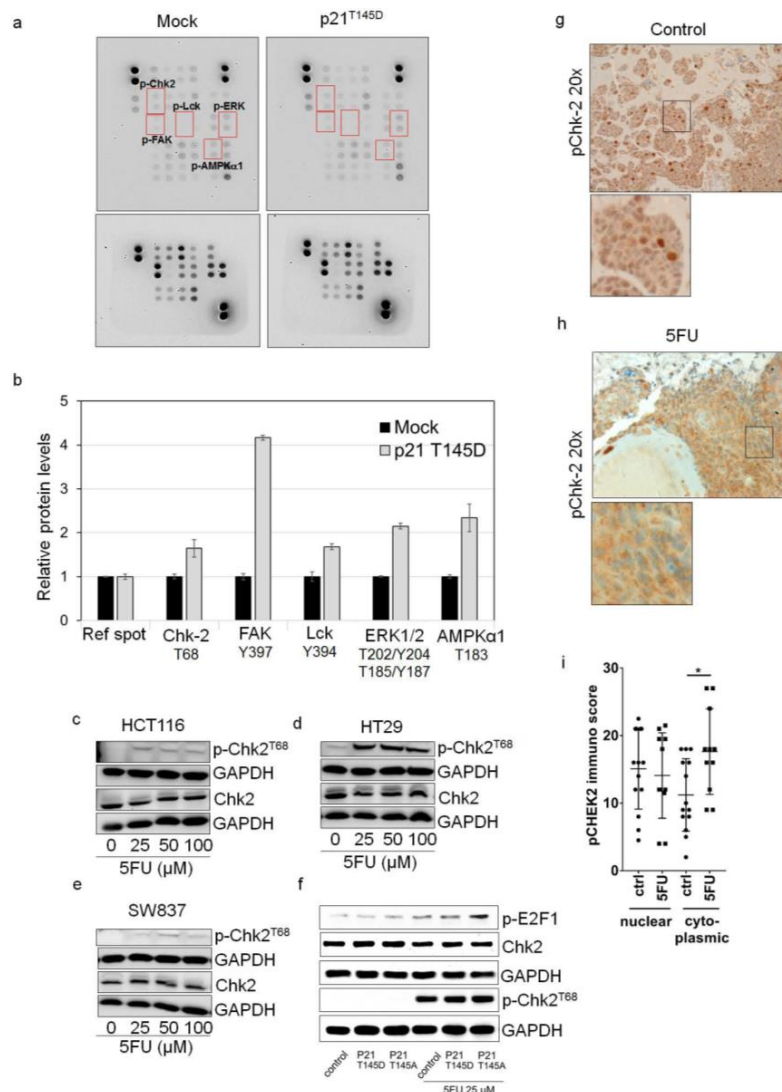


Fig. 5 p21 inhibits pro-apoptotic effect of Chk2. (a-b) Expression levels of phospho-proteins in transfected cells.

(a,b) Expression levels of phospho-proteins in transfected cells. HCT116 cells were transfected with hyperphosphorylated p21T145D. After 48 h of transfection, cells lysates were prepared and subjected to the Human Phospho-Kinase Array Kit (R&D systems). The expression levels of phosphorylated Chk2 (p-Chk2T68) and Chk2 in 5FU-resistant HCT116 (c), HT29 (d), and SW837 (e) cells were determined by Western Blot. (The same lysates were loaded on two different membranes for Chk2 and pChk2 detection). For this, cells were treated with various concentrations of 5FU for 48 h. Dead cells were removed by washing with PBS and the remaining viable cells were collected to prepare protein lysates as mentioned in the Material and Methods sections. The blots were re-probed with GAPDH to confirm equal loading of the samples. (f) The expression levels of phosphorylated Chk2 (p-Chk2T68), Chk2, and p-E2F1 in HCT116 cells transfected with hyperphosphorylated p21T145D and unphosphorylatable p21T145A in response to 5FU treatment were determined by Western Blot analysis. After 24 h transfection, cells were left untreated or were treated with 5FU (25 μ M) for further 48 h. Dead cells were removed by washing with PBS and the remaining viable cells were collected to prepare protein lysates. The expression of p-E2F1, p-Chk2T68 and Chk2 were determined and the blots were re-probed with GAPDH to

confirm equal loading of the samples. Immunohistochemical staining of p-chk2T68 in CAM xenografts formed by HCT116 control (g) and HCT116 5FU-treated (h) cells. (i) p-chk2T68 immunoscore in cytoplasmic and nuclear localizations in tumors of the HCT116 5FU-treated and untreated groups. * $p < 0.05$ versus non-treated control.

In a next step, we stained sections of CAM xenografts with a p-Chk2T68 antibody. As expected, a significant increase of p-Chk2T68 expression in the cytoplasm was observed in vital tumor cells of 5FU-treated xenografts compared to the untreated control group (p -value = 0.0173) with only a slight decrease of p-Chk2T68 expression in the nucleus of 5FU-treated cells when compared to the untreated controls (Figure 5g–i). Taken together, we suggest that after 5FU treatment, p-p21T145 in resistant vital tumor cells could relocate p-Chk2 from the nucleus to the cytoplasm, thus suppressing the recruitment of p-Chk2 to the pro-apoptotic program.

p21 interacts with p-Chk2 in 5-FU resistant cells.

It is well known that p21 directly interacts with several proteins and retains them in the cytoplasm [35–38]. Thus, we raised the question if p-p21T145 and p-Chk2 might be interacting proteins. First, we confirmed a co-localization of p21 and p-Chk2 and p21 and total Chk2 by co-immunofluorescence staining resistant cells after 5FU exposure. Figure 6a–f show that this co-localization was found in both compartments of 5FU-resistant cells in all three cell lines. In a Duo-link assay, we further confirmed a direct physical interaction between p21 and p-Chk2T68 mainly in the nuclei and a few signals also in the cytoplasm of 5FU-resistant HT29 cells (Figure 7a). Images of single antibody staining for untreated and 5FU-treated HT29 cells are given in Figure S5a,b in Supplementary Materials. Confocal microscopy images of Duo-link assay are given in Figure 7b. Additionally, we were able to detect an interaction of p21 and p-Chk2T68 in 5FU-resistant cells in a dose-dependent manner, performing a co-immunoprecipitation in HCT116 cells (Figure 7c).

Additionally, the structural modeling presented in Figure 7d–g provides further evidence that p21 has the capability to interact with Chk2. The interaction site of p21 was found in the second NLS of Chk2 at the arginines of positions 240 and 241 (Figure 7e). When the threonine 145 of p21 and the threonine 68 of Chk2 were phosphorylated, the energy of the complex of both phosphorylated molecules was found to decrease from -907.3 kcal/mol to -1083.5 kcal/mol pointing to a stabilized and stronger binding. The schematic model in Figure 8 describes our hypothesis regarding Chk2 localization and function being controlled by p21 in 5FU-treated cells. Phosphorylation at threonine 68 leads to a blockage of the NLS of Chk2 (Figure 7f). We identified two NES sequences of p21 NES1: amino acids 68–78 with the sequence VRGLGLPKLYL and NES2: at amino acids 102–119 with the sequence LQGTAEEDHVDLSLSSCTL. Two NES sequences of Chk2

were found using the prediction tool LocNES: amino acids 92–106 with the sequence PWARLWALQDGFANL and a second one at amino acids 454–468 with the sequence EVSEKALDLVKLLV with the latter being the relevant NES of Chk2. Examining the interaction profile of the p-p21T145/p-Chk2T68 complex obtained by structural modeling, it is clearly evident that both NES regions of p-Chk2 are without any interaction with p-p21 facilitating export of the complex to the cytoplasm (Figure 7g). Figure 7g shows the NLS and NES regions in the modeled complex. Since we could not find a prominent cytoplasmic p21/p-Chk2 complex with PLA analysis, we suggest that it might dissociate in the cytoplasm. This in silico model is supported by co-immunoprecipitation data where we can show that Chk2 signals increase with higher 5FU concentrations only when immunoprecipitated with p-p21 but not when immunoprecipitated with the p21 antibody (Figure S6a,b, Supplementary Materials). Thus, the function of p-p21T145 might be the permanent export of activated Chk2 from the nucleus, minimizing its pro-apoptotic signaling (Figure 8).

Together, our data demonstrated that interaction of p-p21T145 with p-Chk2T68 is one of the pro-survival mechanisms contributing to 5FU resistance in CRC cells.

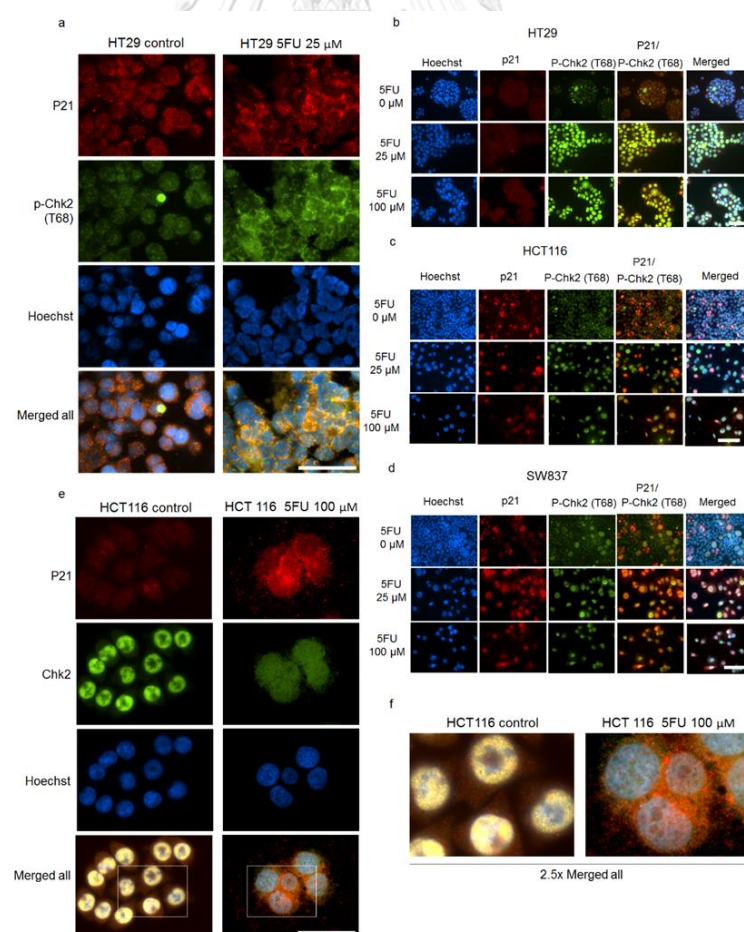


Figure 6 Co-localization of p21 and p-Chk2T68 / Chk2 in 5FU-resistant cells.

(a,b) HT29, (c) HCT116 and (d) SW837 cells were treated with various concentrations of 5FU for 48 h and the expression of p21 and p-Chk2T68 was examined by immunofluorescence staining using mouse anti-p21 monoclonal antibodies followed by an Alexa Fluor 555-labeled secondary antibody to visualize p21 expression (red), rabbit anti-p-Chk2T68 monoclonal antibodies followed by an Alexa Fluor 488-labeled secondary antibody to visualize p-Chk2T68 expression (green) and cell nuclei (Hoechst 33342, blue). (a) Enlarged images of p21 and p-Chk2T68 co-localization in 5FU-resistant HT29 cells. Scale bar: 50 μ m; (e) HCT116 cells were treated with 100 μ M 5FU for 48 h and the expression of p21 and Chk2 was examined by immunofluorescence staining using mouse anti-p21 monoclonal antibodies followed by an Alexa Fluor 555-labeled secondary antibody to visualize p21 expression (red), rabbit anti-Chk2 monoclonal antibodies followed by an Alexa Fluor 488-labeled secondary antibody to visualize Chk2 expression (green) and cell nuclei (Hoechst 33342, blue). Scale bar: 50 μ m; and (f) 2.5-fold computer-enlarged images from merge images in (e).

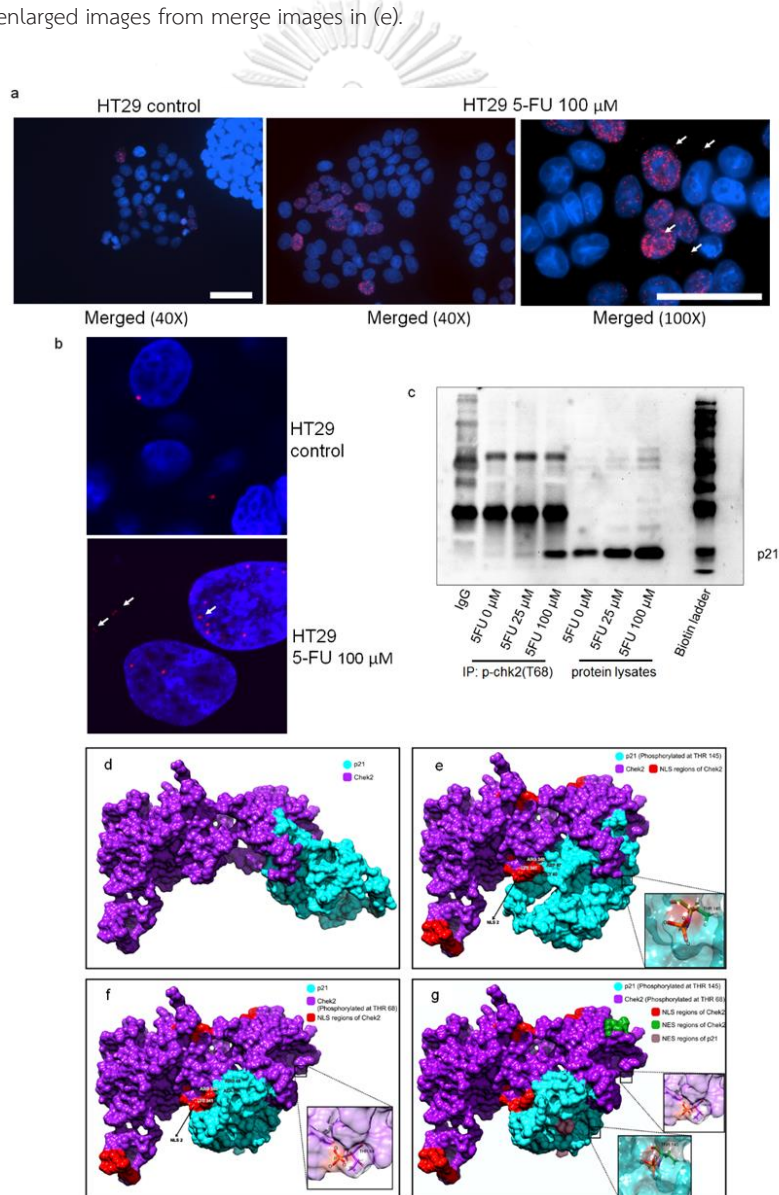


Fig. 7 Interaction between p21 and Chk2 proteins.

Cells were treated with 100 μM 5FU for 48 h and the protein–protein interaction of p21–p-Chk2T68 was analyzed by proximity ligation assay (HT29) (red signals indicate the protein–protein interaction between p21 and p-Chk2T68). (a) Fluorescence images of untreated control HT29 cells (40x magnification) and 5FU-treated HT29 cells (40x and 100x magnification) (scale bar: 50 μm); (b) confocal images. (c) 5FU-treated HCT116 cell lysates were prepared and immunoprecipitated with an anti-p-chk2T68 antibody. The resulting immune complexes were then analyzed for p21 by Western Blot using an anti-p21 antibody. (d) Complex of p21 and Chk2 obtained by structural modelling; p21 (cyan) was modelled using two PDB structures 4I58 and 5EOU as templates using MODELLER [39]. Chk2 (magenta) was obtained from its crystal structure 2WTC after removing the coordinates of the inhibitor. The structures were energy-minimized and docked using ClusPro [40] and rendered using Chimera [40]. (e) Complex of phosphorylated p21 and Chk2: the energy-minimized stable structure of p21 (cyan) was phosphorylated at Threonine residue at position 145 using Chimera [41] and was docked with the structural model of Chk2 (magenta) using ClusPro [40]. The nuclear localization signal (NLS) region of Chk2 is shown in red. The insert shows the phosphorylation of T145 of p21 in the model. The interactions between the proteins were identified using the Protein Interaction Calculator (PIC) [42]. (f) Complex of p21 and phosphorylated Chk2: the energy-minimized stable structure of Chk2 (magenta) was phosphorylated at Threonine residue at position 68 using Chimera [41] and was docked with the structural model of p21 (cyan) using ClusPro [40]. The NLS region of Chk2 is shown in red and the residues around and in the NLS are labelled. The insert shows the phosphorylation of T68 of Chk2 in the model. The interactions between the proteins were identified using the PIC [42]. (g) Complex of phosphorylated p21 (T145) and phosphorylated Chk2 (T68): individual structural models of p21 phosphorylated at T145 and Chk2 phosphorylated at T68 were docked using ClusPro [40] and rendered using Chimera [41]. The NLS of Chk2 is shown in red and the nuclear export signal (NES) is shown in green. The interaction profile of the p-p21/p-Chk2 complex identified by the PIC [42] shows that no amino acid in the NES region of p21 interacts with p-Chk2, hence showing that the NES is free from any interactions facilitating export of the complex to the cytoplasm.

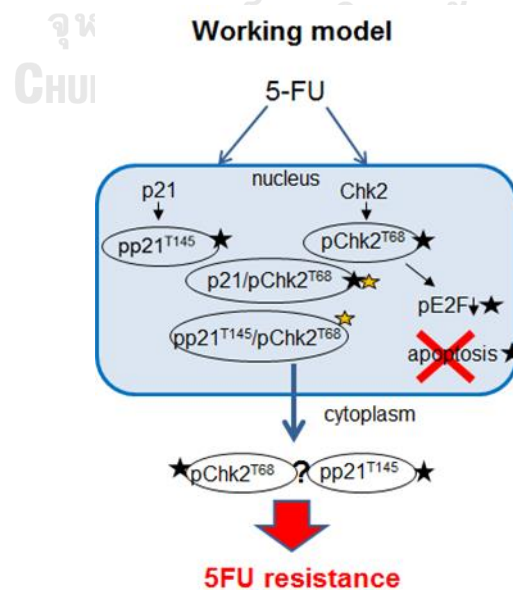


Fig. 8 Schematic model of p21/Chk2 mediated 5-FU resistance.

Black stars mark where experimental evidence is given, and orange star marks in silico analysis. The fate of p-Chk2 in the cytoplasm after detachment of the complex is unclear.

Discussion

Chemoresistance has become the major limitation for 5FU-based therapy in multiple types of cancer [1,3]. Thus, there is an urgent need to better understand the underlying molecular mechanism and to finally identify novel biomarkers with the potential to predict the patient's specific drug response. For the first time, our study revealed that cytoplasmic p21 plays a critical role in controlling 5FU resistance in CRC.

As a classical cell cycle inhibitor and tumor suppressor, p21 mediates diverse cellular functions such as DNA repair, cell cycle arrest, differentiation, and apoptosis induction [4,43]. Interestingly, p21 might also act as an oncogene, which also led to the introduction of the name "cancer gene chameleon" [44,45]. The distinct functions of p21 are mainly dependent on its subcellular localization. Whereas nuclear p21 elicits tumor suppressive activities, the cytoplasmic p21 protein has rather oncogenic effects [4,14].

The cytoplasmic localization of p21 can be ascribed to phosphorylation through different kinases at distinct phosphorylation sites, such as Thr-57, Ser-130, Thr-145, Ser-146, and Ser-153 [46]. Activated AKT was suggested to be an important regulator of p21 and phosphorylates p21 at threonine 145 (p-p21T145), leading to formation of anti-apoptotic complexes [26]. Since the phosphorylation of p21 at threonine 145 was clearly shown to cause cytoplasmic retention of the protein, our findings led to the notion that cytoplasmic p21 might control the susceptibility to 5FU. Previous studies have already shown that cytoplasmic p21 is mediating drug resistance for cisplatin and paclitaxel in ovarian cancer [23–25]. In doxorubicin-chemoresistant breast cancer cells, cytoplasmic re-localization of p21 led to an up-regulation of the anti-apoptotic protein BclxL [47].

Indeed, we showed that, in response to 5FU, the protein levels of p-p21T145 were up-regulated predominantly in the resistant (adherent) cells when compared to apoptotic (detached) cells. In addition, there was a remarkable cytoplasmic increase/shuttling under 5FU treatment in the resistant cells in vitro and in vital (resistant) areas of in vivo xenografts. When conducting ectopic expression of two different forms of p21, the hyperphosphorylated p21T145D and unphosphorylatable p21T145A, we found that the presence of p-p21T145D conferred 5FU resistance, while unphosphorylatable p21 had the opposite effect. In accordance with these findings, apoptosis induction measured by cleaved PARP seemed to be higher in the hypophosphorylated p21T145A group.

Paradoxically, our data provided evidence that the cytoplasmic phosphorylation and sequestration of p21 is not the only pathway by which resistance to 5FU can develop. Thus, our

findings support the general knowledge of a dual functionality of p21 action dependent on the genetic context of cells. It has to be mentioned that HCT116 p21^{-/-} cells show another morphologic differentiation and represent a more mesenchymal phenotype [48]. Mesenchymal colorectal tumor cells are well-known for their high chemotherapy resistance [49]. Therefore, we suggest that cells without p21 take another pathway to develop a resistance to 5FU treatment.

It is well accepted that p21 has the capability to interact with several cellular proteins resulting in its diverse functions [3,4,20–22,25,43,50]. Cyclin E/A-CDK2 or cyclin D-CDK4/6 complexes were identified as the main interaction partners of p21 being involved in cell cycle regulation [4,43,50]. In addition, binding of p21 to pro-caspase 3 or ASK1 has been shown to play a role in apoptotic signaling inhibition [20–22]. In the present study, the expression of a panel of phospho-kinases analyzed by an antibody-based array suggested phosphorylated Chk2 (T68) to be an interaction partner of p21 that is involved in mediating 5FU resistance in CRC. Chk2 is a serine/threonine protein kinase, which can be activated in response to DNA damage [32,33]. It is well established that the Chk2 protein structure contains an FHA domain, which typically binds to phospho-threonine residues of interacting proteins [34]. Using *in silico* modeling, we provided further evidence that this domain might interact with p21T145. The interaction between both proteins becomes even stronger, when both proteins are phosphorylated, which is reflected by the lower energy of the complex. The functions of Chk2 for DNA damage-response are very diverse and include regulation of DNA repair, cell cycle arrest, senescence and apoptosis [32,33,51]. Thus, Chk2 seemed a promising novel candidate that we wanted to study in more detail concerning its interaction with p21 and role in 5FU resistance. In response to stress stimuli, Chk2 is phosphorylated and activated by ATM at Threonine 68 (p-Chk2T68) in the nucleus. Activated p-Chk2 then phosphorylates one of its downstream substrates E2F1, which contributes to the induction of apoptosis [33,34]. In the present study, 5FU treatment caused an increase in the p-Chk2T68 level, and for the first time, we describe that cytoplasmic p21 or p-p21T145 could inhibit the normal function of p-Chk2 in activation of pro-apoptotic p-E2F1.

We provided further evidences for an interaction between p21 and p-Chk2: (1) p-Chk2T68 could be co-immunoprecipitated with p21 after 5FU treatment; (2) cytoplasmic p21 is co-localized with p-Chk2T68 after 5FU treatment as shown by immunofluorescence and immunohistochemistry both *in vitro* and *in vivo*; (3) our proximity ligation assay showed interaction between both proteins in the nucleus, leading to the hypothesis that p21 is responsible for the nuclear export of p-Chk2T68; and (4) *in silico* modeling supported our hypothesis of a p21/Chk2 protein complex formation. According to our working model, p21 and Chk2 exist in a complex in the nucleus. After 5FU treatment, p21 and Chk2 are phosphorylated and the conformation of both proteins triggers the interaction of p-p21T145 and p-Chk2T68 at

the two residues Arg 240 and Arg 241, where the NLS of Chk2 is located leading to a masked NLS. At the same time, the NES sequences of p-p21^{T145} are still accessible, thus facilitating the export of the complex to the cytoplasm. There was a significant cytoplasmic increase of p-Chk2^{T68} in CAM xenografts of cells that had been treated with 5FU. Obviously, p-p21^{T145} seems to decrease the endogenous level of nuclear p-Chk2^{T68} after 5FU stimulus. From our results of the ligation assay, we assume that the complex is falling apart, when p-Chk2^{T68} reaches the cytoplasm. The fate of p-Chk2 in the cytoplasm after detachment of the protein complex is unclear. For B-cell lymphoma, it has been reported that ERK and Chk2 form a cytoplasmic complex and this functional interaction requires Chk2 phosphorylation [52]. We cannot exclude the interaction of p21 with further kinases as the spectrum of deregulated kinases after p21 transfection was remarkable. Moreover, 5FU is also able to induce cancer cell death, independent of p21 signaling [1,3]. Finally, we suggest p-Chk2^{T68}'s nuclear export and cytoplasmic accumulation as a novel mechanism for cytoplasmic p21-mediated resistance to 5FU.

Material and Methods

Cell lines

Human colorectal HCT116, HT29, SW837 cancer cells were cultured in RPMI 1640 (GIBCO Life Technologies, Loughborough, UK) and HCT p21^{-/-} cancer cells were cultured in DMEM (GIBCO Life Technologies) supplemented with 10% fetal bovine serum (PAN Biotech, Aidenbach, Germany), penicillin (100 U/ML) and streptomycin (100 µg/mL) (PAN Biotech), 1% L-glutamine (PAN Biotech) (for HCT p21^{-/-}) and 1% essential amino acid (GIBCO Life Technologies) (for HCT p21^{-/-}). Cells were mycoplasma free. Cell lines were authenticated using Multiplex Cell Authentication by Multiplexion (Heidelberg, Germany)

Cytotoxicity assay

Cell viability was determined by MTT or Crystal Violet assay as previously described [53,54]. Briefly, HCT116, HCT116 p21^{-/-}, HT29, and SW837 cells were seeded in 96-well plates and treated with 5FU at various concentrations (0–100 µM) for 24 h or 48 h and then stained with MTT or Crystal Violet. All analyses were performed in at least three independent replicate experiments.

Annexin-Propidium iodide apoptosis assay by flow cytometry

Quantification of apoptosis was performed by Annexin-PI staining as previously described [55]. Cells were treated with 5FU (10, 25, and 100 µM) for 48 h. Positive Annexin V staining indicates early apoptotic cells, and propidium iodide-positive cells were used to measure

necrotic cells, whereas Annexin V-positive and propidium iodide-positive cells were counted as late apoptotic cells.

Western Blot analysis

Cells were treated with 5FU (25 and 100 μ M) for 48 h. Dead and viable cells were collected separately. Cell lysates were prepared by adding lysis buffer with a protease inhibitor cocktail (Merck KGaA, Darmstadt, Germany) to cell pellets for 90 min on ice. After SDS PAGE, the proteins were transferred onto 0.45 μ M nitrocellulose membranes (GE Healthcare Chalfont, St. Giles, UK). After blocking for 1 h in 5% non-fat dry milk in TBST (25 mM Tris-HCl (Carl Roth, Karlsruhe, Germany) pH 7.5, 125 mM NaCl (Carl Roth, Karlsruhe, Germany), and 0.05% Tween 20 (SERVA) membranes were incubated with a primary antibody at 4 °C overnight. Membranes were washed three times with TBST for 5 min and incubated with horseradish peroxidase-labeled isotype-specific secondary antibodies (anti-mouse or anti-rabbit IgG peroxidase conjugated; Pierce, Rockford, IL, USA) for 2 h at room temperature. The immune complexes were detected by enhancement with a chemiluminescent substrate (IMerck Millipore, Molsheim, France). The level of immunoreactivity was measured as peak intensity using an image capture and analysis system (Syngene Europe, Cambridge, UK). Antibodies used in the present study were as follows: mouse monoclonal anti-p-p21T145 (1:1000, BSA, Santa Cruz Biotechnology, Dallas, TX, USA), mouse monoclonal anti-p21 (1:1000, BSA, Cell Signaling), Rabbit monoclonal anti-Chk2 (1:1000, BSA, Cell Signaling, Cambridge, UK), Rabbit monoclonal anti-P-Chk2T68 (1:1000, BSA, Cell Signaling), mouse monoclonal p-E2F1 (1:250, BSA, Abcam, Cambridge, UK) and Rabbit monoclonal anti-PARP (1:1000, BSA, Cell Signaling). HRP-conjugated anti-GAPDH (1:50,000, BSA, Abnova, Taipei, Taiwan) was used to control equal loading and protein quality. In addition, lysates from HCT116 p21^{-/-} cells were used as a validation control for the p-p21 antibody.

Immunofluorescence

Cells were treated with 5FU (25 and 100 μ M) for 48 h. After the treatment, cells were washed several times with PBS to remove the dead cells. The remaining cells on the slides were fixed with 4% paraformaldehyde for 20 min and permeabilized with 0.1% Triton-X for 10 min. Thereafter, the cells were incubated with 3% bovine serum albumin (BSA) (Carl Roth) for 30 min to prevent nonspecific binding. The cells were washed and incubated with mouse anti-p21 monoclonal antibodies or rabbit anti-p-Chk2T68 monoclonal antibodies (1:400 and 1:200 in BSA, respectively) for 48 h at 4 °C. The primary antibody was removed and cells were washed with PBS and subsequently incubated with secondary antibodies (Alexa Fluor 555-labeled conjugated goat anti-mouse IgG or Alexa Fluor 488-labeled conjugated goat anti-rabbit IgG, respectively, 1:500, Invitrogen, Carlsbad, CA, USA) for 2 h at room temperature. Nuclei were counterstained

with Hoechst 33342 (Sigma-Aldrich, St. Louis, MO, USA). Samples were washed with PBS, and then visualized and imaged by fluorescence microscope.

Plasmids and Transfection

Flag p21 T145D (Addgene plasmid # 16242), Flag p21 T145A (Addgene plasmid # 16241) and HA PKB T308D S473D pcDNA3 (Addgene plasmid # 14751) were provided by Addgene (Cambridge, MA, USA). Transient transfection was performed using Lipofectamine 3000 Transfection Reagent according to the manufacturer's instruction (Thermo Fisher Scientific, Waltham, MA, USA). Briefly, HCT116 cells were seeded to be 70–90% confluent at transfection. Plasmid DNA-lipid complexes were prepared as recommended from the company's protocol. DNA-lipid complexes were added to the cells. Cells were incubated for 2 days at 37 °C before treatment with 5FU (25 µM) for 48 h and evaluation of protein expression by Western Blot analysis. The transcription efficiency was validated by immunofluorescence and Western Blot analysis of targeting gene expression in three independent experiments.

Immunoprecipitation

HCT116 were seeded in 60-mm cell culture dishes at a density of 5×10^5 cells/dish for 24 h. Then, the cells were treated with 5FU (25 and 100 µM) for 48 h. After removing the dead cells, cell lysates of remaining cells were collected and prepared as previously described [56]. Briefly, cells were fixed with 2% formaldehyde before lysed with RIPA buffer. Protein content was determined by using a Bio-Rad Dc Protein Assay (BioRad, Hercules, CA, USA). Equal amounts of lysates (600–900 µg) were adjusted to 500 µL of volume and then incubated with specific antibodies to p-Chk2(T68) immobilized on 50 µL of magnetic Protein G beads overnight at 4 °C (IP Dynabeads Kit). The protein-antibody-bead complexes were recovered (IP Dynabeads Kit) and the protein complexes were analyzed by Western Blotting.

Human phospho-kinase antibody array

To determine levels of phospho-kinases at baseline, and after specific transfection, HCT116 were harvested after 48 h of transfection with Flag p21 T145D pcDNA3 or HA PKB T308D S473D pcDNA3. Cells were lysed using lysis buffer of the Human phospho-kinase array kit (ARY003, Proteome Profiler™, R&D Systems, Minneapolis, MN, USA). The Human phospho-kinase array was performed according the protocol of the manufacturer. In this array, 46 capture antibodies were spotted in duplicate on nitrocellulose membranes. Cell lysates were incubated with the membrane overnight and membranes were incubated with a cocktail of biotinylated detection antibodies and streptavidin-HRP. Finally, proteins were detected using an ECL chemiluminescent system. The level of immunoreactivity was measured as peak intensity using an image capture and analysis system (GeneGnome). The intensity of signal of each spot was

quantified using ImageJ software. The intensity values were corrected for background signals and to compare different membranes levels were normalized to those of the positive controls on each membrane.

Chorioallantoic membrane assay (CAM assay)

The CAM assay represents a well-known and accepted alternative xenograft animal model system. Thus, the present study complies with the commonly accepted “3Rs”. Briefly, fertilized chicken eggs were incubated at 37 °C with a 80% humidity for 8 days. Then, a small hole was pricked into the eggshell of the more rounded pole, where the air sac resided. After dropping of the egg content, a small window (Ø 1–1.5 cm) was carefully cut at the more rounded pole for inoculation of the tumor cells. After another day of incubation (day 9 of embryonic development), 1×10^6 of 5FU pretreated (15 µM) or control HCT116 cells in a 1:1 mixture of Matrigel (Corning Life Sciences, NY, USA) and the medium were implanted onto the CAM and the eggs were incubated for another 5 days. Finally, micro-tumors were harvested, fixed in 4% phosphate-buffered formalin and embedded in paraffin for histological and immunohistochemical analysis.

Immunohistochemistry (IHC) Staining Assay

Serial sections (2 µm) were cut from the paraffin blocks and mounted on pre-coated slides for immunohistochemical analysis of the CAM tumors. All FFPE CAM tissue sections were deparaffinized with xylene and rehydrated with graded ethanol. The antigen retrieval was performed by 1 min steam cooking in TRS-Buffer pH 6 (p21 Waf1/Cip1) or pH 9 (pChk2T68), respectively. Slides were incubated at 4 °C overnight with a primary monoclonal antibody p21 Waf1/Cip1 (12D1, mouse), 1:1.000 dilution (Cell Signaling), or pChk2T68 (2197, rabbit), 1:50 dilution (Cell Signaling). Antibody binding was visualized using the Polymer-Kit (AP, Zytomed, Berlin, Germany) or biotinylated Anti-Rabbit/ABC-Kit (Vector, Olean, NY, USA).

Adjacent slides were stained with hematoxylin and eosin for histomorphological analyses. Immunohistochemical scoring was performed in a semi-quantitative way by two pathologists (Katharina Erlenbach-Wuensch, Asiana Vial Roehe). The intensity was quantified in a range from 1 to 3. The area was quantified by percentage of positive cells in 5% steps. An immunoscore was generated by multiplying intensity (0–3) with the respective percentage of positive cells (0–100%).

Bright field images (Magnification: 200x, 400x) of stained sections were taken with the Olympus XC50 camera (Olympus Corporation, Tokyo, Japan) in combination with the Olympus BX51 microscope (Olympus Corporation).

Proximity ligation assay (In situ PLA)

HT29 cells were grown on 8-well chamber slides until 70–80% confluency and treated with 5FU. Cells were then washed with PBS, fixed in 4% paraformaldehyde in PBS for 30 min, permeabilized in 0.1% Triton X-100 for 20 min, and blocked with a Duolink II blocking solution (Sigma-Aldrich). After blocking, cells were incubated with a combination of primary antibodies anti-p21 and anti-p-Chk2 (T68) in a preheated humidity chamber for 1 h at 37 °C. Cells were then incubated with the PLA probes diluted 1:5 in antibody diluent (Sigma-Aldrich) in a humidified chamber for 1 h at 37 °C. Subsequent hybridization, ligation, amplification, and detection were performed using manufacturer's instruction (Sigma-Aldrich). Fluorescence images were acquired using a confocal laser microscope (LSM-PMT Observer, Carl Zeiss, Oberkochen, Germany).

Structural modeling

Modelling of p21: The full length structure of the 164aa long p21 protein was modelled using two crystallographic structures 4I58 and 5E0U as templates, respectively, for homology by MODELLER [39] and a structure prediction approach using Iterative Threading ASSEmblY Refinement (ITASSER), a hierarchical server for protein structure prediction [57].

For modelling of Chk2, its crystal structure with an inhibitor was taken from the PDB (2WTC) and the coordinates of the inhibitor were then removed to get the structure of Chk2. The structure was energy-minimized and the stable structure was considered for further investigations. Phosphorylation of p21 at T145 and of Chk2 at T68 was modelled using CHIMERA [41]. The complexes of p21 and Chk2 were formed by docking the individual proteins using the protein–protein docking tool ClusPro [40]. The complexes with the lowest energy were chosen for the analysis of interactions between the proteins considered. The cluster scores of the complexes from the ClusPro server were used to understand the energy profiles of the p21–Chk2 complex. The ionic, hydrophobic, and hydrogen bond interactions were identified and analyzed, applying the Protein Interaction Calculator (PIC) [42]. All renderings were performed using CHIMERA [41]. The same protocol was followed for docking of the phosphorylated structures of p21 and Chk2.

Statistics

Data are expressed as means \pm SD of at least three independent experiments. All treatment data were normalized to non-treated controls or transfection controls. Statistical analysis was performed using the non-parametric Mann-Whitney-test. Statistical significance was set to $P < 0.05$.

Conclusions

In summary, our mechanistic study provides novel information on how cytoplasmic p21 controls 5FU resistance in CRC. We suggest that the p21-dependent inhibition of Chk2 majorly

contributes to the resistance for 5FU-based chemotherapy. The formation of a p21–Chk2 complex disrupts the function of Chk2-mediated apoptosis induction by promoting the nuclear export of both proteins. Screening for the subcellular localization of p21 in patient tumor samples could provide information about possible resistance development under 5FU-based therapy and has to be further evaluated in a clinical setting.

Authors' contributions

A.M., C.N., P.C. and R.S.-S. conceived the study. A.M., C.N., P.C. and R.S.-S. designed the experiments. A.M., C.N., J.K.M., B.N., A.C. and C.C. performed the experiments. V.M. and H.A.P. performed the structural modeling analysis. A.H., A.V.R., and K.E.-W. analyzed the immunohistochemical stainings. A.M., C.N., P.C. and R.S.-S. analyzed and interpreted the data. R.S.-S. contributed reagents/materials/analysis tools. A.M. and C.N. drafted the manuscript. R.S.-S., P.C. and J.K.M. revised the manuscript critically before submission. All authors read and approved the final manuscript.

Funding

The authors thank the Emerging Fields Initiative “Cell Cycle in Disease and Regeneration” (CYDER) for supporting this project (RSS). AM was supported by a grant of the Thailand Research Fund through the Royal Golden Jubilee Ph.D. program of the Chulalongkorn University, Bangkok (Grant No. PHD/0063/2557) and The 100th Anniversary Chulalongkorn University Fund for Doctoral Scholarship. AM was a Cotutelle PhD student (FAU Erlangen and Chulalongkorn University Bangkok) and the present work was performed in partial fulfillment of the requirements for obtaining the degree Dr. rer. nat. at the FAU Erlangen-Nürnberg. PC was granted with a Georg-Forster-Stipendium of the Alexander von Humboldt Foundation. C.C. was partially supported by research grant from Faculty of Pharmaceutical Sciences, Chulalongkorn University (Grant no. Phar2561-RGI-02).

Acknowledgement

We thank Adrian Koch and Christa Winkelmann for their excellent technical support.

Conflicts of interest

The authors declare no conflict of interest.

Supplementary materials:

The following are available online at <http://www.mdpi.com/2072-6694/10/10/373/s1> ,

Figure S1: Verification of p-p21^{T145} antibody for Western Blotting analysis, Figure S2: Localization of p21 in 5FU-resistant HT29 and SW837 cells, Figure S3: Transfection efficiency, Figure S4: Effect of hyperphosphorylated AKT on cellular kinase profiles in HCT116, Figure S5: Interaction between p21 and Chk2 proteins, Figure S6: Interaction between p21 and Chk2 proteins.

Figure S1 Verification of p-p21^{T145} antibody for Western Blotting analysis
 Figure S2 Localization of p21 in 5FU-resistant HT29 and SW837 cells
 Figure S3 Transfection efficiency
 Figure S4 Effect of hyperphosphorylated AKT on cellular kinase profiles in HCT116
 Figure S5 Interaction between p21 and Chk2 proteins
 Figure S6 Interaction between p21 and Chk2 proteins

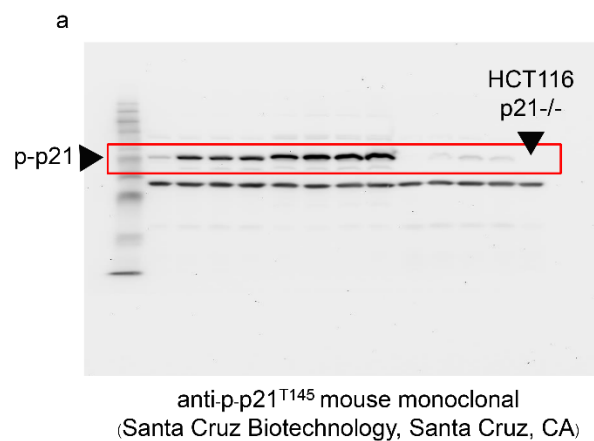


Fig. S1 Verification of p-p21^{T145} antibody for Western Blotting analysis.

(a)p-p21^{T145} showed many unspecific signals in Western Blot analysis, HCT116 p21^{-/-} lysates were used to specify the correct p-p21^{T145} signal.

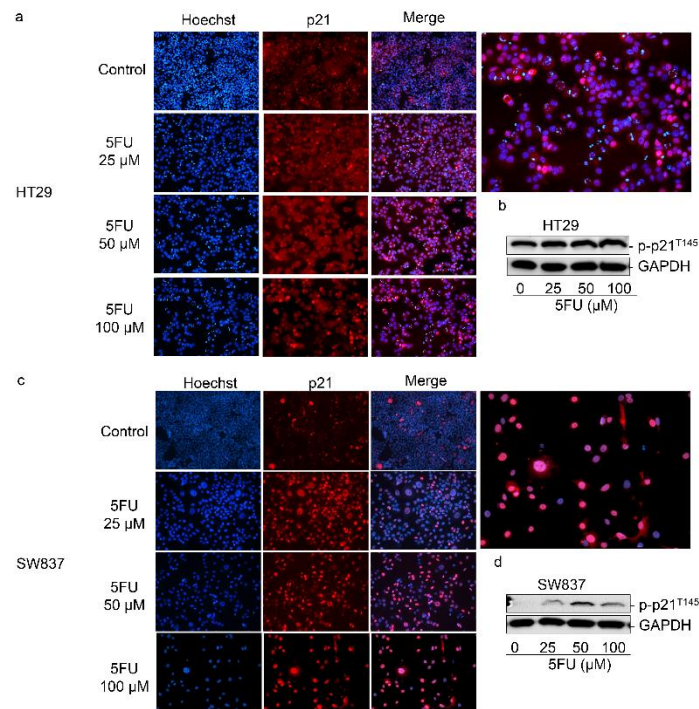


Fig. S2 Localization of p21 in 5FU-resistant HT29 and SW837 cells.

HT29 cells (a,c) and SW837 cells (b,d) were treated with various concentrations of 5FU for 48 h and the expression of p21 was determined by immunofluorescence staining using mouse anti-p21 monoclonal antibodies followed by Alexa Fluor 555-labeled secondary antibody to visualize p21 expression (red) and cell nuclei (Hoechst 33342, blue), scale bar: 50 μm . (c,d) The expression level of phosphorylated-p21 (p-p21^{T145}) in 5FU-resistant HT29 (b) and SW837 (d) cells was determined by Western Blot analysis. Cells were treated with various concentrations of 5FU for 48 h. After incubation, dead cells were discarded by washing 3 times with PBS and the remaining resistant cells were collected to prepare protein lysates. The expression level of p-p21^{T145} was determined and the blots were re-probed with GAPDH to confirm equal loading of the samples.

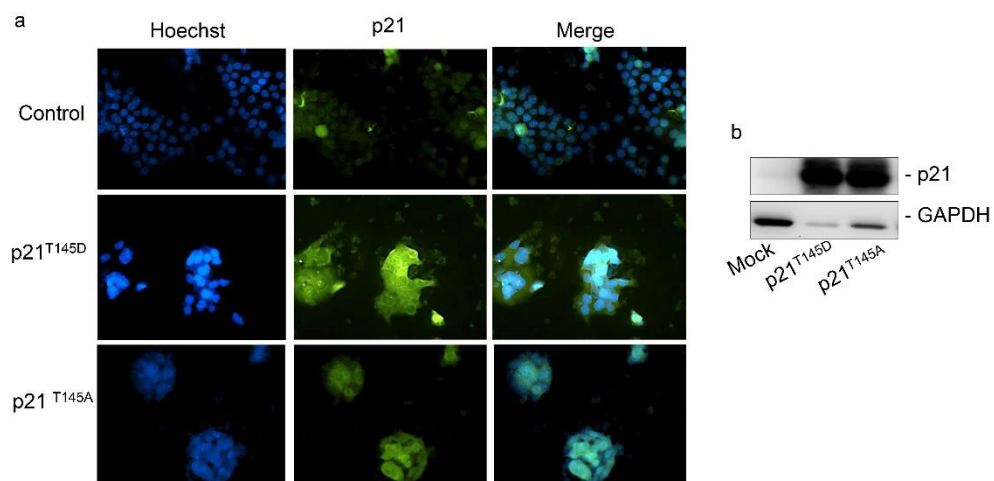


Fig. S3 Transfection efficiency.

HCT116 cells were transfected with plasmids for the hyperphosphorylated p21^{T145D} and unphosphorylatable p21^{T145A} protein forms. After 24 h of transfection, (a) the subcellular localization of p21 was characterized by immunofluorescence staining using mouse anti-p21 monoclonal antibodies followed by Alexa Fluor 488-labeled secondary antibody to visualize p21 expression (green) and cell nuclei (Hoechst 33342, blue), scale bar: 50 μ m. (b) The expression levels of p21 were quantified by Western Blot analysis after 24 h. Blots were re-probed with GAPDH to confirm equal loading of the samples.

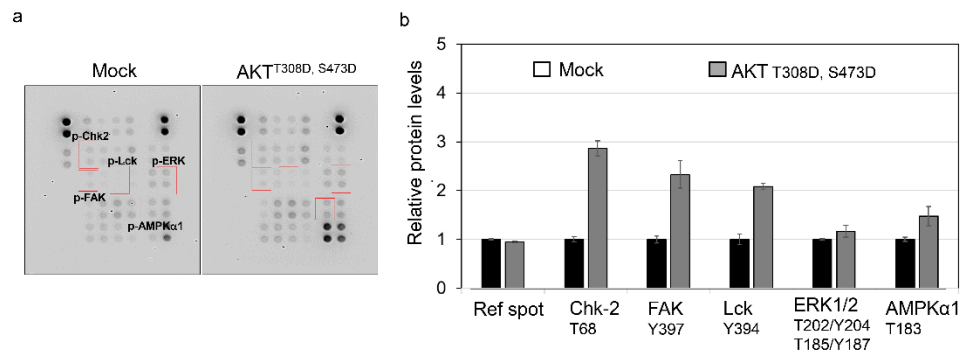


Fig. S4 Effect of hyperphosphorylated AKT on cellular kinase profiles in HCT116.

(a-b) Expression levels of phospho-proteins in transfected cells. HCT116 cells were transfected with hyperphosphorylated AKT^{T308D, S473D}. After 48 h of transfection, cells lysates were prepared and subjected to the Human Phospho-Kinase Array Kit (R&D systems).

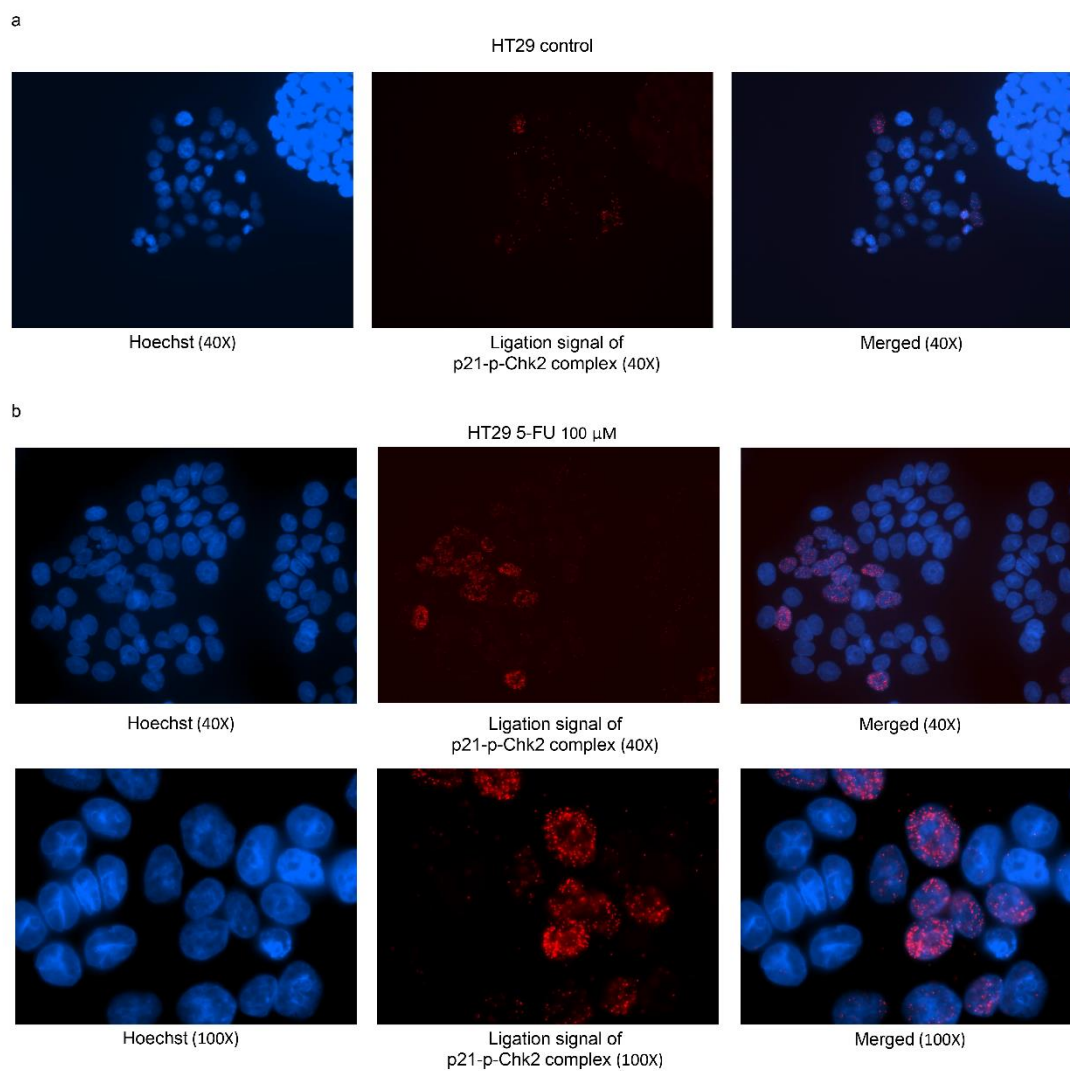


Fig. S5 Interaction between p21 and Chk2 proteins.

Cells were treated with 100 μ M 5FU for 48 h and the protein-protein interaction of p21-p-Chk2T68 was analyzed by proximity ligation assay (HT29 cells) (red signals indicate protein-protein interaction between p21 and p-Chk2T68; Fluorescence images of untreated control HT29 cells (40X magnification) and 5FU treated HT29 cells (40X and 100X magnification).

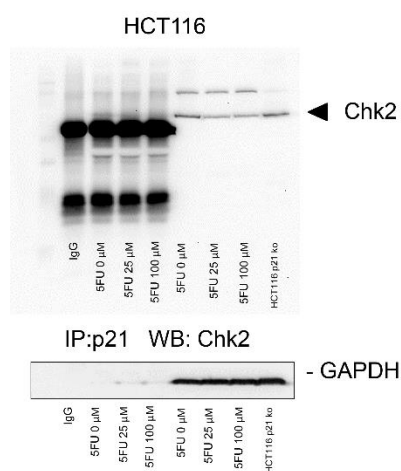


Fig. S6 Interaction between p21 and Chk2 proteins.

Cells were treated with 25 μM and 100 μM 5FU for 48 h and the protein-protein interaction of p21 and Chk2 (a, HCT116 cells) or p-p21T145 and Chk2 (b, HT29 cells) was analyzed by co-immunoprecipitation assay. Cell lysates were prepared and immunoprecipitated with p21 and p-p21 antibody, respectively. The resulting immunocomplexes were then analyzed for Chk2 by Western Blotting using an Chk2 antibody.

References

1. Longley, D.B.; Harkin, D.P.; Johnston, P.G. 5-fluorouracil: Mechanisms of action and clinical strategies. *Nat. Rev. Cancer* 2003, 3, 330–338. [CrossRef] [PubMed]
2. Efficacy of adjuvant fluorouracil and folinic acid in colon cancer. International Multicentre Pooled Analysis of Colon Cancer Trials (IMPACT) investigators. *Lancet* 1995, 345, 939–944.
3. Zhang, N.; Yin, Y.; Xu, S.J.; Chen, W.S. 5-Fluorouracil: Mechanisms of resistance and reversal strategies. *Molecules* 2008, 13, 1551–1569. [CrossRef] [PubMed]
4. Abbas, T.; Dutta, A. p21 in cancer: Intricate networks and multiple activities. *Nat. Rev. Cancer* 2009, 9, 400–414. [CrossRef] [PubMed]
5. Zhang, S.; Hu, B.; You, Y.; Yang, Z.; Liu, L.; Tang, H.; Bao, W.; Guan, Y.; Shen, X. Sorting nexin 10 acts as a tumor suppressor in tumorigenesis and progression of colorectal cancer through regulating chaperone mediated autophagy degradation of p21(Cip1/WAF1). *Cancer Lett.* 2018, 419, 116–127. [CrossRef] [PubMed]
6. Singh, K.; Dong, Q.; TimiriShanmugam, P.S.; Koul, S.; Koul, H.K. Tetrandrine inhibits deregulated cell cycle in pancreatic cancer cells: Differential regulation of p21(Cip1/Waf1), p27(Kip1) and cyclin D1. *Cancer Lett.* 2018, 425, 164–173. [CrossRef] [PubMed]

7. Winters, Z.E.; Leek, R.D.; Bradburn, M.J.; Norbury, C.J.; Harris, A.L. Cytoplasmic p21WAF1/CIP1 expression is correlated with HER-2/ neu in breast cancer and is an independent predictor of prognosis. *Breast Cancer Res.* 2003, 5, R242–R249. [CrossRef] [PubMed]
8. Perez-Tenorio, G.; Berglund, F.; Esguerra Merca, A.; Nordenskjold, B.; Rutqvist, L.E.; Skoog, L.; Stal, O. Cytoplasmic p21WAF1/CIP1 correlates with Akt activation and poor response to tamoxifen in breast cancer. *Int. J. Oncol.* 2006, 28, 1031–1042. [CrossRef] [PubMed]
9. Shiraki, K.; Wagayama, H. Cytoplasmic p21(WAF1/CIP1) expression in human hepatocellular carcinomas. *Liver Int.* 2006, 26, 1018–1019. [CrossRef] [PubMed]
10. Cheung, T.H.; Lo, K.W.; Yu, M.M.; Yim, S.F.; Poon, C.S.; Chung, T.K.; Wong, Y.F. Aberrant expression of p21(WAF1/CIP1) and p27(KIP1) in cervical carcinoma. *Cancer Lett.* 2001, 172, 93–98. [CrossRef]
11. Ferrandina, G.; Stoler, A.; Fagotti, A.; Fanfani, F.; Sacco, R.; De Pasqua, A.; Mancuso, S.; Scambia, G. p21WAF1/CIP1 protein expression in primary ovarian cancer. *Int. J. Oncol.* 2000, 17, 1231–1235. [CrossRef] [PubMed]
12. Shah, M.A.; Kortmansky, J.; Motwani, M.; Drobnjak, M.; Gonen, M.; Yi, S.; Weyerbacher, A.; Cordon-Cardo, C.; Lefkowitz, R.; Brenner, B.; et al. A phase I clinical trial of the sequential combination of irinotecan followed by flavopiridol. *Clin. Cancer Res.* 2005, 11, 3836–3845. [CrossRef] [PubMed]
13. Rau, B.; Sturm, I.; Lage, H.; Berger, S.; Schneider, U.; Hauptmann, S.; Wust, P.; Riess, H.; Schlag, P.M.; Dorken, B.; et al. Dynamic expression profile of p21WAF1/CIP1 and Ki-67 predicts survival in rectal carcinoma treated with preoperative radiochemotherapy. *J. Clin. Oncol.* 2003, 21, 3391–3401. [CrossRef] [PubMed]
14. Child, E.S.; Mann, D.J. The intricacies of p21 phosphorylation: Protein/protein interactions, subcellular localization and stability. *Cell Cycle* 2006, 5, 1313–1319. [CrossRef] [PubMed]
15. Kondo, S.; Barna, B.P.; Kondo, Y.; Tanaka, Y.; Casey, G.; Liu, J.; Morimura, T.; Kaakaji, R.; Peterson, J.W.; Werbel, B.; et al. WAF1/CIP1 increases the susceptibility of p53 non-functional malignant glioma cells to cisplatin-induced apoptosis. *Oncogene* 1996, 13, 1279–1285. [PubMed]
16. Lincet, H.; Poulain, L.; Remy, J.S.; Deslandes, E.; Duigou, F.; Gauduchon, P.; Staedel, C. The p21(cip1/waf1) cyclin-dependent kinase inhibitor enhances the cytotoxic effect of cisplatin in human ovarian carcinoma cells. *Cancer Lett.* 2000, 161, 17–26. [CrossRef]
17. Helt, C.E.; Rancourt, R.C.; Staversky, R.J.; O'Reilly, M.A. p53-dependent induction of p21(Cip1/WAF1/Sdi1) protects against oxygen-induced toxicity. *Toxicol. Sci.* 2001, 63, 214–222. [CrossRef] [PubMed]

18. Zhang, X.; Song, X.; Yin, S.; Zhao, C.; Fan, L.; Hu, H. p21 induction plays a dual role in anti-cancer activity of ursolic acid. *Exp. Biol. Med.* (Maywood) 2016, 241, 501–508. [CrossRef] [PubMed]
19. Gorospe, M.; Cirielli, C.; Wang, X.; Seth, P.; Capogrossi, M.C.; Holbrook, N.J. p21(Waf1/Cip1) protects against p53-mediated apoptosis of human melanoma cells. *Oncogene* 1997, 14, 929–935. [CrossRef] [PubMed]
20. Asada, M.; Yamada, T.; Ichijo, H.; Delia, D.; Miyazono, K.; Fukumuro, K.; Mizutani, S. Apoptosis inhibitory activity of cytoplasmic p21(Cip1/WAF1) in monocytic differentiation. *EMBO J.* 1999, 18, 1223–1234. [CrossRef] [PubMed]
21. Suzuki, A.; Tsutomi, Y.; Miura, M.; Akahane, K. Caspase 3 inactivation to suppress Fas-mediated apoptosis: Identification of binding domain with p21 and ILP and inactivation machinery by p21. *Oncogene* 1999, 18, 1239–1244. [CrossRef] [PubMed]
22. Suzuki, A.; Tsutomi, Y.; Akahane, K.; Araki, T.; Miura, M. Resistance to Fas-mediated apoptosis: Activation of caspase 3 is regulated by cell cycle regulator p21WAF1 and IAP gene family ILP. *Oncogene* 1998, 17, 931–939. [CrossRef] [PubMed]
23. Xia, X.; Ma, Q.; Li, X.; Ji, T.; Chen, P.; Xu, H.; Li, K.; Fang, Y.; Weng, D.; Weng, Y.; et al. Cytoplasmic p21 is a potential predictor for cisplatin sensitivity in ovarian cancer. *BMC Cancer* 2011, 11, 399. [CrossRef] [PubMed]
24. Koster, R.; di Pietro, A.; Timmer-Bosscha, H.; Gibcus, J.H.; van den Berg, A.; Suurmeijer, A.J.; Bischoff, R.; Gietema, J.A.; de Jong, S. Cytoplasmic p21 expression levels determine cisplatin resistance in human testicular cancer. *J. Clin. Investig.* 2010, 120, 3594–3605. [CrossRef] [PubMed]
25. Heliez, C.; Baricault, L.; Barboule, N.; Valette, A. Paclitaxel increases p21 synthesis and accumulation of its AKT-phosphorylated form in the cytoplasm of cancer cells. *Oncogene* 2003, 22, 3260–3268. [CrossRef] [PubMed]
26. Zhou, B.P.; Liao, Y.; Xia, W.; Spohn, B.; Lee, M.H.; Hung, M.C. Cytoplasmic localization of p21Cip1/WAF1 by Akt-induced phosphorylation in HER-2/neu-overexpressing cells. *Nat. Cell Biol.* 2001, 3, 245–252. [CrossRef] [PubMed]
27. Kim, E.J.; Kang, G.J.; Kang, J.I.; Boo, H.J.; Hyun, J.W.; Koh, Y.S.; Chang, W.Y.; Kim, Y.R.; Kwon, J.M.; Maeng, Y.H.; et al. Over-activation of AKT signaling leading to 5-Fluorouracil resistance in SNU-C5/5-FU cells. *Oncotarget* 2018, 9, 19911–19928. [CrossRef] [PubMed]
28. Manapov, F.; Muller, P.; Rychly, J. Translocation of p21(Cip1/WAF1) from the nucleus to the cytoplasm correlates with pancreatic myofibroblast to fibroblast cell conversion. *Gut* 2005, 54, 814–822. [CrossRef] [PubMed]

29. Gravina, G.L.; Senapedis, W.; McCauley, D.; Baloglu, E.; Shacham, S.; Festuccia, C. Nucleocytoplasmic transport as a therapeutic target of cancer. *J. Hematol. Oncol.* 2014, 7, 85. [CrossRef] [PubMed]
30. Boulares, A.H.; Yakovlev, A.G.; Ivanova, V.; Stoica, B.A.; Wang, G.; Iyer, S.; Smulson, M. Role of poly(ADP-ribose) polymerase (PARP) cleavage in apoptosis. Caspase 3-resistant PARP mutant increases rates of apoptosis in transfected cells. *J. Biol. Chem.* 1999, 274, 22932–22940. [CrossRef] [PubMed]
31. Chaitanya, G.V.; Alexander, J.S.; Babu, P.P. PARP-1 cleavage fragments: Signatures of cell-death proteases in neurodegeneration. *Cell Commun. Signal.* 2010, 8, 31. [CrossRef] [PubMed]
32. Zhou, B.B.; Bartek, J. Targeting the checkpoint kinases: Chemosensitization versus chemoprotection. *Nat. Rev. Cancer* 2004, 4, 216–225. [CrossRef] [PubMed]
33. Stevens, C.; Smith, L.; La Thangue, N.B. Chk2 activates E2F-1 in response to DNA damage. *Nat. Cell Biol.* 2003, 5, 401–409. [CrossRef] [PubMed]
34. Antoni, L.; Sodha, N.; Collins, I.; Garrett, M.D. CHK2 kinase: Cancer susceptibility and cancer therapy—Two sides of the same coin? *Nat. Rev. Cancer* 2007, 7, 925–936. [CrossRef] [PubMed]
35. Huang, D.Y.; Chang, Z.F. Interaction of human thymidine kinase 1 with p21(Waf1). *Biochem. J.* 2001, 356, 829–834. [CrossRef] [PubMed]
36. Cayrol, C.; Knibiehler, M.; Ducommun, B. p21 binding to PCNA causes G1 and G2 cell cycle arrest in p53-deficient cells. *Oncogene* 1998, 16, 311–320. [CrossRef] [PubMed]
37. Chen, W.; Sun, Z.; Wang, X.J.; Jiang, T.; Huang, Z.; Fang, D.; Zhang, D.D. Direct interaction between Nrf2 and p21(Cip1/WAF1) upregulates the Nrf2-mediated antioxidant response. *Mol. Cell* 2009, 34, 663–673. [CrossRef] [PubMed]
38. Li, H.; Xie, B.; Rahmeh, A.; Zhou, Y.; Lee, M.Y. Direct interaction of p21 with p50, the small subunit of human DNA polymerase delta. *Cell Cycle* 2006, 5, 428–436. [CrossRef] [PubMed]
39. Webb, B.; Sali, A. Comparative Protein Structure Modeling Using MODELLER. *Curr. Protoc. Bioinform.* 2014, 47, 5.6.1–5.6.32. [CrossRef] [PubMed]
40. Comeau, S.R.; Gatchell, D.W.; Vajda, S.; Camacho, C.J. ClusPro: A fully automated algorithm for protein-protein docking. *Nucleic Acids Res.* 2004, 32, W96–W99. [CrossRef] [PubMed]
41. Pettersen, E.F.; Goddard, T.D.; Huang, C.C.; Couch, G.S.; Greenblatt, D.M.; Meng, E.C.; Ferrin, T.E. UCSF Chimera—A visualization system for exploratory research and analysis. *J. Comput. Chem.* 2004, 25, 1605–1612. [CrossRef] [PubMed]

42. Tina, K.G.; Bhadra, R.; Srinivasan, N. PIC: Protein Interactions Calculator. *Nucleic Acids Res.* 2007, 35, W473–W476. [CrossRef] [PubMed]
43. Karimian, A.; Ahmadi, Y.; Yousefi, B. Multiple functions of p21 in cell cycle, apoptosis and transcriptional regulation after DNA damage. *DNA Repair (Amst)* 2016, 42, 63–71. [CrossRef] [PubMed]
44. Huff, V. Wilms' tumours: About tumour suppressor genes, an oncogene and a chameleon gene. *Nat. Rev. Cancer* 2011, 11, 111–121. [CrossRef] [PubMed]
45. Stepanenko, A.A.; Vassetzky, Y.S.; Kavsan, V.M. Antagonistic functional duality of cancer genes. *Gene* 2013, 529, 199–207. [CrossRef] [PubMed]
46. Kreis, N.N.; Louwen, F.; Yuan, J. Less understood issues: p21(Cip1) in mitosis and its therapeutic potential. *Oncogene* 2015, 34, 1758–1767. [CrossRef] [PubMed]
47. Vincent, A.J.; Ren, S.; Harris, L.G.; Devine, D.J.; Samant, R.S.; Fodstad, O.; Shevde, L.A. Cytoplasmic translocation of p21 mediates NUPR1-induced chemoresistance: NUPR1 and p21 in chemoresistance. *FEBS Lett.* 2012, 586, 3429–3434. [CrossRef] [PubMed]
48. Li, X.L.; Hara, T.; Choi, Y.; Subramanian, M.; Francis, P.; Bilke, S.; Walker, R.L.; Pineda, M.; Zhu, Y.; Yang, Y.; et al. A p21-ZEB1 complex inhibits epithelial-mesenchymal transition through the microRNA 183-96-182 cluster. *Mol. Cell Biol.* 2014, 34, 533–550. [CrossRef] [PubMed]
49. Findlay, V.J.; Wang, C.; Watson, D.K.; Camp, E.R. Epithelial to mesenchymal transition and the cancer stem cell phenotype: Insights from cancer biology with therapeutic implications for colorectal cancer. *Cancer Gene Ther.* 2014, 21, 181–187. [CrossRef] [PubMed]
50. Romanov, V.S.; Rudolph, K.L. p21 shapes cancer evolution. *Nat. Cell Biol.* 2016, 18, 722–724. [CrossRef] [PubMed]
51. Aliouat-Denis, C.M.; Dendouga, N.; Van den Wyngaert, I.; Goehlmann, H.; Steller, U.; van de Weyer, I.; Van Slycken, N.; Andries, L.; Kass, S.; Luyten, W.; et al. p53-independent regulation of p21Waf1/Cip1 expression and senescence by Chk2. *Mol. Cancer Res.* 2005, 3, 627–634. [CrossRef] [PubMed]
52. Dai, B.; Zhao, X.F.; Mazan-Mamczarz, K.; Hagner, P.; Corl, S.; Bahassi el, M.; Lu, S.; Stambrook, P.J.; Shapiro, P.; Gartenhaus, R.B. Functional and molecular interactions between ERK and CHK2 in diffuse large B-cell lymphoma. *Nat. Commun.* 2011, 2, 402. [CrossRef] [PubMed]
53. Ninsontia, C.; Phiboonchaiyanan, P.P.; Chanvorachote, P. Zinc induces epithelial to mesenchymal transition in human lung cancer H460 cells via superoxide anion-dependent mechanism. *Cancer Cell Int.* 2016, 16, 48. [CrossRef] [PubMed]

54. Feoktistova, M.; Geserick, P.; Leverkus, M. Crystal Violet Assay for Determining Viability of Cultured Cells. *Cold Spring Harb. Protoc.* 2016, 2016, pdb.prot087379. [CrossRef] [PubMed]
55. El-Baba, C.; Mahadevan, V.; Fahlbusch, F.B.; Mohan, S.S.; Rau, T.T.; Gali-Muhtasib, H.; Schneider-Stock, R. Thymoquinone-induced conformational changes of PAK1 interrupt prosurvival MEK-ERK signaling in colorectal cancer. *Mol. Cancer* 2014, 13, 201. [CrossRef] [PubMed]
56. Klockenbusch, C.; Kast, J. Optimization of formaldehyde cross-linking for protein interaction analysis of non-tagged integrin beta1. *J. Biomed. Biotechnol.* 2010, 2010, 927585. [CrossRef] [PubMed]
57. Yang, J.; Yan, R.; Roy, A.; Xu, D.; Poisson, J.; Zhang, Y. The I-TASSER Suite: Protein structure and function prediction. *Nat. Methods* 2015, 12, 7–8. [CrossRef] [PubMed]



CHAPTER IV

APOPTOSIS-INDUCING EFFECT OF HYDROQUINONE 5-O-CINNAMOYL
ESTER ANALOG OF RENIERAMYCIN M ON NON-SMALL CELL LUNG
CANCER CELLS

This research had been published in Anticancer Research by year 2017 volume 37 page 6259 - 6267 on the topic namely: Apoptosis-inducing Effect of Hydroquinone 5-O-Cinnamoyl Ester Analog of Renieramycin M on Non-small Cell Lung Cancer Cells (doi:10.21873/anticanres.12077).

The web link of this article as followed: <https://www.ncbi.nlm.nih.gov/pubmed/29061809>

Ph.D. student

Arnatchai Maiuthed

Affiliation

1. Department of Pharmacology and Physiology, Faculty of Pharmaceutical Sciences, Chulalongkorn University, Bangkok 10300
2. Cell-based Drug and Health Products Development Research Unit, Faculty of Pharmaceutical Sciences, Chulalongkorn University, Bangkok 10300

Advisor

Associate Professor Pithi Chanvorachote, Ph.D.

Affiliation

1. Department of Pharmacology and Physiology, Faculty of Pharmaceutical Sciences, Chulalongkorn University, Bangkok 10300
2. Cell-based Drug and Health Products Development Research Unit, Faculty of Pharmaceutical Sciences, Chulalongkorn University, Bangkok 10300

Approval of the co-authors on the use of publication material in the dissertation of Arnatchai Maiuthed

Approval of the co-authors on the use of publication material in the dissertation of Arnatchai Maluthed

Concerns publication:

"Apoptosis-inducing Effect of Hydroquinone 5-O-Cinnamoyl Ester Analog of Renieramycin M on Non-small Cell Lung Cancer Cells"

Amatchai Maiuthed, Tatchakorn Pinkhien, Supakarn Chamni, Khanit Suwanborirux, Naoki Saito, Nareerat Petpiroon, and Pithi Chanvorachote, Anticancer Research 2017, 37, 6259-6267, doi:10.21873/anticancerres.12077

With this I agree that Amatchai Maiuthed uses the publication in text format and pictorial form for his cumulative dissertation "NOVEL REGULATORY MECHANISMS OF PROTEIN KINASE B ON APOPTOSIS SUSCEPTIBILITY AND CANCER DEDIFFERENTIATION" (working title).

Full name	Signature
Tatchakorn Pinkhien	<i>Tatchakorn Pinkhien</i>
Supakarn Chamni	<i>Supakarn Chamni</i>
Khanit Suwanborirux	Retirement
Naoki Saito	<i>Naoki Saito</i>
Nareerat Petpiroon	<i>Nareerat Petpiroon</i>
Pithi Chanvorachote	<i>Pithi Chanvorachote</i>

Abstract

Background: A newly synthesized derivative of renieramycin M (RM), an anticancer lead compound isolated from the blue sponge *Xestospongia* sp., Hydroquinone 5-O-cinnamoyl ester (CIN-RM), was investigated here for activity against non-small cell lung cancer cells.

Materials and Methods: Cytotoxicity effects of CIN-RM and RM on H292 lung cancer cells were determined by MTT assay. We also investigated the mechanism of CIN-RM-mediated apoptosis and mechanism of action of this compound by western blotting.

Results: CIN-RM showed more potent cytotoxicity than its parental compound (RM) against H292 lung cancer cells. At concentrations of 15-60 μ M, CIN-RM significantly induced apoptosis by increasing expression of apoptosis-inducing factor (AIF) and activation of caspase-3 and -9. For up-stream mechanism, CIN-RM mediated apoptosis through a p53-dependent mechanism, which consequently down-regulated anti-apoptotic B-cell lymphoma 2 (BCL2), while increasing the level of pro-apoptotic BCL2-associated X (BAX). In addition, phosphorylation of pro-survival protein AKT was found to be dramatically reduced.

Conclusion: This study revealed the potential of CIN-RM for apoptosis induction and in the development of a novel anticancer agent.

Key words: Renieramycin M, hydroquinone 5-O-cinnamoyl ester analog of renieramycin M, apoptosis, lung cancer, lead drug.

Introduction

Lung cancer is the leading cause of cancer-mediated deaths, and 80-85% of all lung cancers are non-small cell lung cancer (1, 2). Importantly, resistance to anticancer drugs frequently found in patients with lung cancer has long been recognized as one of the most important obstacles to success of cancer therapy (3-5), leading to the urgent need for more effective chemotherapeutic agents.

The main mechanism of action of the currently effective chemotherapeutic drugs is to mediate cancer cell apoptosis. Apoptosis cell death can be triggered by the production of DNA adducts or damage signal that subsequently activates the p53-dependent cascade. The activation of p53 results in the increase of pro-apoptotic proteins which are members of B-cell lymphoma 2 (BCL2) family such as BCL2-associated X (BAX) accompanied by the reduction of anti-apoptotic proteins, including BCL2. The induction of pro-apoptotic signaling leads to the formation of mitochondrial pores, the release of cytochrome c into the cytosol, the activation of caspases, and finally cell apoptosis (6-8). In contrast, resistance to apoptosis in lung cancer can be caused by several mechanisms; however, the up-regulation of expression of pro-survival proteins including ATP-dependent tyrosine kinase (AKT), and anti-apoptotic proteins of the BCL2 family were shown to be the predominant mechanisms (9-11).

In order to overcome drug resistance problems, our group has focused on searching for natural products with anticancer capability. Renieramycin M (RM), a bistetrahydroisoquinolinequinone alkaloid isolated from the Thai blue sponge *Xestospongia* sp., was reported to possess highly potent cytotoxicity against several human cancer cell lines, including lung, colon, prostate, breast, pancreatic, and oral cancer cells (12-15). Recently, RM was shown to have potent anti-metastatic activity by sensitizing anoikis-resistant lung cancer cells to anoikis (16). In addition, RM was shown to suppress cancer stem-like phenotypes in lung cancer cells (17).

Recently, a series of 22-O-acyl and hydroquinone 5-O-acyl ester analogs of RM were synthesized by our group. These RM derivatives were tested for structure–cytotoxicity relationship study in H292 and H460 non-small-cell lung cancer cell lines. (15, 18, 19). Interestingly, most 22-O-acyl ester and hydroquinone 5-O-acyl ester analogs of RM exhibited potent cytotoxicity at nanomolar concentrations and several of them exhibited higher potency than RM. Having a unique aromatic ester substituent, hydroquinone 5-O-cinnamoyl ester (CIN-RM) is structurally attractive as a potential anticancer candidate. CIN-RM was obtained via two-step chemical synthesis involving Pd-catalyzed hydrogenation and esterification and the structural characterization was matched with the reported data (19). Here we investigated the effect of CIN-

RM on lung cancer cells. This information may benefit the further development of new anticancer agents.

Materials and Methods

Preparation of CIN-RM.

A solution of RM (15.0 mg, 0.026 mmol) in EtOAc (10 ml) was added with 20% Pd(OH)₂ on carbon (7.5 mg, 50% w/w). A hydrogen balloon was attached to the reaction flask. The heterogeneous reaction was stirred vigorously at room temperature (25 °C) and 1 atm for 5 h. The reaction was filtered through a pad of celite and washed with EtOAc (10 ml, 3 times) and CHCl₃ (10 ml, 3 times). The filtrates were combined and concentrated in vacuo to yield HQ-RM as a colorless solid. The product was employed in the next step without further purification. Next, the resulted HQ-RM was placed in an oven dried-rounded bottom flask. To a solution of HQ-RM (15.0 mg, 0.026 mmol) in dry CH₂Cl₂ (5 ml) was stirred at room temperature (25 °C) under Ar atmosphere. The reaction was added 1-ethyl-3-(3-dimethylaminopropyl) carbodiimide (EDCI.HCl, 4.0 mg, 0.026 mmol) and 4-dimethylaminopyridine (DMAP, 3.2 mg, 0.026 mmol), followed by cinnamoyl chloride (4.3 mg, 0.026 mmol). The reaction mixture was stirred for 3 h. After completion, the reaction mixture was quenched by addition of water (5 ml). The organic layer was separated by separatory funnel and the aqueous layer was extracted with CHCl₃ (10 ml, 3 times). The organic layers were combined, washed with brine (30 ml), dried over anhydrous Na₂SO₄, filtered and concentrated in vacuo. Purification by the silica gel flash chromatography eluting with hexanes:EtOAc (3:1) gave 7.9 mg (43%) of CIN-RM as a yellow amorphous solid. ¹H NMR (CDCl₃, 400 MHz) δ 7.8 (1H, d, J = 16.0 Hz, CH=CH β), 7.6 (2H, m, H-3' and H-5'), 7.5 (3H, m, H-2', H-6', and H-4'), 6.7 (1H, d, J = 16.0 Hz, CH α =CH), 6.0 (1H, qq, J = 7.4, 1.2 Hz, H-26), 5.8 (1H, s, OH-8), 4.5 (1H, d, J = 11.2 Hz, H-22b), 4.3 (1H, br t, J = 4.0 Hz, H-1), 4.1 (1H, d, J = 2.0 Hz, H-21), 4.1 (1H, dd, J = 11.2, 4.0 Hz, H-22a), 4.0 (1H, br d, J = 3.6 Hz, H-11), 3.9 (3H, s, 17-OCH₃), 3.8 (3H, s, 7-OCH₃), 3.4 (1H, dt, J = 7.2, 2.0 Hz, H-13), 3.2 (1H, d, J = 12.0 Hz, H-3), 2.8 (1H, dd, J = 20.8, 7.2 Hz, H-14 α), 2.6 (1H, dd, J = 14.0, 2.0 Hz, H-4 α), 2.3 (1H, d, J = 20.8 Hz, H-14 β), 2.3 (3H, s, 12-NCH₃), 2.1 (3H, s, 6-CH₃), 1.9 (3H, dq, J = 7.2, 1.4 Hz, H₃-27), 1.9 (3H, s, 16-CH₃), 1.7 (3H, dq, J = 1.4, 1.2 Hz, H₃-28), 1.7 (1H, overlapped, H-4 β); ¹³C NMR (CDCl₃, 100 MHz) δ 186.0 (C-15), 182.6 (C-18), 167.1 (C-24), 164.7 (5-OC=O), 155.5 (C-17), 146.8 (CH=CH β), 143.8 (C-7), 143.1 (C-8), 141.5 (C-20), 140.0 (C-26), 139.1 (C-5), 135.7 (C-19), 134.1 (C-1'), 131.0 (C-4'), 129.1 (C-2' and C-6'), 128.8 (C-16), 128.4 (C-3' and C-5'), 126.8 (C-25), 124.5 (C-10), 122.6 (C-6), 117.6 (21-CN), 117.2 (C, C-9), 116.4 (CH α =CH), 64.5 (C-22), 61.2 (7-OCH₃), 60.6 (17-OCH₃), 59.5 (C-21), 56.5 (C-1), 55.3 (C-3), 54.9 (C-13), 54.6 (C-11), 41.5 (12-NCH₃), 27.8 (C-4), 21.1 (C-14), 20.6 (C-28), 15.9 (C-27), 10.1 (6-CH₃), 8.6 (16-

CH3). Chemicals were purchased from Tokyo Chemical Industry. NMR spectroscopy was performed on JEOL-JNM AL 400 FT-NMR spectrometer. (19)

Chemicals.

Hoechst 33342, 3-(4,5-dimethylthiazol-2-yl)-2,5-diphenyltetrazolium bromide (MTT), dimethylsulfoxide (DMSO), trypsin and phosphate-buffered saline (PBS) were obtained from Sigma Chemical, Inc. (St. Louis, MO, USA). Antibodies to apoptosis-inducing factor (AIF), phosphorylated AKT (p-AKT), total AKT, p53, BCL2, BAX, poly ADP ribose polymerase (PARP), caspase-3, caspase-9, and β -actin were obtained from Cell Signaling Technology, Inc. (Danvers, MA, USA).

Cell culture and treatment.

H292 Non-small cell lung cancer cells were obtained from the American Type Culture Collection (Manassas, VA, USA) and cultured in RPMI medium supplemented with 10% fetal bovine serum, 2 mmol/l L-glutamine and 100 units/ml penicillin/streptomycin. Cells were maintained in a humidified incubator containing 5% CO₂ at 37°C. Compounds were dissolved in DMSO and achieve the working concentrations (0, 15, 30 and 60 μ M). DMSO in the working solution was less than 0.1% and showed no toxicity towards H292 cells.

Cell viability assay.

Cell viability was determined by the MTT assay, which measures the cellular capacity to reduce MTT (yellow) to formazan crystals (purple) by mitochondria dehydrogenase. After 24 h treatment, the medium was replaced by 100 μ l/well of MTT solution (0.4 mg/ml) and the cells were incubated for 4 h at 37°C. Subsequently, the MTT solution was removed and a 100 μ l/well of DMSO were added to dissolve the formazan crystals. The intensity was measured at 570 nm using a microplate reader (SpectraMax M5, Molecular Devices, City, Ca, USA). All analyses were performed in at least three independent replicate cultures. The cell viability was calculated from the ratio of the optical density (OD) of treated to non-treated control cells and is presented as a percentage of the non-treated controls.

Nuclear staining assay.

Cells were treated without or with different concentrations of CIN-RM in RPMI with serum for 24 h at 37°C. Apoptotic and necrotic cell death was determined by Hoechst 33342 staining: cells were incubated with 10 μ M of Hoechst 33342 dye for 30 min at 37°C in the dark. Finally, cells were visualized under a fluorescence microscope (Olympus IX51 with DP70; Olympus, Center Valley, PA, USA). The blue fluorescent Hoechst dye was used for detection of nuclear condensation and DNA fragmentation in apoptosis cell. The data are presented as the percentage of apoptosis as follows: Apoptosis (%) = number of apoptotic cells \times 100/number of total cells.

Membrane integrity analysis.

The cells collected after treatment with compounds were stained with trypan blue dye and subsequently morphologically visualized and quantified under an automated cell counter (TC10 automated cell counter; Bio-Rad, Hercules, CA, USA).

Western blot analysis.

Treated and untreated cells were harvested and lysed on ice for 60 min. The protein content of cell lysate was determined using BSA protein assay kit (Pierce, Rockford, IL, USA). An equal amount of protein from each sample was separated by size using sodium dodecyl sulfate-polyacrylamide gel electrophoresis and then transferred into nitrocellulose membranes. The membrane was blocked in 5% skim milk in 25 mmol/l Tris-HCl (pH 7.4), 125 mmol/l NaCl and 0.1% Tween 20 TBST for 1 h at room temperature and then probed with appropriate primary antibodies at 4°C overnight. Subsequently, the membrane was washed three times with TBST for 8 min then incubated with horseradish peroxidase-conjugated secondary antibodies according to the primary antibodies for 2 h at room temperature. The signal of immunoreactive proteins was detected by enhanced chemiluminescence (Supersignal West Pico; Pierce, Rockford, IL, USA). Protein expression was investigated and β -actin was used as a loading of control in each treatment. Subsequently, the bands were then visualized using a film exposure with a chemiluminescence detection system and were quantified with analystPC densitometric software.

Statistical analysis.

Mean data from at least three independent experiments were normalized to result for the non-treated control. All data are presented as the means \pm standard error of the mean (S.E.M.). Statistical differences between means were determined using analysis of variance (ANOVA) and post hoc test at a significance level of $p < 0.05$.

Results

Evaluation of the cytotoxic effect of CIN-RM and RM on H292 cells.

CIN-RM was synthesized from RM as shown in Figure 1. The cytotoxicity of CIN-RM and its parental compound RM was characterized by treating H292 cells with different concentrations of compounds (0-100 μ M) for 24 h, then cell viability was measured by MTT assay. Figure 2A shows that a concentration of 100 μ M of CIN-RM significantly reduced viability of H460 cells to approximately 40% when compared with 62% with RM at the same concentration. To confirm effect of CIN-RM in mediating cell death, after 24 h of treatment with 0-100 μ M of CIN-RM, the

cells were collected, stained with trypan blue dye, and subsequently morphologically visualized, and quantified by an automated cell counter (Figure 2B-C).

A

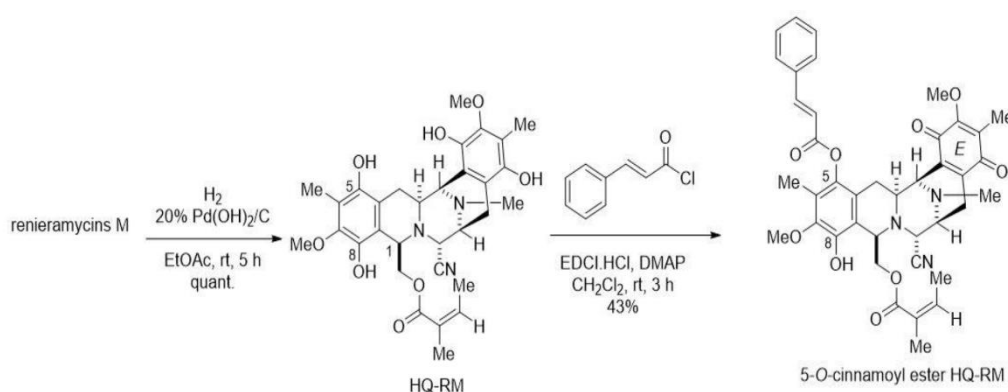


Figure 1. The synthesis of 5-O-cinnamoyl ester analog of renieramycin M (CIN-RM).

CIN-RM was derived from hydrogenation of renieramycin M with 20% Pd(OH)₂/C in ethyl acetate for 5 h to obtain the bishydroquinonerenieramycin M (HQ-RM). HQ-RM was subjected to esterification with cinnamoyl chloride in the presence of 1-ethyl-3-(3-dimethylaminopropyl)carbodiimide hydrochloride (EDCI.HCl) and 4-dimethylaminopyridine (DMAP) yielding CIN-RM

CIN-RM induces apoptotic cell death.

In order to investigate the apoptosis inducing effect of CIN-RM, cells were exposed to CIN-RM and apoptosis was evaluated by Hoechst 33342 staining assay. The nuclear staining assay indicated that 15-60 μ M of CIN-RM caused a significant increase in the number of cells with condensed or fragmented nuclei compared with non-treated control cells (Figure 3 A and B). At a concentration of 60 μ M, CIN-RM-induced cell apoptosis was approximately 55%.

To confirm the above apoptotic activity of CIN-RM, the hallmarks of apoptosis including cleavage of PARP, induction of AIF expression, and activation of caspase-3 and caspase-9 were investigated in cells treated with CIN-RM. Western blot analysis indicated that treatment of H292 cells with CIN-RM increased production of cleaved PARP, while reducing the total intact PARP. Consistent with this, CIN-RM up-regulated AIF and increased activation of caspase-3 and caspase-9 in a dose-dependent manner (Figure 3C and D). Taken together, these results show that CIN-RM induced apoptosis of H292 lung cancer cells.

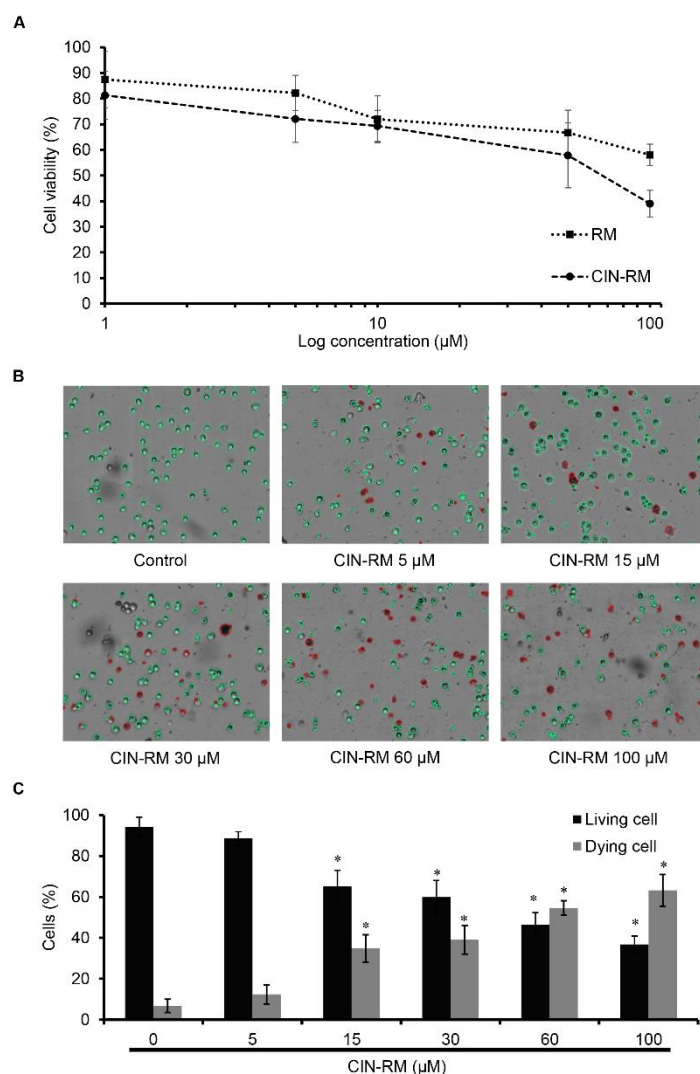


Figure 2. Cytotoxic effect of 5-O-cinnamoyl ester analog of renieramycin M (CIN-RM) on H292 lung cancer cells. A: H292 Human lung cancer

cells were treated with different concentrations (0-100 µM) of CIN-RM or RM for 24 h. The percentage of cell viability was analyzed. Data represent the mean±SD (n=3). Significantly different at *p<0.05 versus non-treated control. B: H292 cells collected after treatment with CIN-RM (0-100 µM) for 24 h were stained with trypan blue dye and subsequently analyzed cell membrane integrity under an automated cell counter. The green color indicates living cells, while the red color indicates dying cells. C: The percentage of living cells and dying cells after treatment with CIN-RM (0-100 µM) for 24 h were quantified. Data represent the mean±SD (n=3). Significantly different at *p<0.05 versus the non-treated control.

CIN-RM triggers apoptosis via a p53-dependent mechanism and suppresses AKT.

It is known that apoptosis induction caused by several chemotherapeutic drugs occurs through p53-mediated death (20-22). A number of studies have indicated the effect of pro-survival AKT signal on chemotherapeutic resistance in cancer (9, 10, 23, 24). Therefore, we tested

whether CIN-RM induced apoptosis of H292 cells via p53 and suppressed pro-survival AKT. Cells were treated with CIN-RM (0-60 μM) for 12 h, and subjected to western blot analysis for the detection of p-AKT, total AKT, p53, BCL2, and BAX. Figure 4 shows that treatment of the cells with CIN-RM dramatically suppressed active AKT (AKT phosphorylated at Ser473), while slightly suppressing total AKT. Importantly, CIN-RM increased the p53 level in the cells relative to the untreated control. As a down-stream protein target of p53 pathway, expression of BAX was found to subsequently increase, while that of BCL2 was down-regulated (Figure 4C and D). Together, these results indicate that CIN-RM induces apoptosis by activating the p53 pathway as well as suppressing the AKT survival signal.

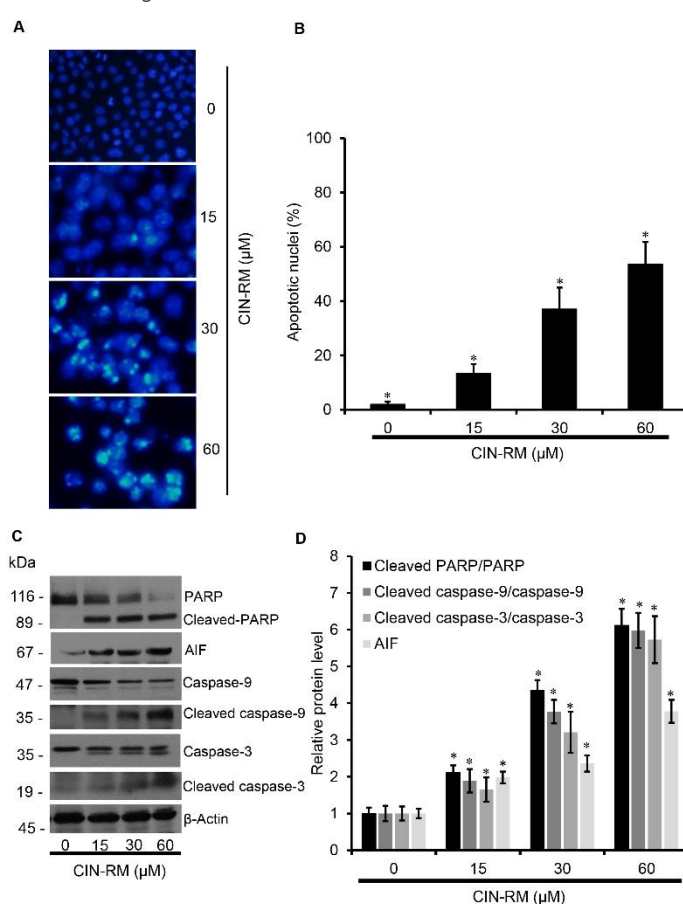


Figure 3. Apoptosis induction by 5-O-cinnamoyl ester analog of renieramycin M (CIN-RM).

A: H292 cells were exposed to CIN-RM for 24 h and subsequently apoptosis was evaluated by Hoechst 33342 staining assay. B: The percentage of apoptotic cells was quantified. Data represent the mean \pm SD (n=3). Significantly different at *p<0.05 versus the non-treated control. C: H292 cells were treated with CINRM (0, 15, 30 and 60 μM) for 24 h. The expression of apoptosis-related proteins in H292 cells was determined by western blotting. The blots were reprobbed with β -actin to confirm equal loading of samples. D: The immunoblot signals were quantified by densitometry and data from independent experiments were normalized and are presented. The data are mean \pm SD (n=3). Significantly different at *p<0.05 versus nontreated cells.

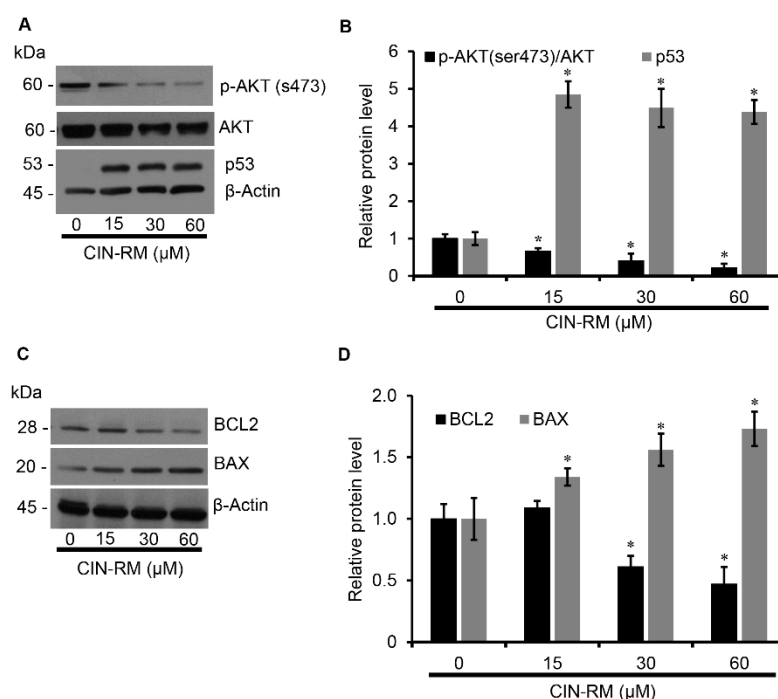


Figure 4. 5-O-Cinnamoyl ester analog of renieramycin M (CIN-RM) induces apoptosis through accumulation of p53 and suppresses ATP-dependent tyrosine kinase (AKT).

H292 cells were treated with CIN-RM (0, 15, 30 and 60 μ M) for 12 h. A: The expression of AKT and phosphorylated (active) AKT [p-AKT(s473)] was determined by western blot assay. The blots were reprobbed with β -actin to confirm equal loading of samples. B: The immunoblot signals were quantified by densitometry and data from independent experiments were normalized and are presented. The data are mean \pm SD (n=3). Significantly different at * $p < 0.05$ versus non-treated cells. C: The expression of anti apoptotic proteins B-cell lymphoma 2 (BCL2) and pro-apoptotic proteins BCL2-associated X (BAX) were determined by western blotting. The blots were reprobbed with β -actin to confirm equal loading of samples. D: The immunoblot signals were quantified by densitometry and data from independent experiments were normalized and are presented. The data are mean \pm SD (n=3). Significantly different at * $p < 0.05$ versus non-treated cells.

Discussion

New drugs and novel strategies to overcome cancer with high efficacy are of the greatest interest in cancer-related and pharmacological research fields. In general, most anticancer drugs are used to kill cancer cells through apoptosis, as it is a mode of cell death with a controlling mechanism (22, 25). Apoptosis is the main mechanism that the human body uses to eliminate unwanted and damaged cells (26, 27). As part of our continuing searching for novel cytotoxic natural products, we isolated and modified a series of RM alkaloids from blue sponge *Xestospongia* sp. (12, 13, 15, 18,) RMs are a group of bistetrahydroisoquinoline quinone alkaloids possessing potent cytotoxicity against several human cancer cell lines (15-18, 28, 29). In addition,

RM was shown to have anti-metastasis potential and suppress cancer stem cells in lung cancer (16, 17, 28).

Successful synthesis of 22-O-acyl and hydroquinone 5-O-acyl ester analogs of RM has led to several more potent compounds for anticancer approaches (15, 18, 19). Interestingly, our previous work of RM derivatives showed that the hydroquinone 5-O-acetyl ester analog of RM was the first analog possessing selective apoptotic induction while reduce its necrosis-inducing effect by reducing oxidative stress (30).

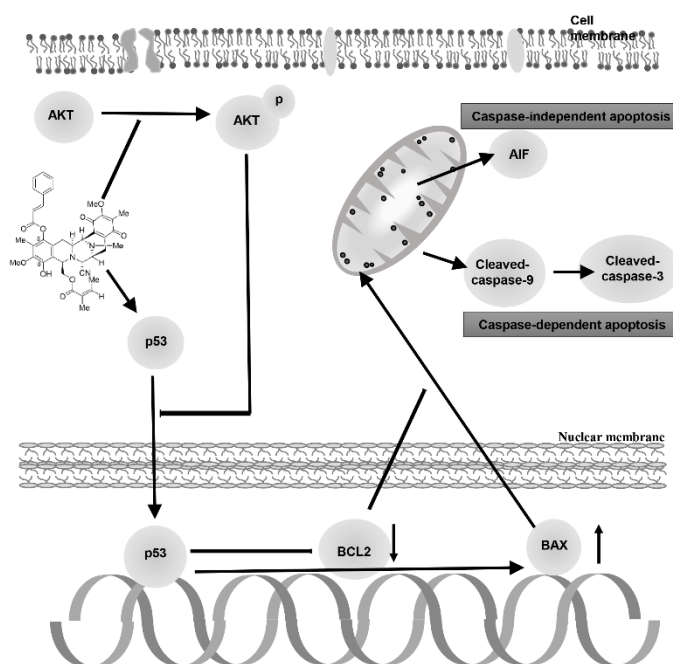


Figure 5. Schematic overview of apoptosis pathway of 5-O-cinnamoyl ester analog of renieramycin M (CIN-RM).

CIN-RM causes apoptosis by reducing expression of pro-survival ATP-dependent tyrosine kinase (AKT) and activating the p53 pathway. The accumulation of p53 suppresses the expression of anti-apoptotic protein B-cell lymphoma 2 (BCL2) while promoting the expression of pro-apoptotic protein BCL2-associated X (BAX). The shift of balance between pro- and anti-apoptotic proteins subsequently triggers the release of apoptosis-inducing factor (AIF), which promotes caspase-independent apoptosis pathway. Moreover, loss of mitochondrial membrane integrity stimulates caspase-dependent apoptosis by activation of caspase-9 and caspase-3.

As chemotherapeutic resistance in lung cancer has been long recognized as an important obstacle to successful therapy (9, 31), new drugs having high potency as well as the ability to inhibit drug resistance of cancer cells are of great interest in anticancer drug discovery. The AKT signaling pathway has been shown to be a central survival pathway playing a key role in drug resistance in many cancer types, including lung cancer (32, 33). Especially, targeting of the AKT pathway was shown to be a good strategy to boost chemotherapy efficacy (34). Figure 4 indicates

that not only does CIN-RM induce apoptosis of lung cancer cells by activation of a p53-dependent mechanism that triggers BCL2 imbalance, the release of AIF, and activation of caspases, the compound also has ability to suppress the AKT survival signal.

In conclusion, we have shown that the newly synthesized CIN-RM has a potent cytotoxic effect against lung cancer cells. The results indicate that the derivative of the lead compound RM possesses a good anticancer activity by inducing apoptosis of lung cancer cells via p53-mediated alteration of BCL2 protein expression and suppression of pro-survival AKT signaling.

Acknowledgements

This work was supported by grants from The Thailand Research Fund through The Royal Golden Jubilee Ph.D. program Grant No. PHD/0063/2557, grant for International Research Integration: Chula Research Scholar, Ratchadaphiseksomphot Endowment Fund grant for Ratchadaphiseksomphot Endowment Fund under Outstanding Research Performance Program.

Conflicts of interest

The Authors declare that there is no conflict of interest in regard to this research.

References

- 1 Esposito L, Conti D, Ailavajhala R, Khalil N and Giordano A: Lung cancer: Are we up to the challenge? *Curr Genomics* 11: 513-518, 2010.
- 2 World Cancer Factsheet. London: International Agency for Research on Cancer and Cancer Research UK, 2012.
- 3 Shanker M, Willcutts D, Roth JA and Ramesh R: Drug resistance in lung cancer. *Lung Cancer: Targets Ther* 1: 23-36, 2010.
- 4 Dai PC, Liu DL, Zhang L, Ye J, Wang Q, Zhang HW, Lin XH and Lai GX: Astragaloside IV sensitizes non-small cell lung cancer cells to gefitinib potentially via regulation of SIRT6. *Tumour Biol* 39: 1-6, 2017.
- 5 Martinez-Jimenez F, Overington JP, Al-Lazikani B and Marti-Renom MA: Rational design of non-resistant targeted cancer therapies. *Sci Rep* 7: 1-18, 2017.
- 6 Wang C and Youle RJ: The role of mitochondria in apoptosis. *Annu Rev Genet* 43: 95-118, 2009.
- 7 Liu C, Wang Y, Xie S, Zhou Y, Ren X, Li X and Cai Y: Liquiritigenin induces mitochondria-mediated apoptosis via cytochrome c release and caspases activation in HeLa Cells. *Phytother Res* 25: 277-283, 2011.

- 8 Tait SWG and Green DR: Mitochondrial regulation of cell death. *Cold Spring Harb Perspect Biol* 5: a008706, 2013.
- 9 Jones VS, Huang R-Y, Chen L-P, Chen Z-S, Fu L and Huang R-P: Cytokines in cancer drug resistance: Cues to new therapeutic strategies. *Biochim Biophys Acta* 1865: 255-265, 2016.
- 10 Luanpitpong S and Chanvorachote P: Nitric oxide and aggressive behavior of lung cancer cells. *Anticancer Res* 35: 4585-4592, 2015.
- 11 Narayanan KB, Ali M, Barclay BJ, Cheng Q, D'Abronzio L, Dornetshuber-Fleiss R, Ghosh PM, Gonzalez Guzman MJ, Lee T-J, Leung PS, Li L, Luanpitpong S, Ratovitski E, Rojanasakul Y, Romano MF, Romano S, Sinha RK, Yedjou C, Al-Mulla F, Al-Temaimi R, Amedei A, Brown DG, Ryan EP, Colacci AM, Hamid RA, Mondello C, Raju J, Salem HK, Woodrick J, Scovassi A, Singh N, Vaccari M, Roy R, Forte S, Memeo L, Kim SY, Bisson WH, Lowe L and Park HH: Disruptive environmental chemicals and cellular mechanisms that confer resistance to cell death. *Carcinogenesis* 36: S89-S110, 2015.
- 12 Suwanborirux K, Amnuoyopol S, Plubrukarn A, Pummangura S, Kubo A, Tanaka C and Saito N: Chemistry of renieramycins. Part 3. Isolation and structure of stabilized renieramycin type derivatives possessing antitumor activity from Thai sponge *Xestospongia* species, pretreated with potassium cyanide. *J Nat Prod* 66: 1441-1446, 2003.
- 13 Amnuoyopol S, Suwanborirux K, Pummangura S, Kubo A, Tanaka C and Saito N: Chemistry of renieramycins. Part 5. Structure elucidation of renieramycin-type derivatives O, Q, R and S from Thai marine sponge *Xestospongia* species pretreated with potassium cyanide. *J Nat Prod* 67: 1023-1028, 2004.
- 14 Saito N, Tanaka C, Koizumi Y-i, Suwanborirux K, Amnuoyopol S, Pummangura S and Kubo A: Chemistry of renieramycins. Part 6: Transformation of renieramycin M into jorumycin and renieramycin J including oxidative degradation products, mimosamycin, renierone and renierol acetate. *Tetrahedron* 60: 3873-3881, 2004.
- 15 Charupant K, Daikuhara N, Saito E, Amnuoyopol S, Suwanborirux K, Owa T and Saito N: Chemistry of renieramycins. Part 8: synthesis and cytotoxicity evaluation of renieramycin M-jorunnamycin A analogues. *Bioorg Med Chem* 17: 4548-4558, 2009.
- 16 Sirimangkalakitti N, Chamni S, Suwanborirux K and Chanvorachote P: Renieramycin M sensitizes anoikis-resistant h460 lung cancer cells to anoikis. *Anticancer Res* 36: 1665-1671, 2016.
- 17 Sirimangkalakitti N, Chamni S, Suwanborirux K and Chanvorachote P: Renieramycin M attenuates cancer stem cell-like phenotypes in h460 lung cancer cells. *Anticancer Res* 37: 615-621, 2017.

- 18 Sirimangkalakitti N, Chamni S, Charupant K, Chanvorachote P, Mori N, Saito N and Suwanborirux K: Chemistry of renieramycins. 15. Synthesis of 22-O-ester derivatives of jorunnamycin A and their cytotoxicity against non-small-cell lung cancer cells. *J Nat Prod* 79: 2089-2093, 2016.
- 19 Chamni S, Sirimangkalakitti N, Chanvorachote P, Saito N and Suwanborirux K: Chemistry of renieramycins. 17. A new generation of renieramycins: hydroquinone 5-O-monoester analogues of renieramycin m as potential cytotoxic agents against non-small-cell lung cancer cells. *J Nat Prod*, 2017. doi:10.1021/acs.jnatprod.7b00068 [Epub ahead of print]
- 20 Fiandalo MV and Kyprianou N: Caspase control: protagonists of cancer cell apoptosis. *Exp Oncol* 34: 165-175, 2012.
- 21 Ricci MS and Zong W-X: Chemotherapeutic approaches for targeting cell death pathways. *Oncologist* 11: 342-357, 2006.
- 22 Johnstone RW, Ruefli AA and Lowe SW: Apoptosis: a link between cancer genetics and chemotherapy. *Cell* 108: 153-164, 2002.
- 23 Fresno Vara JA, Casado E, Castro J, Cejas P, Belda-Iniesta C, and González-Barón M: PI3K/AKT signaling pathway and cancer. *Cancer Treat Rev* 30: 193-204, 2004.
- 24 Ghadimi MP, Lopez G, Torres KE, Belousov R, Young ED, Liu J et al.: Targeting the PI3K/mTOR axis, alone and in combination with autophagy blockade, for the treatment of malignant peripheral nerve sheath tumors. *Mol Cancer Ther* 11: 1758-1769, 2012.
- 25 Lopez J and Tait SWG: Mitochondrial apoptosis: killing cancer using the enemy within. *Br J Cancer* 112: 957-962, 2015.
- 26 Elmore S: Apoptosis: a review of programmed cell death. *Toxicologic pathology* 35: 495-516, 2007.
- 27 Fuchs Y and Steller H: Programmed cell death in animal development and disease. *Cell* 147: 742-758, 2011.
- 28 Halim H, Chunchacha P, Suwanborirux K and Chanvorachote P: Anticancer and antimetastatic activities of renieramycin M, a marine tetrahydroisoquinoline alkaloid, in human non-small cell lung cancer cells. *Anticancer Res* 31: 193-201, 2011.
- 29 Pinkhien T, Maiuthed A, Chamni S, Suwanborirux K, Saito N and Chanvorachote P: Bishydroquinone renieramycin M induces apoptosis of human lung cancer cells through a mitochondria-dependent pathway. *Anticancer Res* 36: 6327-6333, 2016.
- 30 Cheun-Arom T, Chanvorachote P, Sirimangkalakitti N, Chuanasa T, Saito N, Abe I, and Suwanborirux K: Replacement of a quinone by a 5-O- acetylhydroquinone abolishes the accidental necrosis-inducing effect while preserving the apoptosis-inducing effect of renieramycin M on lung cancer cells. *J Nat Prod* 76: 1468-1474, 2013.

- 31 Sui X, Chen R, Wang Z, Huang Z, Kong N, Zhang M, Han W, Lou F, Yang J, Zhang Q, Wang X, He C and Pan H: Autophagy and chemotherapy resistance: a promising therapeutic target for cancer treatment. *Cell Death Dis* 4: e838, 2013.
- 32 David O, Jett J, LeBeau H, Dy G, Hughes J, Friedman M and Brody AR: Phospho-AKT overexpression in non-small cell lung cancer confers significant stage-independent survival disadvantage. *Clin Cancer Res* 10: 6865-6871, 2004.
- 33 Tsvetkova E and Goss GD: Drug resistance and its significance for treatment decisions in non-small-cell lung cancer. *Curr Oncol* 19: S45-S51, 2012.
- 34 Grand ML, Berges R, Pasquier E, Montero MP, Borge L, Carrier A, Vasseur S, Bourgarel V, Buric D andré N, Braguer D and Carré M: AKT targeting as a strategy to boost chemotherapy efficacy in non-small cell lung cancer through metabolism suppression. *Sci Rep* 7: 45136, 2017.



CHAPTER V

CONCLUSION AND SUGGESTION FOR FUTHER STUDY

Conclusion

This research project provides the better understanding how PKB, also known as Akt, regulating apoptosis susceptibility and dedifferentiation of differentiated cancer cells to be CSC. In general, Akt primarily controls cancer virulence by phosphorylation and activation its downstream signalling, whereas these novel findings revealed that Akt can direct modulates certain proteins functions including Cav-1 and p21 via phosphorylation induced protein conformational changed. For p21, activated-Akt changes p21 function and sub-cellular localization leading to favor p21 oncogenic capability instead of its tumor suppressive potential. Oncogenic-p21 can inhibit pro-apoptotic function of Chk2 under treatment with cytotoxic drug, 5FU, leading to more chemoresistance phenotype. For Cav-1, activated-Akt omits CSC suppressive function of Cav-1 leading to formation of CSC through non-CSC dedifferentiation. Moreover, we synthesis and test apoptosis induction effects of the semi-synthetic natural compound, CIN-RM. The results show that CIN-RM induces apoptosis in lung cancer cell by inhibiting Akt function which promotes p53-induced apoptosis. This meaningful knowledge would applicable for designing novel targeted cancer drug and therapy.

Suggestion for further projects

This project mainly performed *in vitro* system which could not represented all feature of cancer biology. For further research, it would be better to include *in vivo* experiments or data from patients' tissue for verifying the novel discoveries of this research and confirming the anti-tumor effect of the semi-synthetic natural compound. Moreover, the main objectives of this project are study the deep biological mechanisms controlling aggressive phonotype of lung cancer and colorectal cancer, there would be investigated this aggressiveness regulatory control in other cancer types to confirm that the discovered mechanisms are not cell type or tissue specific and can apply to design treatment intervention in other cancer types. In addition, the novel protein-protein interaction finding in this research would be more extensively study for precise understanding of important amino acid moieties which essential for its interaction. This knowledge would be use for designing a new therapeutic intervention by suppressing the interaction of the proteins.

REFERENCES



จุฬาลงกรณ์มหาวิทยาลัย
CHULALONGKORN UNIVERSITY



จุฬาลงกรณ์มหาวิทยาลัย
CHULALONGKORN UNIVERSITY

VITA

NAME Arnatchai Maiuthed

DATE OF BIRTH 14 December 1983

PLACE OF BIRTH Phetchaburi province

INSTITUTIONS ATTENDED

1. 2014 – present
Ph.D. student in Pharmacology and Toxicology programme,
Faculty of Pharmaceutical Science, Chulalongkorn University,
Bangkok Thailand
Ph.D. student (cotutelle) in Institute of Pathology,
Friedrich-Alexander-University Erlangen-Nürnberg
Spend time for doctoral research in Germany from 16th January
2017 to 31st January 2018 at Friedrich-Alexander-University
Erlangen-Nürnberg
2. 2007 – 2012
Master of Science in Pharmacy (Pharmacology),
Faculty of Pharmacy, Mahidol university, Bangkok, Thailand
Cumulative GPA 3.70 (4.00-based)
3. 2000 - 2005
Bachelor of Science in Pharmacy with the 2nd class honor,
Faculty of Pharmacy, Mahidol university, Bangkok, Thailand
GPA 3.32 (4.00-based)

HOME ADDRESS 372 Radchadumnaen Road,
Kronggrachang, Muang Phetchaburi,
Thailand, 76000

PUBLICATION

1. Cytoplasmic p21 mediates 5-Fluorouracil resistance by
inhibiting proapoptotic Chk2.
Arnatchai Maiuthed, Chuanpit Ninsontia, Katharina Erlenbach-
Wuensch, Benardina Ndreshkjana, Julienne K. Muenzner, Aylin
Caliskan, Husayn P. Ahmed, Chatchai Chaotham, Arndt Hartmann,
Adriana Vial Roehe, Vijayalakshmi Mahadevan, Pithi

Chanvorachote, and Regine Schneider-Stock. *Cancers*. 2018 Oct, 10 (10); 373. doi: 10.3390/cancers10100373.

2. Nitric oxide promotes cancer cell dedifferentiation by disrupting an Oct4:caveolin-1 complex: A new regulatory mechanism for cancer stem cell formation.

Maiuthed A, Bhummaphan N, Luanpitpong S, Mutirangura A, Apornthewan C, Meeprasert A, Rungrotmongkol T, Rojanasakul Y, Chanvorachote P. *J Biol Chem*. 2018 Aug, 31;293(35):13534-13552. doi: 10.1074/jbc.RA117.000287. Epub 2018 Jul 9.

3. Lung Cancer Stem Cells and Cancer Stem Cell-targeting Natural Compounds (Review).

Maiuthed A, Chantarawong W, Chanvorachote P. *Anticancer Res*. 2018 Jul;38(7):3797-3809. doi: 10.21873/anticancerres.12663. Review.

4. Apoptosis-inducing Effect of Hydroquinone 5-O-Cinnamoyl Ester Analog of Renieramycin M on Non-small Cell Lung Cancer Cells.

Maiuthed A, Pinkhien T, Chamni S, Suwanborirux K, Saito N, Petpiroon N, Chanvorachote P. *Anticancer Res*. 2017 Nov;37(11):6259-6267.

5. Bishydroquinone Renieramycin M Induces Apoptosis of Human Lung Cancer Cells Through a Mitochondria-dependent Pathway.

Pinkhien T, Maiuthed A, Chamni S, Suwanborirux K, Saito N, Chanvorachote P. *Anticancer Res*. 2016 Dec;36(12):6327-6333.

6. Nitric oxide increases the migratory activity of non-small cell lung cancer cells via AKT-mediated integrin αv and $\beta 1$ upregulation.

Saisongkorh V, Maiuthed A, Chanvorachote P. *Cell Oncol (Dordr)*. 2016 Oct;39(5):449-462. Epub 2016 Jul 4.

7. Cisplatin at sub-toxic levels mediates integrin switch in lung cancer cells.

Maiuthed A, Chanvorachote P. Anticancer Res. 2014
Dec;34(12):7111-7.

AWARD RECEIVED

1. Outstanding poster presentation at GRJ-PhD congress 19th, “Innovation towards Thailand 4.0”: Research inspiration, Connectivity and Transformation. June 7- 9 2018 at Pattaya, Thailand.

